学位論文

Visible and dark matter genesis through the Affleck-Dine mechanism

(アフレック・ダイン機構を通じた物質および暗黒物質生成)

平成27年12月博士（理学）申請

東京大学大学院理学系研究科
物理学専攻
山田 將樹

Abstract

The origins of baryon asymmetry and dark matter are outstanding mysteries in cosmology and particle physics. In particular, the observed amount of energy densities of baryon and dark matter are equal to each other up to a factor of unity, which is known as the baryon–dark-matter coincidence problem. In this thesis, we investigate the Affleck-Dine baryogenesis in supersymmetric theories to account for the origins of baryon asymmetry and dark matter, and propose two scenarios to account for the coincidence between their energy densities. In the first scenario, we consider the case that non-topological solitons called Q-balls form after the Affleck-Dine baryogenesis and decay into baryons and light supersymmetric particles before the big-bang nucleosynthesis epoch. The light supersymmetric particles then decay into the lightest one, which is the candidate of dark matter. Thanks to the fact that the branchings of Q-ball decay are determined by the Pauli blocking effect, there is a natural coincidence of energy densities of baryon and dark matter. The second scenario is based on our new scenario of the Affleck-Dine baryogenesis, where the baryon asymmetry is generated just after the end of inflation in contrast to the ordinary scenario. When inflaton decays mainly into gravitinos, the subsequent decay of gravitinos is a non-thermal source of dark matter. We find that the resulting baryon-to-dark-matter ratio is naturally of order unity in hybrid inflation models. As a result of these two scenarios, we conclude that the Affleck-Dine baryogenesis is a promising mechanism to explain the origins of baryon asymmetry and dark matter and the coincidence between their energy densities. Those scenarios would be tested by future collider experiments and direct and indirect dark-matter searches.

Contents

Chapter 1

Introduction

The discovery of the Higgs boson completes the contents of particles in the Standard Model (SM) of particle physics [1, 2]. However, there are several mysteries in cosmology that cannot be explained by the SM: the origin of baryon-anti-baryon asymmetry, existence of dark matter (DM), and inflation.

The Big Bang theory explains the expansion of the Universe, the cosmic microwave background (CMB), and the amounts of light element abundances, which says that the Universe was filled with the thermal plasma in the early Universe with a certain baryon abundance. In fact, the Big Bang nucleosynthesis (BBN) theory explains observed helium (^{4}He) [3, 4] and deuterium (D) [5] abundances by only one parameter $Y_b \equiv n_b/s$, where n_b is baryon number density and s is the entropy density at present. In addition, the spectrum of CMB temperature anisotropies is sensitive to the baryon abundance and the observed spectrum is consistent with the one obtained from the BBN theory [6]. Those facts implies that there is baryon asymmetry of $Y_b \simeq 8.6 \times 10^{-11}$ at least at the temperature of order 1 MeV [7].

However, it confronts severe initial-condition problems, such as the horizon problem and the flatness problem. Then the paradigm of cosmology is shifted to the inflation theory, where those initial condition problems are explained by an exponentially expanding era in the early Universe [8, 9, 10, 11]. It also provides a natural mechanism of producing primordial perturbations that seed the large-scale structure of the Universe [12, 13, 14]. It predicts a spectral index of the spectrum of primordial perturbations. It is precisely measured by the observations of CMB temperature anisotropies, so that we could say that the inflation theory is confirmed experimentally [15, 6].

Unfortunately, the inflation theory implies that the baryon abundance is washed out by the exponential expansion of the Universe. Therefore, we still have a problem to generate

the baryon asymmetry. There should be a mechanism to generate the observed amount of baryon asymmetry after inflation.

In order to generate baryon asymmetry, we have to satisfy the Sakharov conditions, which clarify that it is generically difficult to generate the baryon asymmetry [16]. First, we of course need a baryon number violation operator to generate baryon asymmetry. Secondly, charge conjugation symmetry (C) and parity and charge conjugation symmetry (CP) need to be broken. This is because baryon and anti-baryon are odd under these symmetries. Thirdly, we need departure from thermal equilibrium. In particular, if the above symmetry-violating operators are in thermal equilibrium, no net baryon asymmetry is generated. Although all of these conditions are satisfied in the SM, we cannot generate enough baryon asymmetry to explain that observed. This means that we need physics beyond the SM to explain the baryon asymmetry.

In addition, cosmological and astrophysical observations reveal that there must be invisible massive particles in the Universe, called dark matter (DM). There is no candidate of such an invisible particle in the SM, so that we require new physics beyond the SM. Since inflation washes out the abundance of DM, we also need a mechanism to generate it after inflation. Remarkably, observations reveal that the energy densities of baryon and DM are equal with each other within of order unity [6]. This is known as the baryon-DM coincidence problem. This coincidence may imply that the baryon and DM may have a common origin or at least have a common parameter dependence in their production mechanism.

The origin of baryon asymmetry and DM imply new physics beyond the SM. Supersymmetry (SUSY) is a promising candidate of new physics in particle physics. It is a symmetry that relates fermions and bosons, which results in a cancellation of the quadratic divergences of scalar fields and addresses the hierarchy problem between the electroweak scale and the Planck scale. SUSY is assumed to be softly broken about the TeV scale, so that new particles are introduced around the TeV scale via SUSY. In particular, the lightest SUSY particle is stable and is a good candidate of DM.

In SUSY theories, baryon asymmetry can be generated by the Affleck-Dine mechanism, where $B-L$ asymmetry is generated via the dynamics of scalar partner of quarks and/or leptons [17, 18, 19]. A $B-L$ charged scalar field with a flat potential, called an Affleck-Dine (AD) field, can obtain a large tachyonic effective mass and have a large vacuum expectation value (VEV) during and after inflation. As the energy of the Universe decreases, the effective mass becomes inefficient and the AD field starts to oscillate coherently around the origin of

its potential. At the same time, the phase direction of the AD field is kicked by its A-term potential, which breaks C, CP, and $B-L$ symmetry. Since the $B-L$ number density is proportional to the phase velocity of the AD field, the $B-L$ asymmetry is generated through this non-equilibrium dynamics. When the coherent oscillation of the AD field decays and dissipates into thermal plasma, the $B-L$ asymmetry is converted to the desired baryon asymmetry through the sphaleron effects [20, 21].

Depending on the potential of the AD field, the Affleck-Dine baryogenesis (ADBG) may predict formation of localized lumps composed of condensation of the AD field carrying enormously large baryon charges [22, 23, 24, 25]. The lump is referred to as a Q-ball [26], which is long-lived due to the conservation of baryon charge. The Q-balls emit quarks from their surfaces and release their charges into standard model particles [27]. In this scenario, baryons are generated from the decay of Q-balls. In addition, since Q-balls consist of squarks, their decay produces light SUSY particles. Therefore, their decay may be the origins of DM as well as baryons, which may provide us a solution to the baryon-DM coincidence problem [24, 28].

In this thesis, we focus on ADBG in SUSY theories to explain the origin of baryon asymmetry and the coincidence problem, which are partially related to inflation models. We provide two scenarios to account for the coincidence between the energy densities of baryon and DM. We also provide a new scenario of ADBG, which broaden parameter spaces explaining the observed amount of baryon asymmetry. These topics are based on the works by the author [29, 30, 31, 32, 33].

In Chap. 5, we explain a scenario to account for the coincidence via Q-ball decay. The decay rate of Q-ball is determined by the Pauli blocking effect, so that its branching ratios into quarks and SUSY particles are determined by simple counting of degrees of freedom [27, 34, 35, 30]. As a result, the resulting baryon-to-DM ratio from Q-ball decay is found to be naturally of order unity.

In Chap. 7, we provide a new scenario of ADBG, where the AD field starts to oscillate around the minimum just after inflation [33]. Then in Chap. 8, we show that the resulting baryon-to-DM ratio is naturally of order unity in hybrid inflation models, which is another possibility to account for the coincidence problem [31].

As a result of these two studies, we conclude that the Affleck-Dine baryogenesis is a promising candidate for baryogenesis to account not only for the observed baryon asymmetry but also for the baryon-DM coincidence problem.

This thesis is organized as follows.

In Chap. 2, we explain the mysteries of baryon asymmetry, DM, and inflation. In particular, the observed energy densities of baryon and DM are equal to each other up to a factor of order unity. This coincidence is known as the baryon-DM coincidence problem. In Chap. 3, we review the ADBG in the conventional scenario. Then in Chap. 4, we explain Q-ball, which is a non-topological soliton of a complex scalar field. It sometimes form after ADBG and modifies its scenario. Its decay rates into quarks and SUSY particles are important to discuss the co-genesis of baryon and DM.

Chapter 5 is one of the main part of this thesis. In Sec. 5.1, we explain the scenario for co-genesis in general models of gravity mediation. In Sec. 5.2, we apply it to the constrained minimal SUSY SM (CMSSM) and show that the observed baryon asymmetry, DM abundance, and the 126 GeV Higgs boson can be simultaneously explained in that scenario. We determine a parameter region to realize the scenario and find that it would be tested by future collider experiments and direct and indirect DM searches.

In Chap. 6, we explain the relation between ADBG and inflation. We focus on three important inflation models; F-term hybrid inflation, D-term hybrid inflation, and chaotic inflation. In particular, we investigate the backreaction of the AD field to inflaton dynamics. We also explain that the scenario for co-genesis from Q-ball decay is naturally realized after a chaotic inflation model.

Chapter 7 and 8 are the other main part of this thesis. In Chap. 7, we provide a new scenario of ADBG, where the AD field starts to oscillate around the minimum just after the end of inflation. The resulting baryon asymmetry is independent of low-energy SUSY parameters but is dependent on parameters in inflaton sector. We investigate the scenario in F-term hybrid inflation, chaotic inflation, and D-term hybrid inflation and show that the observed baryon asymmetry can be explained in this new scenario. In Chap. 8, we apply the new scenario to some models and consider non-thermal DM production from gravitino decay. Although the baryon and DM are not generated from a common origin, their resulting abundances are related through same parameters in inflaton sector. As a result, the energy densities of baryon and DM naturally coincide with each other. This is another scenario to account for the baryon-DM coincidence problem.

Chapter 9 is devoted to the conclusion of this thesis.

Chapter 2

Cosmological problems

In this chapter, we briefly explain mysteries in cosmology: the origin of baryon-anti-baryon asymmetry, dark matter (DM), and inflation. The observed amount of light elements implies that the baryon-to-entropy ratio is of order 10^{-10}, whose origin cannot be explained in the Standard Model (SM) of particle physics and cosmology. Astrophysical and cosmological observations reveal that the Universe is partially filled with DM, which is an unknown particle beyond the SM. In the early Universe, there is an era of exponential expansion called inflation, which explains initial condition problems in the Big Bang cosmology.

2.1 Origin of baryon asymmetry

The Universe seems to be isotropic and homogeneous for a scale larger than of order 100 Mpc. The metric of its geometry $g_{\mu\nu}$ is then described by the Friedmann-Robertson-Walker metric:

$$g_{\mu\nu} = \mathrm{diag}[-1, a^2(t), a^2(t), a^2(t)], \tag{2.1}$$

where $a(t)$ is the scale factor and we neglect the curvature of the space. When the energy-momentum tensor for matter is isotropic and homogeneous, Einstein's field equations lead to the following equations called the Friedmann equations:

$$H^2 = \frac{\rho}{3M_{\rm Pl}^2} \tag{2.2}$$

$$\dot{\rho} = -3H\left(\rho + p\right), \tag{2.3}$$

where ρ and p are the energy density and pressure of matter, and

$$H(t) \equiv \frac{\dot{a}}{a} \equiv \frac{1}{a}\frac{\mathrm{d}a}{\mathrm{d}t}, \tag{2.4}$$

is the Hubble parameter. When the Universe is filled with the thermal plasma, the energy density and the pressure is given by

$$\rho = g_* \frac{\pi^2}{30} T^4 \tag{2.5}$$

$$p = \frac{\rho}{3}, \tag{2.6}$$

where g_* is the effective degrees of freedom of relativistic particles. This implies that the Hubble parameter is given by $H(t) = 1/2t$, $T \propto a^{-1}(t)$, and $a(t) \propto t^{1/2}$. Therefore, the temperature increases as we look at the earlier Universe. The early Universe is filled with a high temperature plasma, which is called the Big Bang cosmology.

The early Universe is filled with a hot dense plasma, so that the quarks and anti-quarks are in thermal equilibrium and are relativistic. Their abundance is determined by the thermal abundance and the fraction to entropy density is of order 1/10. As the temperature decreases due to the expansion of the Universe, the QCD phase transition occurs and baryon and anti-baryon form. Then their abundance exponentially decreases due to annihilation. Here, if there is asymmetry between the abundance of baryon and anti-baryon, baryons remain in the thermal plasma while anti-baryons completely disappear. The light element abundances, including ^{4}He and D, form from the remaining baryons. The observed abundance of these light elements implies that the baryon-to-entropy ratio after the annihilation is of order 1/10000000000. The origin of this small amount of asymmetry between baryon and anti-baryon is a mystery in cosmology.

2.1.1 BBN theory

The Big Bang theory explains the expanding Universe, cosmic background radiation called CMB, and light-element abundance. The light-element abundance is calculated by using only well-known physics such as the quantum electrodynamics, weak interactions, and nucleosynthesis. The initial condition is the Universe filled with the hot plasma with some abundance of baryon asymmetry. The resulting amount of light-element abundance thus depends on the initial baryon asymmetry. In this subsection, we briefly explain the BBN theory and estimate deuterium (D) and helium (^{4}He) abundance following Ref. [36]. We then compare the results with observed abundance, which gives us information of initial baryon abundance.

Suppose that the Universe is filled with a hot plasma with a temperature higher than 1 MeV and below the QCD scale. At such a high temperature, there are protons and neutrons, where the weak interaction $p + e \leftrightarrow n + \nu_e$ is in the thermal equilibrium. The ratio

of their number densities at a temperature of T is given by

$$\frac{n_n}{n_p} = \exp\left(-\Delta m/T\right) \tag{2.7}$$

$$\Delta m \equiv m_n - m_p \simeq 1.293 \text{ MeV}, \tag{2.8}$$

where m_p ($\simeq$ 938.272 MeV) and m_n ($\simeq$ 939.565 MeV) are proton and neutron masses, respectively [7]. The weak interaction freezes out at the temperature of T_f given by $\Gamma(T_f) \simeq H(T_f)$, where $\Gamma(T_f) \approx G_F^2 T^5$ is the reaction rate of weak interaction and $G_F \simeq 1.17 \times 10^{-5}$. We obtain

$$T_f \sim \left(G_F^2 M_{\rm Pl}\right)^{-1/3} \sim 0.8 \text{ MeV}. \tag{2.9}$$

The ratio of number densities is fixed at this time such as $n_n/(n_p + n_n) \simeq 1/6$. After that, the neutron abundance decreases via its decay and we obtain

$$\frac{n_n}{n_p + n_n} \simeq \frac{1}{6} \exp\left[-\frac{t - t_f}{\tau_n}\right], \tag{2.10}$$

where τ_n ($\simeq$ 880 sec) is the lifetime of neutron [7]. Since the ratio of number densities is determined by this relation, their number densities are determined once we set the baryon abundance, i.e., their total abundance. Note that neutrons do not decay after deuterium formation.

Next we estimate deuterium abundance. We can understand the reactions of nucleosynthesis by minimizing the Hermhortz free energy $F = E - TS$, where E is energy and S is entropy. At a high temperature, protons and neutrons, whose binding energy is about 2.2 MeV, move independently so that the entropy can be small. As the temperature decreases due to the expansion of the Universe, deuteriums form because of the energy loss of their binding energy:

$$p + n \rightarrow {\rm D} + \gamma. \tag{2.11}$$

The binding energy of deuterium is 2.2 MeV, so that their abundance is related as

$$\frac{n_{\rm D}}{n_n n_p} = \frac{3}{4}\left(\frac{4\pi}{m_p T}\right)^{3/2} e^{2.2 \text{ MeV}/T}, \tag{2.12}$$

by the detailed balance. Using $n_n \sim n_p \sim n_b$ and the photon number density of $n_\gamma \sim T^3$, we rewrite this as

$$\frac{n_D}{n_b} \sim \eta_b \left(\frac{T}{m_p}\right)^{3/2} e^{2.2 \text{ MeV}/T}, \tag{2.13}$$

where $\eta_b \equiv n_b/n_\gamma$ is the baryon-to-photon ratio. Deuteriums form at a much low temperature than the energy scale of the binding energy because photons are much abundant than protons (i.e., $\eta_b \ll 1$). The deuterium abundance is sufficiently generated at the time when $n_D \approx n_b$, or, at the temperature of

$$T = T_{\rm D} \simeq 0.06 \text{ MeV} \left(1 + 0.03 \text{ Log}\eta_{10}\right), \tag{2.14}$$

where $\eta_{10} \equiv \eta_b/10^{-10}$. This corresponds to the time of

$$t = t_{\rm D} \simeq 200 \sec \left(1 - 0.06 \text{ Log}\eta_{10}\right) \left(\frac{3.36}{g_*}\right)^{1/2}. \tag{2.15}$$

For a very rough estimation, we could assume that deuteriums are generated at this time and then combine into heavier elements ^{3}H and ^{3}He:

$$\begin{aligned} {\rm D} + {\rm D} &\rightarrow {}^3{\rm H} + p & (2.16)\\ {\rm D} + {\rm D} &\rightarrow {}^3{\rm He} + n. & (2.17) \end{aligned}$$

In this assumption, the Boltzmann equation of deuterium is approximately written as [36]

$$\begin{aligned} \frac{{\rm d}X_{\rm D}}{{\rm d}t} &= -\frac{1}{2}\langle\sigma v\rangle_{\rm DD} n_B X_{\rm D}^2, & (2.18)\\ \langle\sigma v\rangle_{\rm DD} &\simeq 82 \text{ GeV}^{-2} T_9^{-2/3} \exp\left(-4.258/T_9^{1/3}\right) & (2.19)\\ &\simeq 0.86 \text{ GeV}^{-2} \qquad \text{for} \quad T = 0.06 \text{ MeV}, & (2.20) \end{aligned}$$

where $X_D \equiv 2n_D/n_B$ is the mass fraction of deuterium. Once we approximate the cross section as a constant value with $T = 0.06$ MeV ($T_g \simeq 0.7$), we can calculate the deuterium abundance such as

$$\begin{aligned} X_{\rm D} &\simeq 1.2 \times 10^{-4} \frac{\sqrt{g_*}}{g_{*s}} \frac{10^{-10}}{Y_b} & (2.21)\\ &\simeq 5.6 \times 10^{-5} \frac{10^{-10}}{Y_b}, & (2.22) \end{aligned}$$

where $Y_b \equiv n_b/s$ and g_{*s} is the effective degrees of freedom of relativistic particles for entropy density. We have used $g_* = 3.36$ and $g_{*s} = 3.91$ in the second line. Note that $s = 7.04 n_\gamma$ (i.e., $Y_b = \eta_b/7.04$) at present. The deuterium mass fraction is inversely proportional to the initial baryon abundance. This is because the deuterium abundance is determined by its cross section and is almost independent of its initial abundance.

We can easily estimate ^{4}He abundance. It is so stable that we can assume that all neutrons are contained in ^{4}He. Thus we obtain

$$X_{^4\mathrm{He}} \equiv \frac{4n_{^4\mathrm{He}}}{n_b}, \tag{2.23}$$

$$\simeq \left.\frac{2n_n}{n_p+n_n}\right|_{T=T_\mathrm{D}} \tag{2.24}$$

$$\simeq 0.25 + 0.005 \ \mathrm{Log}\ \eta_{10}. \tag{2.25}$$

For larger baryon asymmetry, the temperature of deuterium formation increases, so that more neutrons are contained in nucleons before they decay. As a result, ^{4}He abundance increases as baryon asymmetry increases.

Here let us compare the above results with observations. Aver *et al.* reported ^{4}He abundance such as [3]

$$X_{^4\mathrm{He}}^{(\mathrm{obs,Aver})} = 0.2465 \pm 0.0097. \tag{2.26}$$

It was also reported by Izotov *et al.* such as [4]

$$X_{^4\mathrm{He}}^{(\mathrm{obs,Izotov})} = 0.2551 \pm 0.0022. \tag{2.27}$$

Observed deuterium abundance is usually expressed by the ratio of number densities of deuterium and hydrogen:

$$\mathrm{D/H} = \frac{X_\mathrm{D}}{2X_\mathrm{H}} \tag{2.28}$$

$$\simeq \left. X_\mathrm{D}\frac{n_p+n_n}{2(n_p-n_n)}\right|_{T=T_\mathrm{D}} \approx 0.4X_\mathrm{D}. \tag{2.29}$$

It is measured such as [5]

$$(\mathrm{D/H})^{(\mathrm{obs})} = (2.53 \pm 0.04) \times 10^{-5}. \tag{2.30}$$

These observed values can be explained by the above rough estimation with the baryon asymmetry of order $Y_b = \mathcal{O}(10^{-10})$. More detailed calculations show that observations of light element abundance imply the baryon abundance of

$$\Omega_b^{(\mathrm{BBN})}h^2 = 0.02202 \pm 0.00046, \tag{2.31}$$

which can be rewritten as

$$Y_b^{(\mathrm{BBN})} = (8.33 \pm 0.17) \times 10^{-11}. \tag{2.32}$$

2.1.2 CMB temperature anisotropies

The CMB temperature anisotropies also have information of baryon abundance at the time of recombination epoch. Since protons, electrons, and photon interact strongly before the recombination epoch, they behave like fluid. There is a typical frequency for their density perturbation, which is related to the sound velocity. Since the sound velocity is smaller for larger baryon abundance, the typical frequency for density perturbation becomes larger. In addition, the free-streaming length of photon is inversely proportional to the number density of electrons, so that the length scale of damping due to its free-streaming, called the Silk damping, is smaller for larger baryon abundance. The observed CMB temperature anisotropies therefore give us information of baryon abundance and it is given by [6]

$$\Omega_b^{(\mathrm{CMB})} h^2 = (0.02222 \pm 0.00023). \tag{2.33}$$

This remarkably agrees to the results of the BBN theory and observations of light-element abundances [see Eq. (2.31)].

In this thesis, we use the following values reported in Ref. [7]:

$$Y_b^{(\mathrm{obs})} = 8.6 \times 10^{-11} \tag{2.34}$$

$$\Omega_b^{(\mathrm{obs})} h^2 = 0.0227. \tag{2.35}$$

2.1.3 Sakharov conditions

In order to generate baryon asymmetry, we need to satisfy the Sakharov conditions [16]. First, we need a reaction that violates baryon number conservation. Otherwise the time evolution of baryon number vanishes:

$$\dot{n}_b \propto \left[\hat{H}, \hat{B}\right] = 0, \tag{2.36}$$

where $\hat{H}$ and $\hat{B}$ are operators of Hamiltonian and baryon charge, respectively. Secondly, we need C and CP violations, where C is the charge conjugate symmetry and P is the parity. This is because if C (CP) is conserved, the reaction rate for baryon production is the same with that C (CP) conjugated, which produce anti-baryon. Thus the net baryon asymmetry cannot be generated in C or CP conserving theory. The third condition is realization of departure from thermal equilibrium. If the baryon violating interaction is in

thermal equilibrium, the density matrix can be written as $e^{-\hat{H}/T}$. In this case, we obtain

$$\begin{aligned}
\left\langle \hat{B} \right\rangle &= \mathrm{Tr}\left[e^{-\hat{H}/T} \hat{B} \right], && (2.37)\\
&= \mathrm{Tr}\left[e^{-\hat{H}/T} \hat{B} (CPT)(CPT)^{-1} \right], && (2.38)\\
&= -\mathrm{Tr}\left[e^{-\hat{H}/T} (CPT) \hat{B} (CPT)^{-1} \right], && (2.39)\\
&= -\mathrm{Tr}\left[(CPT) e^{-\hat{H}/T} \hat{B} (CPT)^{-1} \right], && (2.40)\\
&= -\mathrm{Tr}\left[e^{-\hat{H}/T} \hat{B} \right], && (2.41)\\
&= 0, && (2.42)
\end{aligned}$$

where T is the time-reversal. Thus we need non-equilibrium process to generate baryon asymmetry.

The baryon number is violating in the SM due to anomaly [37, 38]:

$$\partial_\mu j^\mu_B = \partial_\mu j^\mu_L = n_f \left(\frac{g_2^2}{64\pi^2} \epsilon_{\mu\nu\sigma\rho} (W^{\mu\nu})^a (W^{\sigma\rho})^a - \frac{g_1^2}{64\pi^2} \epsilon_{\mu\nu\sigma\rho} (F^{\mu\nu})(F^{\sigma\rho}) \right), \tag{2.43}$$

where n_f is the number of family, g_1 and g_2 are the gauge couplings of $U(1)_Y$ and $SU(2)$, respectively, and $(F^{\mu\nu})$ and $(W^{\mu\nu})^a$ are their field strength tensors. The baryon violating process requires a tunnelling effect associated with instanton and its rate is exponentially suppressed at the vacuum [39]. At a higher temperature than the electroweak scale, on the other hand, the process is efficient and in thermal equilibrium due to thermal effect called sphaleron effect [40, 20]. Since $B + L$ number is washed out via the sphaleron effect, we need a $B - L$ violating interaction to realize baryogenesis at higher temperature than the electroweak scale. Therefore, the first Sakharov condition is rephrased such that we need a reaction violating $B - L$ asymmetry to generate baryon asymmetry at higher temperature than the electroweak scale. By the detailed valance, resulting baryon asymmetry is related to $B - L$ asymmetry such as [41]

$$n_b \simeq \frac{8}{23} n_{B-L}, \tag{2.44}$$

at higher temperature than the electroweak scale in SUSY theories. Note that when we aim to generate baryon asymmetry after the electroweak symmetry breaking, we still need a baryon violating process rather than the $B - L$ violating one.

2.2 DM

The idea of DM is first proposed by Zwicky, motivated by the unexpected high velocities of nebulae in the Coma cluster [42]. Then, in 1978, Rubin *et al.* found that the rotation curve of velocity distribution around galaxies becomes constant with increasing distance from their galaxy center [43]. This behavior cannot be explained by the energy density of visible matter around the galaxies, while an uniformly distributing DM can. Gravitational lensing measurements give a further hint for the existence of DM [44, 45]. Trajectory of light is deformed by the gravitational lensing effect, which results in the deformation of observable's image. The mass distribution can be reconstructed via observations of such deformed images and it reveal that there must be energy density other than luminous objects. In particular, mass distribution reconstructed around galaxy-cluster collisions is separated from luminous gas clouds. This indicates that DM is collisionless (see, e.g., Ref. [46]).

The observations of CMB temperature anisotropies reveal that the plasma is homogeneous within of order 10^{-5} at the recombination epoch. If there was no DM, the density perturbation of baryons, which are tightly coupled with photons, cannot develop to form large scale structures because of the lack of time after the recombination. In addition, its density perturbation is smoothed out by the free-streaming of baryon-photon plasma before the recombination and the density perturbations are smoothed out for the scale of galaxies. These problems can be addressed when we introduce DM. Since DM is non-baryonic, the evolution of its density perturbation is different from that of baryons. In particular, DM is decoupled from photons, so that its density perturbation can develop before the recombination epoch and its diffusion length is smaller than that of baryons.

If DM is relativistic at present, it is called hot DM. In this case, density perturbations are smoothed out for the scale of superclusters so that the large scale structure of the Universe forms by fragmentation, where superclusters form first and subsequently fragment into smaller objects. This disagrees with the observed large scale structure. On the other hand, when DM is non-relativistic, i.e., when DM is cold, the large scale structure forms hierarchically, where smaller objects form first and then cluster into larger ones. This scenario agrees with observations very well. This implies that DM is cold, and in particular, relativistic neutrinos cannot play its role [47]. Therefore we need new physics beyond the SM to account for DM.

The CMB temperature anisotropies are affected by the contents of the Universe. While baryons are tightly coupled with photons, DM is decoupled from these particles. The gravitational potential of DM with density perturbations gives rise to the characteristic oscillation

pattern in the spectrum of CMB temperature anisotropies. If the DM abundance is less than that observed, the epoch of matter-radiation equality becomes close to the recombination epoch. As a result, the peak height of the spectrum of CMB temperature anisotropies is lower for less DM abundance. In addition, since the gravitational potential well is not constant, the integrated Sacks-Wolfe effect contributes more significant to the final anisotropy spectrum than the case withe larger DM abundance. The results of Planck measurement are given as [6]

$$\Omega_{\rm DM}h^2 = 0.1197 \pm 0.0022. \tag{2.45}$$

This can be rewritten as

$$\frac{\rho_{\rm DM}}{s} \simeq (3.55\ {\rm eV}) \times \Omega_{\rm DM}h^2, \tag{2.46}$$

$$\simeq (0.425 \pm 0.008)\ {\rm eV}. \tag{2.47}$$

To construct a consistent cosmological scenario, it is necessary to account for the above DM density as well as the baryon density.

2.3 Inflation

Inflation solves some initial condition problems in the Big Bang cosmology, including the flatness problem and the horizon problem. It can be realized by a potential of a scalar field called an inflaton when it is specially homogeneous and slowly rolls towards its potential minimum. After the slow roll ends, the inflaton starts to oscillate around its potential minimum and then decay into radiation. The resulting Universe is then consistent with the Big Bang theory. Here we shortly explain the motivation of inflation while in Appendix B we briefly explain inflation, its realization by a scalar field, reheating, and its predictions.

If the curvature of the Universe K is nonzero, the Friedmann equation is written as

$$H^2 = \frac{\rho}{3M_{\rm Pl}^2} - \frac{K}{a^2}, \tag{2.48}$$

where ρ is the total energy density of the Universe, a is the scale factor, and $M_{\rm Pl}$ ($\simeq 2.4 \times 10^{18}$ GeV) is the reduced Planck scale. The parameter K is bounded above by the observation of CMB temperature anisotropies such as $|\Omega_K| \equiv |K|/(a_0^2H_0^2) \lesssim 0.01$, where a_0 and H_0 are the scale factor and the Hubble parameter at present. However, the curvature term in the Friedmann equation is proportional to a^{-2}, so that the combination of $|K|/a^2H^2(t)$ has to be

extremely smaller than unity in the early Universe. Such an extremely small dimensionless parameter is a mystery known as the flatness problem.

The observations of CMB temperature anisotropies show that the background temperature of the Universe is homogeneous up to a factor of of order 10^{-5}. However, if the Universe begins from the radiation or matter dominated era, there is no correlation for the whole observable Universe. There is no reason that the whole Universe is homogeneous without correlations. This is known as the horizon problem.

The above flatness and horizon problems are explained by an era of exponential explanation called inflation. Suppose that the early Universe is dominated by a constant energy density. In this case, the Friedmann equation implies that $H = H_{\rm inf} = $ const. and the scale factor exponentially increases such as $a(t) = a(t_{\rm ini}) \exp[H_{\rm inf}(t - t_{\rm ini})]$, where $t_{\rm ini}$ is the time at the beginning of inflation. Therefore the curvature term in the Friedmann equation decreases exponentially compared with the constant energy term, which explains the smallness of the curvature term. Note that the Hubble-horizon length is given by $a(t_{\rm ini})H(t_{\rm ini})$ at the beginning of inflation. The volume of this correlated region exponentially increases due to inflation, so that it explains the homogeneous Universe. Finally, the constant energy density is converted to radiation at a time denoted by $t_{\rm end}$. When we define e-folding number such as $N(t) \equiv \log\left(a(t_{\rm end})/a(t)\right)$, $N(t_{\rm ini}) \approx 50 - 60$ is sufficient to solve those problems.

Inflation can be realized by a potential energy of a scalar field called inflaton. The quantum fluctuations of inflaton during inflation is a seed of large scale structure. In particular, the observations of CMB temperature anisotropies give us information of density perturbations and confirm predictions of inflation models (see Appendix B for a short review). Unfortunately, inflation washes out baryon asymmetry and DM. Therefore we need mechanisms to generate them after inflation.

2.4 Discussion

Here let us consider some solutions to the origin of baryon asymmetry and DM.

The thermal leptogenesis is a simple mechanism to generate baryon asymmetry via the decay of heavy right-handed neutrinos and the $B + L$ violating sphaleron process [21]. It can be realized when the mass of the lightest right-handed neutrino is larger than of order 10^9 GeV and the reheating temperature of the Universe after inflation is larger than its mass (see, e.g., Ref. [48]). Unfortunately, such a high reheating temperature may be inconsistent with the gravitino and/or LSP overproduction problem in SUSY theories, unless the gravitino mass is larger than of order 100 TeV and the LSP mass is sufficiently small [49, 50]. The

electroweak baryogenesis is another candidate of baryogenesis, where the baryon asymmetry is generated via the sphaleron process in front of bubble of Higgs phase transition [20]. This requires a modification of Higgs potential to realize a first-order electroweak phase transition, so that it is expected that some signals are observed in collider experiments in the near future. However, it might be inconsistent with the experiments of the neutron electric dipole moment unless we allow some amount of cancellation in CP phases.

The relic density of DM can be explained by freeze-out mechanism when the DM is a weakly-interacting massive particle (WIMP). The WIMP is thermal equilibrium in the hot plasma and then decoupled at a temperature below its mass. Its annihilation cross section determines its relic density, which is of order the observed amount of DM for the WIMP with mass of order the electroweak scale. It is motivated also by particle physics, such as supersymmetric theories. However, the non-observation of new physics at the LHC puts questions on this scenario because there should be new particles around the electroweak scale.

Here let us reconsider the baryon and DM abundance. From Eqs. (2.35) and (2.45), we obtain the baryon-to-DM ratio such as

$$\frac{\Omega_b}{\Omega_{\rm DM}} \simeq \frac{1}{5} = \mathcal{O}(1). \tag{2.49}$$

Therefore, there is a coincidence between the energy densities of baryon and DM. This coincidence may imply that the baryon and DM are generated from a common origin. However, the above mechanisms generate baryon asymmetry and DM independently, so that they cannot explain the coincidence.

In this thesis, we focus on another mechanism to generate baryon asymmetry called the Affleck-Dine baryogenesis (ADBG). It is based on SUSY theories, where SUSY partners of quarks called squarks are introduced. The ADBG generates baryon asymmetry via the dynamics of squarks in the early Universe, which subsequently decay and release their baryon charge into SM particles. Here, in SUSY, the lightest SUSY particle (LSP) is stable and is good candidate of DM when we assume R-parity conservation. Therefore, the decay of squarks may be a non-thermal source of DM in the scenario of ADBG. This fact may result in a coincidence between the resulting energy density of baryon and DM. In Chap. 5 and 8, we show that ADBG can in fact account for the coincidence problem as well as the observed baryon asymmetry.

Chapter 3

Affleck-Dine baryogenesis

In this chapter, we review the conventional scenario of Affleck-Dine baryogenesis (ADBG).

3.1 Overview of ADBG

Before we explain the detail of the ADBG, in this section we overview its mechanism. In supersymmetric (SUSY) theories, baryon asymmetry can be generated by ADBG using a $B-L$ charged flat direction called an AD field [17, 19]. The AD field is assumed to have a negative effective mass term, called a Hubble-induced mass term, due to a finite energy density of the Universe via supergravity effects, which implies that it obtains a large VEV during and after inflation. As the energy density of the Universe decreases, the effective mass decreases. Eventually, the effective mass becomes comparable to the soft mass of the AD field, and then the AD field starts to oscillate around the origin of its potential, whose dynamics is far from thermal equilibrium. Non-renormalizable terms, which break B (or $B-L$) symmetry in general, are relevant for the dynamics of the AD field due to its large initial amplitude. The difference between the initial phase of the AD field and the phase in the potential minimum (along a nonzero VEV) leads to CP violation. In this way, the Sakharov conditions for baryogenesis [16] are satisfied and B (or $B-L$) asymmetry is generated. In fact, its phase direction is kicked by its non-renormalizable A-term potential at the beginning of oscillation. The asymmetry is actually generated through this dynamics because the $B-L$ number density is proportional to the phase velocity of the AD field. Note that the amplitude of the oscillation decreases due to the Hubble expansion, the non-renormalizable terms becomes irrelevant and B (or $B-L$) symmetry is approximately restored soon after the beginning of oscillation. Finally, the coherent oscillation of the AD field decays and dissipates into the thermal plasma. If the AD field releases its charge into the standard model particles after

the sphaleron process [20] freezes out, the AD field should have B charge to account for the baryon asymmetric Universe. On the other hand, if the AD field releases its charge before the sphaleron process freezes out, the AD field should have $B-L$ charge so that the sphaleron process does not wash out the asymmetry.

3.2 Flat directions in the MSSM

In SUSY theories, there are SUSY partners of quarks and leptons, called squarks and sleptons, which are complex scalar fields carrying $B-L$ charges. Let us consider one of them and denote it as ϕ. When we write its $B-L$ charge as q, the number density of $B-L$ asymmetry associated with ϕ is written as

$$n_{B-L} = iq\left(\dot{\phi}^*\phi - \phi^*\dot{\phi}\right) = 2q\mathrm{Im}\left[\phi^*\dot{\phi}\right]. \tag{3.1}$$

This implies that we can obtain a large amount of $B-L$ asymmetry when the field ϕ rotates in the complex plane with a large amplitude. Thus we focus on a $B-L$ charged scalar field that has a very flat potential. In fact, the potentials for scalar fields are severely restricted by SUSY, which especially results in existence of many flat directions. Flat directions are scalar fields whose potentials are absent within the renormalizable level as long as SUSY is unbroken.

Here, we illustrate how the potentials for scalar fields are absent in SUSY theories by taking a flat direction called the $u^c d^c d^c$ flat direction as an example. Let us focus on a scalar field constructed by right-handed squarks through the following orthogonal matrix:

$$\begin{pmatrix} \phi \\ \cdot \\ \cdot \end{pmatrix} = \frac{1}{\sqrt{3}} \begin{pmatrix} 1 & 1 & 1 \\ & \cdot & \\ & \cdot & \end{pmatrix} \begin{pmatrix} (u^c)_1^R \\ (d^c)_1^G \\ (d^c)_2^B \end{pmatrix}, \tag{3.2}$$

where the lower and upper indices represent flavour and color, respectively. The dots represent other directions, which we are not interested in. Since the inverse matrix is given by the transposed matrix, we obtain

$$\begin{pmatrix} (u^c)_1^R \\ (d^c)_1^G \\ (d^c)_2^B \end{pmatrix} = \frac{1}{\sqrt{3}} \begin{pmatrix} 1 & & \\ 1 & \cdot & \cdot \\ 1 & & \end{pmatrix} \begin{pmatrix} \phi \\ \cdot \\ \cdot \end{pmatrix}. \tag{3.3}$$

In the MSSM, the superpotential is given by Eq. (A.7) within the renormalizable level. F-term potentials are determined by superpotential W as

$$V_F(\phi) = \sum_i \left|\frac{\partial W}{\partial \varphi_i}\right|^2, \tag{3.4}$$

where φ_i generically denote the fields in W. It is easy to see that the F-term potential for the field ϕ is absent. The D-term potential is also absent like

$$|D_3^a|^2 = g_3^2 \left|(u^c)_1^{R*} T^a (u^c)_1^R + (d^c)_1^{G*} T^a (d^c)_1^G + (d^c)_2^{B*} T^a (d^c)_2^B\right|^2 \tag{3.5}$$

$$= \frac{g_3^2}{9}|\phi|^4 \left|\mathrm{Tr}\,(T^a)\right|^2 = 0, \tag{3.6}$$

$$|D_1|^2 = \left|-\frac{2}{3}\left|(u^c)_1^R\right|^2 + \frac{1}{3}\left|(d^c)_1^G\right| + \frac{1}{3}\left|(d^c)_2^B\right|\right|^2 = 0, \tag{3.7}$$

where $|D_3^a|^2$ and $|D_1|^2$ are D-term potentials for $SU(3)$ and $U(1)_Y$, respectively. Therefore, the field ϕ has a flat potential and is called a flat direction. The above example consists of right handed squarks of u^c, d^c, d^c, and is called the $u^c d^c d^c$ flat direction. It is known that every flat direction is characterized by gauge-invariant monomial in this manner.

The following combination is another famous example of flat directions called LH_u flat direction [18]:

$$L_i = \frac{1}{\sqrt{2}}\begin{pmatrix} 0 \\ \phi \end{pmatrix}, \quad H_u = \frac{1}{\sqrt{2}}\begin{pmatrix} \phi \\ 0 \end{pmatrix}, \tag{3.8}$$

where L and H_u are left-handed slepton and up-type Higgs, respectively. The directions in the MSSM are listed in Table. 3.1 with their $B-L$ and B charges [51].[1] Note that there are many flat directions even in such a simple model. It is expected that the dynamics of such a flat direction can generate a large amount of $B-L$ asymmetry. Hereafter, we call a B (or $B-L$) charged flat direction as an AD field and investigate its dynamics in the early Universe.

Although flat directions have no potential within the exact SUSY limit and the renormalizable level, they obtain nonzero potentials through SUSY breaking and nonrenormalizable operators (i.e., underlying higher energy theory). These potentials induce non-trivial dynamics of flat directions. The next section is devoted to discussing this point.

3.3 Potentials for flat directions

In this section, we discuss the induced potentials for flat directions through SUSY breaking, thermal effect, and nonrenormalizable operators. Flat directions have soft (SUSY breaking) masses of the order of sparticle masses, which are subject to collider experiments and should

[1] Although LH_u flat direction has a potential coming from the Higgs μ-term, it is assumed that μ is of order the soft mass scale and absorb it to the meaning of m_ϕ [see Eq. (3.9)].

Table 3.1: Flat directions in the MSSM and their $B-L$ and B charges [51].

flat directions	$B-L$	B
LH_u	-1	0
H_uH_d	0	0
$u^cd^cd^c$	-1	-1
LLe^c	-1	0
Qd^cL	-1	0
$QQQL$	0	1
Qu^cQd^c	0	0
Qu^cLe^c	0	0
$u^cu^cd^ce^c$	0	-1
$d^cd^cd^cLL$	-3	-1
$u^cu^cu^ce^ce^c$	1	-1
$Qu^cQu^ce^c$	1	0
$QQQQu^c$	1	1
$(QQQ)_4LLLe^c$	-1	1
$u^cu^cd^cQd^cQd^c$	-1	-1

be larger than $\mathcal{O}(10^{2\text{-}3})$ GeV [52, 53]. In addition, the finite energy density of the Universe contributes to potentials for flat directions. For instance, scalar fields obtain so-called Hubble induced terms through supergravity effects during inflation because inflation is driven by a finite energy density [19]. This is also the case during the inflaton oscillation dominated era as we explain in Sec. 3.3.2. In a finite temperature plasma, flat directions acquires thermal potentials due to thermal effects [19, 54, 55, 56]. Finally, when a flat direction has a large VEV, nonrenormalizable operators become important.

3.3.1 Soft terms

In low energy, the AD field obtains soft terms coming from the low-energy SUSY breaking effect. In gravity-mediated SUSY breaking models, soft terms of the AD field is given by [see Eq. (A.37)]

$$V_{\rm soft} = m_\phi^2(\phi)\left|\phi\right|^2 + am_{3/2}W^{(\rm AD)} + \text{c.c.}, \tag{3.9}$$

where m_ϕ is the soft mass of the AD field, $m_{3/2}$ is gravitino mass, and a ($=\mathcal{O}(1)$) is a constant. The higher-dimensional superpotential of the AD field $W^{(\rm AD)}$ is determined below.

Note that not only soft masses but μ-term can also contribute to m_ϕ if the flat direction consists of Higgs field.

In models of gravity-mediated SUSY breaking, the soft mass is approximately constant such as

$$m_\phi(\phi) \simeq m_\phi, \tag{3.10}$$

where m_ϕ is roughly of order the gravitino mass [see Eq. (A.37)]. We take into account the renormalization running effect in the next chapter but we neglect it for simplicity in this chapter. On the other hand, in models of gauge-mediated SUSY breaking, SUSY breaking in a hidden sector is transmitted to the standard model sector by gauge interactions mediated by a messenger sector.[2] Since the AD field has some gauge charge, gauge fields acquire effective masses of the order of $g|\phi|$, where g generically stands for the Standard Model gauge coupling. The transmission of SUSY breaking effect is therefore suppressed for $g|\phi| \gg M_m$, where M_m is a messenger scale [57], and thereby the soft mass of the AD field is suppressed. The following potential is well fitted with an analytical result [see Eqs. (A.51) and (A.58)]:

$$m_\phi^2(\phi)|\phi|^2 = \begin{cases} m_\phi^2|\phi|^2 & \text{for } g|\phi| \ll M_m \\ M_F^4 \left[\log \frac{g^2|\phi|^2}{M_m^2}\right]^2 & \text{for } g|\phi| \gg M_m. \end{cases} \tag{3.11}$$

A parameter M_F^2 is proportional to the VEV of the F component of a gauge-singlet chiral multiplet in the messenger sector as

$$M_F^2 = \frac{m_\phi^2 M_s^2}{g^2} = \frac{gy}{(4\pi)^2}\langle F_s \rangle, \tag{3.12}$$

where y is a coupling constant for the interaction between the gauge singlet chiral multiplet and the messenger field [see Eq. (A.42)]. The mass of the gravitino is related to the SUSY breaking F-term as

$$\langle F_s \rangle = k\sqrt{3} m_{3/2} M_{\rm Pl}, \tag{3.13}$$

$$k \leq 1, \tag{3.14}$$

where a factor k is less than one when the messenger sector indirectly couple to the SUSY breaking sector. Hereafter we redefine the combination of yk as k ($\lesssim 1$).

[2]Here we implicitly assume that the AD field is not identified with LH_u flat direction. It has a SUSY mass from the Higgs μ term, which is not suppressed above the messenger scale.

The above potential can be understood as follows. Since soft masses are proportional to the SUSY breaking parameter F_s, $m_\phi^2 \propto |F_s|^2$. From the dimensional analysis, its proportionality coefficient is given as $m_\phi^2(\mu^2) \sim |F_s|^2/\mu^2$ at the energy scale of μ that is higher than the messenger scale. Since we consider the potential of the AD field, μ should be replaced by ϕ, so that we obtain a suppressed mass term such as $m_\phi^2(\phi^2)|\phi|^2 \sim |F_s|^2$. Note that in gravity mediated SUSY breaking models, the cutoff scale is of order the Planck scale and $m_\phi^2 \sim |F_s|^2/M_{\rm Pl}^2$, so that there is no suppression up to the Planck scale.

3.3.2 Hubble-induced terms

During and after inflation, the AD field obtains effective potentials from the energy density of inflaton I via supergravity effects [19]. The potential for a flat direction ϕ is modified by supergravity effects during and after inflation. The energy density of the Universe is so large that we have to consider its effects on the potential for the flat direction. In the supergravity, scalar potentials are written in terms of superpotential, W, and Kähler potential, K. The potential of scalar fields is written as Eq. (A.29).

We introduce an inflaton I and treat it as a background field. As explained in Appendix B, the potential energy of inflaton drives inflation. We assume that the F-term potential of I drives inflation and satisfies $|W_I|^2 \simeq 3H_{\rm inf}^2 M_{\rm Pl}^2$, where $H_{\rm inf}$ is the Hubble parameter during inflation. We consider a Kähler potential of

$$K = |\phi|^2 + |I|^2 + \frac{c}{M_{\rm Pl}^2}|\phi|^2|I|^2, \tag{3.15}$$

where c is an $O(1)$ constant. In this case, the supergravity potential of Eq. (A.29) includes the following interaction:

$$V \supset \exp\left(\frac{K}{M_{\rm Pl}^2}\right) W_I (K^{I\bar{I}})^{-1} W_I^* \tag{3.16}$$

$$\simeq |F_I|^2 \left(1 + (1-c)\frac{|\phi|^2}{M_{\rm Pl}^2}\right), \tag{3.17}$$

where we assume $\langle\phi\rangle, \langle I\rangle \ll M_{\rm Pl}$ and neglect irrelevant higher-dimensional terms. Thus the AD field ϕ obtains an effective mass term of order the Hubble parameter during inflation:

$$V_H = c_H H_{\rm inf}^2 |\phi|^2 \tag{3.18}$$

$$c_H = -3(c-1), \tag{3.19}$$

where we use $|F_I|^2 = 3H_{\rm inf}^2 M_{\rm Pl}^2$. This is called a Hubble-induced mass term.

If there is a Kähler potential of $I|\phi|^2/M_{\rm Pl} + c.c.$, it leads to a Hubble-induced A-term such as

$$\left(\frac{-\lambda a_H}{nM_{\rm Pl}^{n-3}} H\phi^n + c.c.\right), \tag{3.20}$$

where a_H is an $\mathcal{O}(1)$ constant. However, the above Kähler potential is absent and the Hubble-induced A-term is suppressed when the field which has a non-zero F-term during inflation is charged under some symmetry and its VEV is less than the Planck scale during inflation [58]. These conditions are satisfied for models of hybrid inflation [59, 60] and high-scale inflation in supergravity [61, 62] and thus we set $a_H = 0$ in this thesis. Note that other small A-terms play important roles in our new scenario of ADBG explained in Chap. 7 though they do not in the conventional scenario explained in this chapter.

After inflation ends, the inflaton starts to oscillate around the potential minimum and its oscillation energy dominates the Universe. During this inflaton-oscillation dominated era, the Hubble-induced mass comes also from higher-dimensional kinetic interactions, which are determined by the Kähler potential as

$$\mathcal{L}_{\rm kin} = K_{i\bar{j}}\partial_\mu\phi^i\partial^\mu\phi^{*j}, \tag{3.21}$$

where ϕ_i generically represents the fields of ϕ and I. There is a kinetic interaction of

$$\mathcal{L}_{\rm kin} \supset K_{I\bar{I}}\left|\dot{I}\right|^2 \supset \frac{c}{M_{\rm Pl}^2}\left|\dot{I}\right|^2|\phi|^2. \tag{3.22}$$

A typical time scale of the dynamics of the AD field is at most of order the Hubble parameter as shown below. That of inflaton is the curvature of its potential, which is larger than the Hubble parameter during inflaton-oscillation dominated era. Thus we can take a time-average over the inflaton-oscillation time scale to investigate the dynamics of the AD field. Assuming that the inflaton oscillates in a quadratic potential after inflation, we obtain an effective Hubble-induced mass for ϕ after inflation:

$$V_H = c_H H^2(t)|\phi|^2 \tag{3.23}$$

$$c_H = -3\left(c - \frac{1}{2}\right), \tag{3.24}$$

where we use the Virial theorem and include the contribution from the F-term potential.[3]

[3] Inflation may be driven by a D-term potential of inflaton [63, 64]. In this case, the Hubble-induced mass is absent during inflation but the AD field stays at a nonzero VEV due to the Hubble-friction effect [67, 65, 66]. The inflaton obtains nonzero F-term after inflation ends, so that the AD field obtains a Hubble-induced mass during the inflaton oscillation dominated era. Thus the scenario of ADBG and resulting $B-L$ asymmetry are the same with the ones in F-term inflation.

3.3.3 Thermal-log potential

After inflation ends and before reheating completes, inflaton gradually decays into radiation (see Appendix B.4). Therefore, even if the energy density of the Universe is dominated by that of oscillating inflaton, there is a background plasma with temperature of Eq. (B.18). In the finite temperature plasma, the AD field acquires an effective potential via the thermal effect [55, 56]. In this subsection, we explain the origin of thermal-log potential, focusing on LH_u flat direction.

The free energy of the thermal plasma F depends on QCD coupling g_3 in the next-to-leading order as

$$F = \frac{3}{8}(1 + N_f^{(\rm th)}) g_3^2(T) T^4, \tag{3.25}$$

where $N_f^{(\rm th)}$ is the number of family in the thermal plasma. Here, quark multiplets obtain effective masses via the Yukawa interactions when LH_u flat direction has a large VEV [see Eq. (A.7)]. When its VEV is larger than the temperature of the plasma, the renormalization running of g_3 is affected and its value at the energy scale of T depends on the VEV of LH_u flat direction [see Eq. (A.25)]:

$$\frac{\rm d}{{\rm dlog}\mu}\frac{8\pi^2}{g^2} = (3N - F)\,, \tag{3.26}$$

$$g(\mu) = g_0 \left(1 - \frac{g_0^2}{16\pi^2}\left[(3N - F){\rm log}\left(\frac{\mu}{\mu_0}\right)\right]\right), \tag{3.27}$$

where the renormalization scale μ should be replaced by ϕ. When there are ΔF particles that obtain the effective mass larger than the temperature, the renormalization running is given by

$$g(\mu) = g_0 \left(1 - \frac{g_0^2}{16\pi^2}\left\{[3N - F]{\rm log}\left(\frac{\mu}{\mu_0}\right) + \Delta F {\rm log}\left(\frac{\mu}{\phi}\right)\right\}\right). \tag{3.28}$$

Therefore the free energy depends on ϕ and LH_u flat direction acquires a potential depending on temperature. Since the renormalization running has a logarithmic dependence, it is written as [55, 56]

$$V_T(\phi) \simeq c_T \alpha_s^2 T^4 {\rm log}\left(\frac{|\phi|^2}{T^2}\right), \tag{3.29}$$

with $c_T = 45/32$ for $y\,|\phi| \gg T$, where $\alpha_s \equiv g_s^2/4\pi$ and y generically stands for Yukawa couplings for quarks. This is sometimes called thermal log potential.

Note that temperature is given by Eq. (B.18) during the inflaton-oscillation dominated era. Since many MSSM particles are decoupled from the thermal plasma due to the effective mass from the VEV of the AD field, it is calculated as $g_*(T) \simeq 142.5$ before the LH_u flat direction starts to oscillate around the origin of the potential. Assuming that the reheating completes after the oscillation, we obtain $g_*(T_{\rm RH}) = 228.75$.

3.3.4 Higher-dimensional terms

As we explain in the next section, we assume that c_H is negative during and after inflation to realize ADBG. This means that the AD field has a large tachyonic mass and obtains a large VEV during the time of $H(t) \gtrsim m_\phi$. Since the AD field has a large VEV, we have to take into account non-renormalizable terms to investigate its dynamics. Although the superpotential of the AD field is absent within the renormalizable level, it may have a higher-dimensional superpotential such as

$$W^{(\rm AD)} = \lambda \frac{\phi^n}{n M_{\rm Pl}^{n-3}}, \tag{3.30}$$

where n (≥ 4) is an integer depending on flat directions and $M_{\rm Pl}$ ($\simeq 2.4 \times 10^{18}$ GeV) is the reduced Planck scale. For example, since the neutrinos have nonzero masses (denoted as m_{ν_i}), we introduce a superpotential of

$$W^{(LH_u)} = \frac{m_{\nu_i}}{2\langle H_u \rangle^2} (L_i H_u)^2, \tag{3.31}$$

$$\equiv \frac{\lambda}{4M_{\rm Pl}} \phi^4 \qquad \text{for} \qquad \frac{\phi^2}{2} = LH_u, \tag{3.32}$$

where $\langle H_u \rangle = \sin\beta \times 174\,\text{GeV}$ and $\tan\beta \equiv \langle H_u \rangle / \langle H_d \rangle$. Thus LH_u flat direction corresponds to the case of $n = 4$ in Eq. (3.30). In the case of the $u^c d^c d^c$ flat direction, it may come from a term like

$$W = \lambda \frac{(u^c d^c d^c)^2}{6M_{\rm Pl}^3} = \lambda \frac{\phi^6}{6M_{\rm Pl}^3}, \tag{3.33}$$

where we use Eq. (3.3). In this case, the power of superpotential n is 6. The superpotential leads to a F-term potential of ϕ as

$$V_F(\phi) = \lambda^2 \frac{|\phi|^{2n-2}}{M_{\rm Pl}^{2n-6}}, \tag{3.34}$$

where we neglect irrelevant higher-dimensional terms in the supergravity potential.

3.3.5 Summary of this section

Here we summarize the potential for the AD field. It is given by

$$\begin{aligned} V(\phi) &= V_{\rm soft} + V_H + V_F + V_T \qquad (3.35) \\ &= m_\phi^2(\phi)\,|\phi|^2 + a m_{3/2} W^{(\rm AD)} + \text{c.c.} \\ &\quad + c_H H^2(t)\,|\phi|^2 + \lambda^2 \frac{|\phi|^{2n-2}}{M_{\rm Pl}^{2n-6}} + c_T \alpha_s^2 T^4 \log\left(\frac{|\phi|^2}{T^2}\right), \qquad (3.36) \end{aligned}$$

where the soft term $V_{\rm soft}$ depends on SUSY breaking models and is given by Eqs. (3.10) or (3.11). We assume negative Hubble induced mass term ($c_H < 0$) during and after inflation. Hereafter, we set the phase of the AD field and the SUSY-breaking F-term such that $\text{Im}[a] = 0$.

In the next section, we investigate the dynamics of the AD field with the above potential.

3.4 Dynamics of AD fields and baryon asymmetry

In this section, we explain the dynamics of the AD field and calculate $B-L$ asymmetry.

As explained in the previous section, the potential of the AD field is given by

$$\begin{aligned} V(\phi) &\simeq V_H + V_F \qquad (3.37) \\ &= c_H H_{\rm inf}^2\,|\phi|^2 + \lambda^2 \frac{|\phi|^{2n-2}}{M_{\rm Pl}^{2n-6}}, \qquad (3.38) \end{aligned}$$

during inflation, where we assume $H_{\rm inf}^2 \gg |\phi|^{-1} V'_{\rm soft}$ and neglect the soft terms. The coefficient c_H is assumed to be negative so that the AD field has a tachyonic mass and obtains a large VEV. The VEV of the AD field at the potential minimum is given by

$$\langle|\phi|\rangle_{\rm min} \simeq \left(\frac{|c_H|\,H_{\rm inf}^2 M_{\rm Pl}^{2n-6}}{\lambda^2 (n-1)}\right)^{1/(2n-4)}. \qquad (3.39)$$

When we decompose the AD field as $\phi = \varphi e^{i\theta}/\sqrt{2}$, the equations of motion are written as

$$\begin{aligned} \ddot{\varphi} + 3H_{\rm inf}\dot{\varphi} - \dot{\theta}^2\varphi + \frac{\partial V(\varphi)}{\partial \varphi} &= 0 \qquad (3.40) \\ \ddot{\theta} + 3H_{\rm inf}\dot{\theta} + 2\frac{\dot{\varphi}}{\varphi}\dot{\theta} + \frac{\partial V}{\partial \theta} &= 0. \qquad (3.41) \end{aligned}$$

Since $H_{\rm inf}$ is almost constant during inflation, the AD field damps to the potential minimum exponentially fast:

$$|\phi| - \langle|\phi|\rangle_{\rm min} \approx \exp\left[-\frac{3}{2}H_{\rm inf}t\left(1-\sqrt{1-\frac{4\,|c_H|}{9}}\right)\right]. \tag{3.42}$$

The phase direction has a Hubble-friction term ($3H\dot{\theta}$), so that it stays at a certain phase during inflation. We denote the initial phase of the AD field as $\theta_{\rm ini}$, which is expected to be of order unity.

During the inflaton-oscillation dominated era and the time satisfying $H(t) \gg (|\phi|^{-1}\,V'_{\rm soft} + |\phi|^{-1}\,V'_T)^{1/2}$, the potential of the AD field is given by

$$\begin{aligned} V(\phi) &= V_H + V_F & (3.43)\\ &= c_H H^2(t)\,|\phi|^2 + \lambda^2\frac{|\phi|^{2n-2}}{M_{\rm Pl}^{2n-6}}, & (3.44)\end{aligned}$$

where $H(t) = 2/3t$. Here, we redefine the parameters such as [19]

$$\begin{aligned} z &\equiv \log t, & (3.45)\\ \phi &\equiv \chi(z)\left(\frac{4|c_H|}{9(n-1)\lambda^2}\right)^{1/2(n-2)}\left(M_{\rm Pl}^{n-3}e^{-z}\right)^{1/(n-2)}. & (3.46)\end{aligned}$$

Then the equation of motion is written as

$$\ddot{\chi} + \frac{n-4}{n-2}\dot{\chi} - \left(\frac{4|c_H|}{9} + \frac{n-3}{(n-2)^2}\right)\chi + \frac{4|c_H|}{9}\chi^{2n-3} = 0. \tag{3.47}$$

We find that the parameter χ oscillates around the minimum of

$$\chi_0 = \left(1 + \frac{9(n-3)}{4|c_H|(n-2)^2}\right)^{1/2(n-2)}. \tag{3.48}$$

The oscillation amplitude is damped for the case of $n > 4$. Therefore, the AD field follows the potential minimum of Eq. (3.39) with the replacement of $H_{\rm inf} \to H(t)$.

When the Hubble parameter decreases to $(|\phi|^{-1}\,V'_{\rm soft} + |\phi|^{-1}\,V'_T)^{1/2}$, the potential of the AD field is dominated by these terms and it starts to oscillate around the origin of the potential. We write the Hubble parameter at the time of oscillation as

$$H_{\rm osc} \simeq \left(|\phi|^{-1}\,V'_{\rm soft} + |\phi|^{-1}\,V'_T\right)^{1/2}. \tag{3.49}$$

The VEV of the AD field at that time is given by

$$\phi_{\rm osc} \simeq \left(\frac{|c_H|\, H_{\rm osc}^2 M_{\rm Pl}^{2n-6}}{\lambda^2 (n-1)} \right)^{1/(2n-4)} . \tag{3.50}$$

Note that the curvature of the phase direction is given by

$$m_\theta^2 \equiv \frac{1}{\langle\varphi\rangle^2} \frac{\partial^2 V}{\partial \theta^2} \simeq \frac{n|\lambda a_g|}{2^{n/2}} \frac{m_{3/2}\varphi^{n-2}}{M_{\rm Pl}^{n-3}}. \tag{3.51}$$

Since the amplitude of the flat direction decreases as time evolves due to the Hubble expansion, the curvature of the phase direction, which is proportional to some powers of φ, decreases fast. Thus we can estimate the phase velocity of the AD fields such as

$$\dot\theta \approx \frac{m_\theta^2}{H_{\rm osc}} \theta_{\rm ini}. \tag{3.52}$$

This means that the AD field starts to rotate in the phase space, which is the dynamics that generates the $B-L$ asymmetry [see Eq. (3.1)]:

$$\begin{aligned} \frac{a^3(t)}{a^3(t_{\rm osc})} n_{B-L}(t) &= 2\dot\theta\, |\phi|^2 \Big|_{\rm osc} && (3.53) \\ &\equiv \epsilon q H_{\rm osc} \phi^2 && (3.54) \\ \epsilon &\sim \frac{m_\theta^2}{H_{\rm osc}^2} \sin\left(n\theta_{\rm ini}\right), && (3.55) \end{aligned}$$

where $a(t)$ is the scale factor and we define the ellipticity parameter ϵ. Since the $B-L$ density is smaller than the charge times the number density of AD field, ϵ is smaller than unity. The amplitude of the flat direction decreases as time evolves due to the Hubble expansion and the $B-L$ breaking effect (i.e., the A-term) becomes irrelevant soon after the oscillation. Thus, the generated $B-L$ asymmetry within a comoving volume is conserved soon after the AD field starts to oscillate.

In the case that the oscillating AD field decays and dissipates into radiation before the sphaleron process freezes out [68], the sphaleron effect relates the $B-L$ asymmetry to the baryon asymmetry as Eq. (2.44) [20, 21]. We can calculate the resulting baryon-to-entropy ratio Y_b such as

$$\begin{aligned} Y_b &\equiv \frac{n_b}{s} \simeq \frac{8}{23} \frac{n_{B-L}}{s} \Big|_{\rm RH} && (3.56) \\ &\simeq \frac{8}{23} \frac{3 T_{\rm RH} n_{B-L}}{4\rho_{\rm inf}} \Big|_{\rm osc} && (3.57) \\ &\simeq \frac{8}{23} \frac{\epsilon q T_{\rm RH}}{4 H_{\rm osc}} \left(\frac{\phi_{\rm osc}}{M_{\rm Pl}} \right)^2, && (3.58) \end{aligned}$$

where $\rho_{\rm inf}$ ($\simeq 3H^2(t)M_{\rm Pl}^2$) is the energy density of the inflaton and $T_{\rm RH}$ is reheating temperature. On the other hand, in the case that the oscillating AD field decays and dissipates into radiation after the sphaleron process freezes out [68], e.g., in the case that Q-balls form after the oscillation and decay after the sphaleron process freezes out as explained in the next chapter, we should replace the $B-L$ charge q with the B charge q_B and remove the factor of 8/23 to calculate present baryon asymmetry in the above equations.

In the following subsections, we consider the cases that the dynamics is determined by the soft mass term in gravity-mediated and gauge-mediated SUSY breaking models and the thermal-log potential. We explicitly write $H_{\rm osc}$ and derive the epsilon parameter to calculate baryon asymmetry in each case.

3.4.1 Gravity-mediated SUSY breaking models

In this subsection, we consider gravity-mediated SUSY breaking model where the soft mass of the AD field is given by Eq. (3.10). We neglect the thermal-log potential, which is discussed in Sec. 3.4.3.

When the Hubble parameter decreases to m_ϕ, the potential of the AD field is dominated by the soft mass term and it starts to oscillate around the origin of the potential. Here we denote the Hubble parameter at the time of beginning of oscillation as $H_{\rm osc}$:

$$H_{\rm osc} \simeq \frac{m_\phi}{\sqrt{|c_H|}}. \tag{3.59}$$

For a rough estimation, we can use Eq. (3.55) and obtain

$$\epsilon \sim \frac{m_{3/2}}{m_\phi} \sin\left(n\theta_{\rm ini}\right), \tag{3.60}$$

where we use Eq. (3.50).

Here we calculate $B-L$ asymmetry in more detail. The evolution of equation for the $B-L$ number density is written as

$$\dot{n}_{B-L} + 3Hn_{B-L} = -q\varphi^2 \left(\frac{\partial V}{\partial \theta}\right), \tag{3.61}$$

where q denotes the $B-L$ charge of the AD field. We semi-analytically and numerically solve this equation and obtain

$$\begin{aligned} a^3 n_{B-L}(t) &= -\int {\rm d}t q a^3(t)\varphi^2 \frac{\partial V}{\partial \theta} && (3.62)\\ &\equiv \epsilon q H_{\rm osc}\phi_{\rm osc}^2 a^3(t_{\rm osc}) && (3.63)\\ \epsilon &\simeq (1-2)\times \frac{a(n-2)}{\sqrt{n-1}(n-3)}\frac{m_{3/2}}{m_\phi}\sin\left(n\theta_{\rm ini}\right) \quad \text{for} \quad \epsilon \lesssim 1, && (3.64) \end{aligned}$$

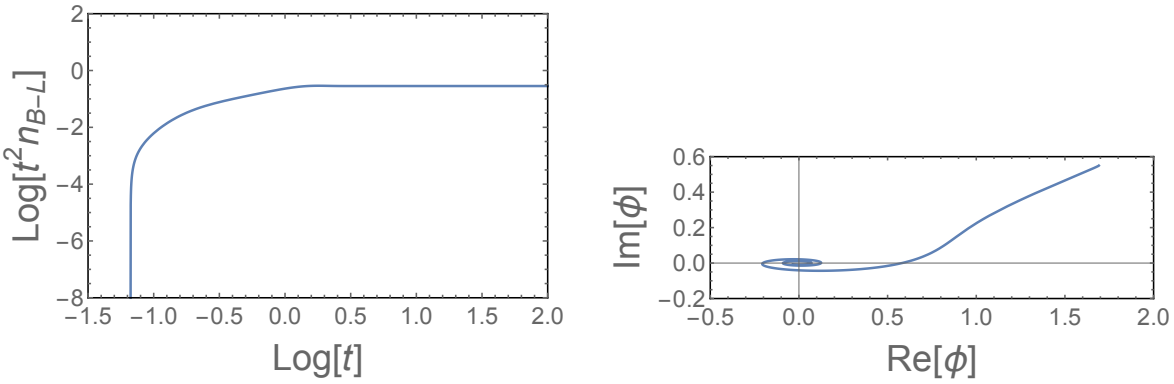

Figure 3.1: Evolution of $B-L$ number density in a comoving volume (left panel) and the AD field (right panel) in the conventional scenario of ADBG. We set $n=6$, $c_H=-1$, $am_{3/2}/m_\phi=-1$, and $\theta_0=\pi/10$. The dimensionfull quantities are rescaled such as $t\to t/m_\phi$ and $\phi\to\phi/\langle|\phi|\rangle_{t=H_{\rm osc}^{-1}}$.

where we assume $c_H=-1$ in the last line. This result confirms the rough estimation of Eq. (3.60). We have numerically solved the equation of motion for ϕ and have obtained the numerical factor of $(1-2)$ in Eq. (3.64) for $c_H=-1$ and $\epsilon\lesssim 1$. One of the numerical results is shown in Fig. 3.1, where we set $n=6$, $c_H=-1$, $am_{3/2}/m_\phi=-1$, and $\theta_0=\pi/10$. One can see that the phase direction is kicked and the $B-L$ asymmetry is generated at $t\sim m_\phi^{-1}\simeq H_{\rm osc}^{-1}$. The generated $B-L$ asymmetry within a comoving volume is conserved soon after the AD field starts to oscillate as one can see in Fig. 3.1.

We can calculate the resulting baryon-to-entropy ratio Y_b such as

$$Y_b \simeq \frac{8}{23}\frac{\epsilon q T_{\rm RH}}{4H_{\rm osc}}\left(\frac{\phi_{\rm osc}}{M_{\rm Pl}}\right)^2 \tag{3.65}$$

$$\simeq 1.2\times 10^{-10}\epsilon q\lambda^{-1/2}\left(\frac{T_{\rm RH}}{100\ {\rm GeV}}\right)\left(\frac{m_\phi}{1\ {\rm TeV}}\right)^{-1/2} \quad \text{for} \quad n=6. \tag{3.66}$$

In the last line, we use Eq. (3.50). The resulting baryon asymmetry can be consistent with the observed baryon asymmetry of $Y_b^{(\rm obs)}\simeq 8.6\times 10^{-11}$ [7]. Since we expect $\epsilon q\sim 1$, a relatively low reheating temperature is required to explain the observed amount of baryon asymmetry unless the parameter λ is much larger than unity.

3.4.2 Gauge-mediated SUSY breaking models

In models of gauge mediation, the gravitino mass is much smaller than the soft mass of the AD field. In addition, the soft mass term of the AD field (other than LH_u flat direction) becomes flat for a larger VEV than the messenger scale such as Eq. (3.11). In this case, the

Hubble parameter at the beginning of oscillation is determined as[4]

$$H_{\rm osc} \simeq \sqrt{\phi^{-1} V'_{\rm gauge}}. \tag{3.67}$$

As a result, the ellipticity parameter may be much smaller than unity. Since the curvature of the potential at the energy scale of $|\phi_{\rm osc}|$ is roughly given by $M_F^2/|\phi_{\rm osc}|$, the AD filed begins to oscillate at the time of $H_{\rm osc} \sim M_F^2/|\phi_{\rm osc}|$. Using this and Eqs. (3.50), (3.12), and (3.13), the VEV of the AD field at the beginning of its oscillation is calculated as

$$|\phi_{\rm osc}| \simeq \begin{cases} 3 \times 10^{13}\ k^{1/3} \left(\frac{m_{3/2}}{1\ {\rm GeV}}\right)^{1/3} \left(\frac{\lambda}{10^{-6}}\right)^{-1/3}, & \text{for } n = 4, \\ 10^{15}\ k^{1/5} \left(\frac{m_{3/2}}{1\ {\rm GeV}}\right)^{1/5} \left(\frac{\lambda}{10^{-4}}\right)^{-1/5}, & \text{for } n = 6. \end{cases} \tag{3.68}$$

We can calculate the ellipticity parameter ϵ ($\simeq m_{3/2}/H_{\rm osc}$) and the required reheating temperature as

$$\epsilon \simeq \begin{cases} 10^{-3}\ k^{-2/3} \left(\frac{m_{3/2}}{1\ {\rm GeV}}\right)^{1/3} \left(\frac{\lambda}{10^{-6}}\right)^{-1/3}, & \text{for } n = 4, \\ 4 \times 10^{-2}\ k^{-4/5} \left(\frac{m_{3/2}}{1\ {\rm GeV}}\right)^{1/5} \left(\frac{\lambda}{10^{-4}}\right)^{-1/5}, & \text{for } n = 6, \end{cases} \tag{3.69}$$

and

$$T_{\rm RH} \simeq \begin{cases} 3 \times 10^{6}\ {\rm GeV}\ k^{2/3} \left(\frac{m_{3/2}}{1\ {\rm GeV}}\right)^{-1/3} \left(\frac{\lambda}{10^{-6}}\right)^{4/3}, & \text{for } n = 4, \\ 3\ {\rm GeV}\ k^{6/5} \left(\frac{m_{3/2}}{1\ {\rm GeV}}\right)^{1/5} \left(\frac{\lambda}{10^{-4}}\right)^{4/5}, & \text{for } n = 6, \end{cases} \tag{3.70}$$

respectively. Here we use the observed value of baryon-to-entropy ratio.

3.4.3 Case with thermal effects: LH_u flat direction

In this section, we take into account thermal log potential. It is particularly important for the case of $n = 4$, including the case of LH_u flat direction.

In the previous two subsections, we neglect the thermal potential and the AD field starts to oscillate around the origin of the potential at $H(t) \simeq \sqrt{|\phi|^{-1} V'_{\rm soft}}$. When the thermal log potential dominates the potential before that time, the AD field starts to oscillate at the time of

$$H_{\rm osc} \simeq \sqrt{\phi^{-1} V'_T}. \tag{3.71}$$

Using Eqs. (3.50) and (B.18), this can be rewritten as

$$H_{\rm osc} \simeq 0.6 \alpha_s \sqrt{\lambda} T_{\rm RH}, \tag{3.72}$$

[4]Here we implicitly assume that $H_{\rm osc}$ is larger than the gravitino mass. Otherwise the AD field starts to oscillate due to the soft mass from the gravity-mediated SUSY breaking effect and $H_{\rm osc}$ is given by $m_{3/2}$ [69].

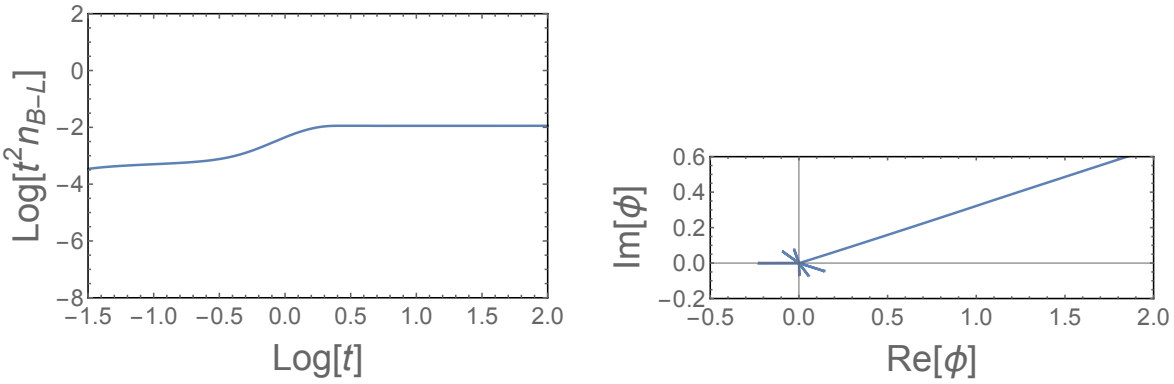

Figure 3.2: Evolution of $B-L$ number density in a comoving volume (left panel) and the phase direction of the AD field (right panel) in the conventional scenario of ADBG. We set $c_H = -1$, $a_H m_{3/2}/H_{\rm osc} = -0.01$, and $\theta_0 = \pi/10$. The dimensionfull parameters are rescaled as $t \to t/H_{\rm osc}$ and $\phi \to \phi/\langle|\phi|\rangle_{t=H_{\rm osc}^{-1}}$.

where we assume $|c_H| = 1$ and $n = 4$.

We numerically solve the equation of motion for ϕ and obtain the ellipticity parameter as

$$\epsilon = (0.4 - 3.5) \times a \sin(n\theta_0) \frac{m_{3/2}}{H_{\rm osc}} \tag{3.73}$$

$$\equiv \tilde{\epsilon} \frac{m_{3/2}}{H_{\rm osc}}, \tag{3.74}$$

where we define $\tilde{\epsilon}$ that is expected to be of order unity. One of our results is shown in Fig. 3.2, where we set $c_H = 1$, $am_{3/2}/H_{\rm osc} = -0.01$, and $\theta_0 = \pi/10$. The ellipticity parameter ϵ is much smaller than unity in this numerical calculation, so that the phase direction is kicked slightly. We are difficult to see that the AD field rotates in the phase space in the right panel of Fig. 3.2 though it actually does.

The large numerical uncertainty comes from the fact that the AD field does not stay at the VEV of Eq. (3.39) during the inflaton oscillation dominated era for the case of $n = 4$. Rather, it continues to oscillate around a VEV of order Eq. (3.39). Then at the time of $H \simeq H_{\rm osc}$ it starts to oscillate and rotate around the origin of the potential. The amount of the baryon asymmetry depends on the oscillation amplitude, which depends on the evolution of the AD field during the inflaton oscillation dominated era.

The baryon-to-entropy ratio is calculated as

$$Y_b \simeq \frac{8}{23} \frac{q\tilde{\epsilon} m_{3/2}}{4\alpha_s \lambda^{3/2} M_{\rm Pl}} \tag{3.75}$$

$$\simeq 3.7 \times 10^{-10} \tilde{\epsilon} \left(\frac{\lambda}{10^{-4}}\right)^{-3/2} \left(\frac{m_{3/2}}{1\ {\rm TeV}}\right), \tag{3.76}$$

where we assume $|c_H| = 1$, $n = 4$, and $\alpha_s = 0.1$ and use $\epsilon = \tilde{\epsilon} m_{3/2}/H_{\rm osc}$. This result is independent of the reheating temperature [56].

The observed baryon asymmetry can be explained when the coupling λ satisfies

$$\lambda \simeq 2.6 \times 10^{-4} \left(\frac{m_{3/2}}{1 \text{ TeV}} \right)^{2/3}, \tag{3.77}$$

where we assume $\tilde{\epsilon} = 1$. When we identify the AD field as LH_u flat direction, this result implies that the lightest left-handed neutrino has a tiny mass of

$$m_\nu \simeq 1.6 \times 10^{-9} \text{ eV} \left(\frac{\lambda}{2.6 \times 10^{-4}} \right) \tag{3.78}$$

$$\simeq 1.6 \times 10^{-9} \text{ eV} \left(\frac{m_{3/2}}{1 \text{ TeV}} \right)^{2/3}. \tag{3.79}$$

Since the mass squared differences of the left-handed neutrinos are measured by observations of atmospheric and solar neutrino oscillations, this determines the total neutrino mass such as

$$\sum m_\nu \simeq \begin{cases} 0.06 \text{ eV} & \text{for NH} \\ 0.1 \text{ eV} & \text{for IH}, \end{cases} \tag{3.80}$$

for the cases of normal hierarchy (NH) and inverted hierarchy (IH), respectively. We can also calculate the upper and lower bounds on the effective Majorana mass for the $0\nu\beta\beta$ decay process such as [56, 70]

$$0.001 \text{ eV} \lesssim |m_{\beta\beta}| \lesssim 0.004 \text{ eV} \qquad \text{for NH} \tag{3.81}$$

$$0.01 \text{ eV} \lesssim |m_{\beta\beta}| \lesssim 0.04 \text{ eV} \qquad \text{for IH}, \tag{3.82}$$

where we take the values for the experimentally measured parameters from Ref. [71]. These results of total neutrino mass and effective Majorana mass are too small to measure in the near future at least for the case of NH. Therefore, if we would measure the total neutrino mass or the effective Majorana mass in the near future, we can falsify the scenario of the ADBG by LH_u flat direction.

Here we write the condition that the thermal effect dominates the soft mass term at the oscillation in the case of $n = 4$. It is written as $T_{\rm RH} \gtrsim m_\phi(\phi)/(0.6\alpha_s\sqrt{\lambda})$ [see Eq. (3.72)]. For a typical parameter set, it is rewritten as

$$T_{\rm RH} \gtrsim 2 \times 10^6 \text{ GeV} \left(\frac{m_\phi(\phi)}{1 \text{ TeV}} \right) \left(\frac{\lambda}{10^{-4}} \right)^{-1/2}, \tag{3.83}$$

where we use $\alpha_s \approx 0.1$. Next we write the condition that the thermal effect can be neglected in the case of $n = 6$. It can be given by $V_T \lesssim V_{\rm soft}$ at the time of oscillation, so that in gravity-mediated SUSY breaking models,

$$T_{RH} \lesssim \frac{M_{\rm Pl}^{(n-3)/(n-2)}}{\alpha M_{\rm Pl}^{1/2}} m_\phi^{n/(2n-4)}, \tag{3.84}$$

$$\simeq 7.0 \times 10^7 {\rm GeV} \left(\frac{0.1}{\alpha}\right) \left(\frac{m_\phi}{\rm TeV}\right)^{3/4} \left(\frac{M_{\rm Pl}}{M_{\rm Pl}}\right)^{3/2} \quad \text{for } n = 6, \tag{3.85}$$

while in gauge-mediated SUSY breaking models,

$$T_{RH} \lesssim \frac{M_{\rm Pl}^{(n-3)/(2n-2)}}{\alpha M_{\rm Pl}^{1/2}} V_{\rm gauge}^{n/(4n-4)}, \tag{3.86}$$

$$\simeq 10^8 {\rm GeV} \left(\frac{0.1}{\alpha}\right) \left(\frac{V_{\rm gauge}^{1/4}}{10^9 {\rm GeV}}\right)^{6/5} \left(\frac{M_{\rm Pl}}{M_{\rm Pl}}\right)^{3/10} \quad \text{for } n = 6. \tag{3.87}$$

For reheating temperature below these values, we can neglect the thermal-log potential and can use the results of the previous two sections. In fact, observed abundance of baryon asymmetry favours reheating temperature much lower than these bounds for the case of $n = 6$ [see Eqs. (3.66) and (3.70)].

3.5 Baryonic isocurvature constraint

Hubble-induced A-terms are absent during inflation if the field which has a non-zero F-term during inflation is charged under some symmetry and its VEV is less than the Planck scale during inflation [58]. In this case, since the phase direction of the AD field is massless during inflation, it has quantum fluctuations during inflation. As a result, baryonic isocurvature density perturbations, which are tightly constrained by recent observations of CMB temperature anisotropies, are produced. The ADBG after high-scale inflation results in a sizable baryonic isocurvature fluctuation [65, 66, 58], unless the vacuum expectation value (VEV) of the AD field is very large during inflation.

The phase direction of the AD field acquires quantum fluctuations during inflation as [65, 66, 58]

$$|\delta\theta_{\rm ini}| \simeq \frac{\sqrt{2} H_{\rm inf}}{2\pi |\phi_{\rm inf}|}. \tag{3.88}$$

Since the baryon number is related to the initial phase [see Eq. (3.55)], this fluctuation induces a sizable baryonic isocurvature fluctuation as

$$\mathcal{S}_{b\gamma} \equiv \frac{\delta Y_B}{Y_B} \simeq n \cot\left(n\theta_{\rm ini}\right) \delta\theta_{\rm ini}. \tag{3.89}$$

The baryonic isocurvature perturbation is constrained by observations of the cosmic microwave background, which have shown that the density perturbations are predominantly adiabatic [15, 6]. The Planck Collaboration puts an upper bound on the totally uncorrelated isocurvature fraction as [72]

$$\frac{\mathcal{P}_{\mathcal{SS}}(k_*)}{\mathcal{P}_{\mathcal{RR}}(k_*) + \mathcal{P}_{\mathcal{SS}}(k_*)} \lesssim 0.038, \tag{3.90}$$

where $\mathcal{P}_{\mathcal{RR}}$ and $\mathcal{P}_{\mathcal{SS}}$ are power spectra of the adiabatic fluctuation and isocurvature fluctuation, respectively, and k_* $(= 0.05{\rm Mpc}^{-1})$ is a pivot scale. Since we are interested in the baryonic isocurvature fluctuation, we use the following relation:

$$\mathcal{P}_{\mathcal{SS}} = \left(\frac{\Omega_{\rm b}}{\Omega_{\rm DM}}\right)^2 \mathcal{P}_{\mathcal{S}_{b\gamma}\mathcal{S}_{b\gamma}}. \tag{3.91}$$

Thus we obtain an upper bound on the baryonic isocurvature fluctuation as

$$|S_{\rm b\gamma}| \lesssim \frac{\Omega_{\rm DM}}{\Omega_{\rm b}} \left(0.038 \times 2.2 \times 10^{-9}\right)^{1/2} \simeq 5.0 \times 10^{-5}, \tag{3.92}$$

where we have used ${\mathcal{P}_{\mathcal{RR}}}^{1/2} \simeq 2.20 \times 10^{-9}$ [6]. This implies that the VEV of the AD field during inflation is bounded from below:

$$|\phi_{\rm inf}| \gtrsim 4 \times 10^{17}\,{\rm GeV} \times n\,|\cot(n\theta_{\rm ini})| \left(\frac{H_{\rm inf}}{10^{14}\ {\rm GeV}}\right). \tag{3.93}$$

Using Eq. (3.39), the baryonic isocurvature constraint can be rewritten as

$$\lambda \lesssim \begin{cases} 2.6 \times 10^{-4} \left(\frac{H_{\rm inf}}{2.1\times 10^{13}\ {\rm GeV}}\right)^{-1} & \text{for} \quad n = 4 \\ 1.1 \left(\frac{H_{\rm inf}}{2.6\times 10^{12}\ {\rm GeV}}\right)^{-3} & \text{for} \quad n = 6, \end{cases} \tag{3.94}$$

where we assume $|c_H| = 1$ and $|\cot n\theta_{\rm ini}| = 1$. This constraint is severe for high-scale inflation models such as chaotic inflation, where the energy scale of inflation is of order 10^{14} GeV.

Chapter 4

Q-ball

In this section, we explain the dynamics of Q-ball, which is a non-topological soliton formed after the Affleck-Dine mechanism in many SUSY models [26, 22, 23, 24, 25]. We first explain the condition of the Q-ball to form and then review its decay processes.

4.1 Q-balls in SUSY theories

After the AD field starts to oscillate and rotate around the low energy vacuum, the amplitude of the oscillation decreases due to the Hubble expansion. Since baryon number-violating terms are higher-dimensional ones, their effects become irrelevant and the generated baryon number is conserved soon after the beginning of the oscillation. Thus, in this section, we assume baryon number to be conserved and investigate the stable configuration of the AD field in a system with non-zero baryon charge.

4.1.1 Formation of Q-ball

Let us first consider an AD field with conserved baryon symmetry. The Lagrangian density is written as

$$\mathcal{L} = -\partial_\mu \phi^* \partial^\mu \phi - V(\phi). \tag{4.1}$$

The energy of the AD field is given as

$$E = \int \mathrm{d}^3 x \left[\left|\dot{\phi}\right|^2 + \left|\nabla\phi\right|^2 + V\left(\left|\phi\right|\right) \right]. \tag{4.2}$$

We are interested in the case with sufficiently small value of the VEV of the AD field, for which the potential is approximated by $V = m_\phi^2(\phi)\left|\phi\right|^2$. Since the baryon density is already

generated via ADBG, we consider a system with non-zero baryon charge. The baryon charge is given by

$$Q = -2\int \mathrm{d}^3x \mathrm{Im}\left[\phi^*\dot{\phi}\right], \tag{4.3}$$

[see Eq. (3.1)], where we have omitted the factor q for notational simplicity. The scalar field configuration which minimizes the energy given in Eq. (4.2) with a fixed baryon charge Q_0 is obtained by minimizing the following combination;

$$E + \omega_0\left[Q_0 + 2\int \mathrm{d}^3x \mathrm{Im}\left[\phi^*\dot{\phi}\right]\right], \tag{4.4}$$

where ω_0 is a Lagrange multiplier. Terms with time derivatives are rewritten as

$$\left|\dot{\phi}\right|^2 + 2\omega_0 \mathrm{Im}\left[\phi^*\dot{\phi}\right] = \left|\dot{\phi} + i\omega_0\phi\right|^2 - \omega_0^2\left|\phi\right|^2. \tag{4.5}$$

Thus, the minimization condition determines the time dependence of the AD field as

$$\phi(\boldsymbol{r}, t) = \varphi(\boldsymbol{r})e^{-i\omega_0 t}/\sqrt{2}. \tag{4.6}$$

Assuming a spherically symmetric ansatz, $\varphi(\boldsymbol{r}) = \varphi(r)$, we obtain the following equation which determines $\varphi(r)$:

$$\frac{\partial^2}{\partial r^2}\varphi + \frac{2}{r}\frac{\partial}{\partial r}\varphi + \omega_0^2\varphi - \frac{\partial}{\partial\varphi}V(\varphi) = 0. \tag{4.7}$$

The boundary conditions are $\varphi'(0) = 0$ and $\varphi(\infty) = 0$ since we are interested in smooth and localized configurations. Regarding φ and r as a position x and a time variable t, we can interpret Eq. (4.7) as the equation of motion of a particle in one dimension with a friction term $(2/t)\partial x/\partial t$ and a potential of $\omega_0^2x^2/2 - V(x)$ (see Fig. 4.1). In this analogy, the boundary conditions imply that the initial velocity is absent and the position is asymptotic to the origin at $t \to \infty$. Since the total energy decreases due to the friction term, there is a solution only when the initial potential energy is larger than the one at $x = 0$. This requires a condition of $\mathrm{Max}_x\left[\omega_0^2x^2/2 - V(x)\right] > 0$, which can be rewritten as $\mathrm{Min}_x\left[2V(x)/x^2\right] < \omega_0^2$. It is also needed that the curvature of the potential at the origin is negative so that there is an asymptotic solution. This requires another condition of $\omega_0^2 - V''(x) < 0$. Thus, one can find the following condition for existence of a spatially localized configuration, referred to as Q-ball [26]:

$$\mathrm{Min}_\varphi\left[\frac{2V(\varphi)}{\varphi^2}\right] < \omega_0^2 < \frac{\partial^2V(0)}{\partial\varphi^2}. \tag{4.8}$$

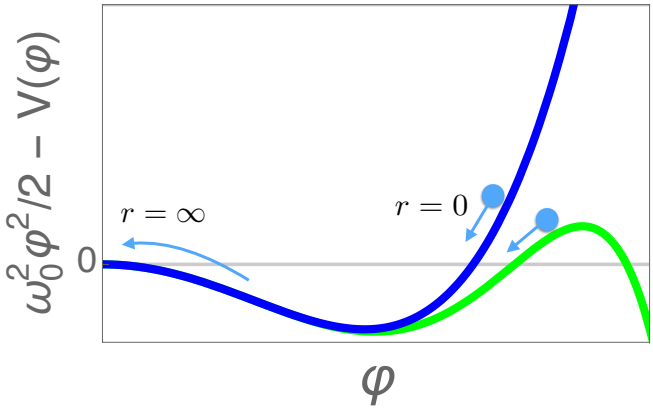

Figure 4.1: Examples of potential that have Q-ball solutions. These examples satisfy the condition of Eq. (4.8).

The energy of the Q-ball per unit charge is given by ω_0 because

$$\delta E = \int \mathrm{d}^3x \left[\omega_0 \delta\omega_0 \varphi^2 + \omega_0^2 \varphi\delta\varphi - \Delta\varphi\delta\varphi + V'(\varphi)\delta\varphi\right] \tag{4.9}$$

$$= \omega_0 \int \mathrm{d}^3x \left[\delta\omega_0 \varphi^2 + 2\omega_0\varphi\delta\varphi\right] \tag{4.10}$$

$$= \omega_0 \delta Q. \tag{4.11}$$

If there is a Q-ball solution, a condensed scalar field is more stable in the Q-ball configuration than in the homogeneous one. Therefore, the AD field, which is homogeneous for the first time, is unstable and fragments into Q-balls soon after the beginning of oscillation. In fact, linear analyses indicate that there are instability bands during the oscillation of the AD field if the condition of Q-ball formation Eq. (4.8) is satisfied [23, 24]. This means that the coherently oscillating AD field is unstable and fragments into Q-balls soon after the onset of its oscillation. A typical charge of Q-balls is roughly estimated by the charge which is contained in the volume of a typical instability wavelength (which is roughly equal to the Q-ball size R) at the formation time:

$$Q \sim n_B(t_{\rm form}) R^3 \sim \left(\frac{a(t_{\rm osc})}{a(t_{\rm form})}\right)^3 \omega_0 \left|\phi_{\rm osc}\right|^2 R^3, \tag{4.12}$$

where we have included the dependence on the scale factors a because it needs some time

for Q-ball to be formed completely. The numerical simulations have shown that Q-balls are indeed formed when the condition of Q-ball formation Eq. (4.8) is satisfied, and have determined the proportional constant including $a^3(t_{\rm osc})/a^3(t_{\rm form})$ of Eq. (4.12) for the cases we are interested in [see Eqs. (4.32) and (4.40)] [25, 73].

In the following subsections, we consider gravity-mediated and gauge-mediated SUSY breaking models, where $m_\phi(\phi)$ is given by Eqs. (3.10) and (3.11), respectively, and derive solutions of Q-ball.

4.1.2 Q-balls in gravity-mediated SUSY breaking models

In gravity-mediated SUSY breaking models, the soft mass term $m_\phi(\phi)$ is approximately constant of order the gravitino mass. However, the mass of the AD field $m_\phi(\phi)$ logarithmically depends on $|\phi|$ due to the renormalization group running of squark masses (see Appendix A.1.2). We simply write the potential of the AD field in gravity mediation as

$$V = m_\phi^2(\phi)\,|\phi|^2 \tag{4.13}$$

$$\simeq m_\phi^2|\phi|^2\left(1 + K\log\frac{|\phi|^2}{M_{\rm Pl}^2}\right), \tag{4.14}$$

where the second term in the parenthesis represents renormalization group running. In many cases in gravity mediation, the strong interaction dominates quantum corrections for a typical flat direction, and we obtain $K < 0$ and $|K| \sim 0.01 - 0.1$ [24], which satisfies the condition for Q-ball formation of Eq. (4.8). The configuration of the AD field is obtained by solving Eq. (4.7) with the above potential. The solution is well approximated by [24]

$$\phi(r,t) \simeq \frac{1}{\sqrt{2}}\phi_0 e^{-r^2/2R^2} e^{-i\omega_0 t}, \tag{4.15}$$

where R, ω_0, and ϕ_0 are given as

$$R \simeq \frac{1}{|K|^{1/2} m_\phi(\phi_0)}, \tag{4.16}$$

$$\omega_0 \simeq m_\phi(\phi_0), \tag{4.17}$$

$$\phi_0 \simeq \left(\frac{|K|}{\pi}\right)^{3/4} m_\phi(\phi_0) Q^{1/2}, \tag{4.18}$$

where $m_\phi(\phi_0)$ is the mass of the AD field at the energy scale of ϕ_0. Since the energy of the Q-ball, M_Q, is calculated from Eq. (4.2) as

$$M_Q \simeq m_\phi(\phi_0) Q, \tag{4.19}$$

we find that the energy of the Q-ball per unit charge is equal to $\omega_0 \simeq m_\phi(\phi_0)$. Note that this is of order the TeV scale and is much larger than the proton mass, which fact is important to discuss the decay of Q-ball as explained in Sec. 4.3.

Here we consider the instability of the AD field by the linear analysis. When we decompose the AD field as $\phi = \varphi e^{i\theta}/\sqrt{2}$, their equations of motion are given by

$$\ddot{\varphi} + 3H\dot{\varphi} - \frac{1}{a^2}\Delta\varphi - \dot{\theta}^2\varphi + \frac{1}{a^2}(\partial_i\theta)^2\varphi + \frac{\partial V}{\partial\varphi} = 0 \tag{4.20}$$

$$\ddot{\theta} + 3H\dot{\theta} - \frac{1}{a^2}\Delta\theta + \frac{2\dot{\varphi}}{\varphi}\dot{\theta} - \frac{2}{a^2\varphi}(\partial_i\theta)(\partial^i\varphi) = 0. \tag{4.21}$$

Let us consider the time just after the AD field starts to oscillate coherently. The coherent oscillation of the AD field is approximately specially homogeneous, so that we set a perturbation such as

$$\varphi = \varphi(t) + \delta\varphi(x,t), \tag{4.22}$$

$$\theta = \theta(t) + \delta\theta(x,t), \tag{4.23}$$

so that their equations of motion are written as

$$\ddot{\delta\varphi} + 3H\dot{\delta\varphi} - \frac{1}{a^2}\Delta(\delta\varphi) - 2\varphi\dot{\theta}(\dot{\delta\theta}) + V''\delta\varphi - \dot{\theta}^2\delta\varphi = 0, \tag{4.24}$$

$$\ddot{\delta\theta} + 3H\dot{\delta\theta} - \frac{1}{a^2}\Delta(\delta\theta) + \frac{2\dot{\varphi}}{\varphi}\dot{\delta\theta} + \frac{2\dot{\theta}}{\varphi}\dot{\delta\varphi} - \frac{2\dot{\varphi}\dot{\theta}}{\varphi^2}\delta\varphi = 0. \tag{4.25}$$

Let us expand the solution such as

$$\delta\varphi = \delta\varphi_0\varphi(t)e^{\alpha t - ikx}, \tag{4.26}$$

$$\delta\theta = \delta\theta_0 e^{\alpha t - ikx}, \tag{4.27}$$

and seek a growing mode $\alpha > 0$. Eliminating $\delta\chi_0$ and $\delta\theta_0$, we obtain a dispersion relation such as

$$\left[\alpha^2 + 3H\alpha + \frac{k^2}{a^2} + \frac{2\dot{\varphi}}{\varphi}\alpha + V'' - \frac{V'}{\varphi}\right]\left[\alpha^2 + 3H\alpha + \frac{k^2}{a^2} + \frac{2\dot{\varphi}}{\varphi}\alpha\right] + 4\dot{\theta}^2\alpha^2 = 0, \tag{4.28}$$

when we assume $V = V_0\varphi^{2n}$ and use the Vilial theorem of $\dot{\varphi}\varphi = -3H/(n+1)$, we obtain

$$\left[\alpha^2 - 3\frac{1-n}{1+n}H\alpha + \frac{k^2}{a^2} - 4n(1-n)\varphi^{2n-2}V_0\right]\left[\alpha^2 - 3\frac{1-n}{1+n}H\alpha + \frac{k^2}{a^2}\right] + 4\dot{\theta}^2\alpha^2 = 0. \tag{4.29}$$

Then we can find that for the case of $0 < n < 1$, the mode in the interval of $[0, k_{\rm max}]$ grows, where $k_{\rm max}$ is given by

$$k_{\rm max}(t) \simeq a(t)\sqrt{4n(1-n)V/\varphi^2}. \tag{4.30}$$

We expect that Q-balls are originated from these growing modes, so that a typical size of Q-balls are given by of order $k_{\rm max}$. The logarithmic potential of the AD field of Eq. (4.14) can be approximated as $V \sim \phi^{2(1+K)}$, so that $k_{\rm max}$ is given by

$$\frac{k_{\rm max}^2}{a^2(t)} \simeq 2\,|K|\,m_\phi^2. \tag{4.31}$$

Note that $k_{\rm max}$ is of order R^{-1} [see Eq. (4.16)].

Using $\omega_0 \simeq m_\phi$ and $R \sim m_\phi^{-1}$ in Eq. (4.12), we estimate a typical charge of Q-ball formed after the Affleck-Dine baryogenesis as

$$Q \sim \beta \left(\frac{|\phi_{\rm osc}|}{m_\phi}\right)^2, \tag{4.32}$$

$$\simeq 2\times 10^{23} \left(\frac{|\phi_{\rm osc}|}{3\times 10^{15}\,{\rm GeV}}\right)^2 \left(\frac{m_\phi}{1{\rm TeV}}\right)^{-2}. \tag{4.33}$$

The numerical simulations have shown that the coefficient β is approximately given by [25, 73]

$$\beta \simeq \begin{cases} 2\times 10^{-2}\epsilon & \text{for } \epsilon \gtrsim 0.01, \\ 2\times 10^{-4} & \text{for } \epsilon \lesssim 0.01, \end{cases} \tag{4.34}$$

which we have used in the second line in Eq. (4.33).

4.1.3 Q-balls in gauge-mediated SUSY breaking models

In this subsection, we consider the AD field in gauge-mediated SUSY breaking models and calculate the solution of Q-ball.[1] As shown in Sec. A.1.5, the soft mass term for the AD field is absent for a VEV larger than the messenger scale because the transmission of SUSY breaking effect is suppressed for such a large VEV. Thus the potential of the AD field is written as Eq. (3.11).

[1] We implicitly assume that the AD field is not identified with LH_u flat direction. It has a SUSY mass from the Higgs μ term, so that there is no Q-ball solution.

For the potential in Eq. (3.11), there exists a Q-ball solution, approximated to be [74][23]

$$\phi(r,t) \simeq \begin{cases} \frac{1}{\sqrt{2}}\phi_0 \frac{\sin(\omega_0 r)}{\omega_0 r} e^{-i\omega_0 t} & \text{for} r \le R \equiv \frac{\pi}{\omega_0}, \\ 0 & \text{for} r > R, \end{cases} \tag{4.35}$$

where ω_0 and ϕ_0 are given as

$$\omega_0 \simeq \sqrt{4\pi c} M_F Q^{-1/4}, \tag{4.36}$$

$$\phi_0 \simeq \sqrt{\frac{c}{\pi}} M_F Q^{1/4} \left(\simeq c \frac{M_F^2}{\omega_0} \right). \tag{4.37}$$

Here, the parameter c is fitted as [77]

$$c \simeq 1.7 \log(m_s/\omega_0) + 2. \tag{4.38}$$

The energy of the Q-ball is calculated as

$$M_Q \simeq \frac{4\sqrt{4\pi c}}{3} M_F Q^{3/4}. \tag{4.39}$$

Using $R \simeq \pi/\omega_0$ and $\omega_0 \sim M_F^2/\phi$ in Eq. (4.12), a typical charge of Q-balls formed after the Affleck-Dine baryogenesis is estimated as

$$Q \sim \beta \left(\frac{|\phi_{\rm osc}|}{M_F} \right)^4, \tag{4.40}$$

$$\simeq 3 \times 10^{23}\ k^{-6/5} \lambda^{-4/5} \left(\frac{m_{3/2}}{1\ \text{MeV}} \right)^{-6/5} \qquad \text{for } n = 6. \tag{4.41}$$

We have used Eq. (3.68) in the last line. The numerical parameter β has been calculated by the numerical simulation of Q-ball formation and is given by [25]

$$\beta \simeq \begin{cases} 6 \times 10^{-4} \epsilon & \text{for } \epsilon \sim 1 \\ 6 \times 10^{-5} & \text{for } \epsilon \ll 1. \end{cases} \tag{4.42}$$

Note that there are instability modes even if $\epsilon \to 0$, which means that the baryon charge does not generated by the dynamics of the AD field. This implies that both anti-Q-balls, which carry negative baryon charge, and Q-balls form to compensate the total baryon charge. This feature is actually found in numerical simulations.

[2]If $\phi_{\rm osc}$ or ϕ_0 is less than about the messenger mass M_s ($\simeq g M_F^2/m_\phi$), the suppression on the transmission of SUSY breaking effect is absent and the situation is similar to models of gravity mediation [75, 76]. We have checked that $\phi_{\rm osc}$ and ϕ_0 is larger than M_s in the case we are interested in, if the mass of the AD field m_ϕ is larger than 10 TeV or that of gravitino $m_{3/2}$ is less than 10 GeV.

[3]If $\phi_0 \gtrsim M_F^2/m_{3/2}$, the potential of the AD field is dominated by the soft mass of the form $m_{3/2}^2|\phi|^2$, which is induced by gravity mediated SUSY breaking effect. In this case, a Q-ball solution is known as a "new type Q-ball" [69], which is stable and is a DM candidate for the case of $m_{3/2}/|q| \lesssim 1$ GeV. Note that if $k \sim 1$, a "new type Q-ball" is never formed.

4.2 Evaporation and dissipation of Q-ball

After Q-balls form, they interact with particles in the thermal plasma and release their charges. There are two important processes: dissipation and evaporation.

4.2.1 Evaporation

Q-balls evaporate via collisions of particles in the thermal plasma [78]. The evaporation rate par unit time is given by

$$\Gamma_{\rm evap} = \frac{{\rm d}Q}{{\rm d}t} \sim -\zeta(\mu_Q - \mu_{\rm plasma})T^2 4\pi R^2, \tag{4.43}$$

where $\mu_Q = \omega_0$ is the energy of Q-ball per unit charge. The parameter ζ ($\lesssim 1$) is the collision rate of particles in the thermal plasma. In the case of $T \gtrsim m_\phi$, the AD field (i.e., squarks) exists in the thermal plasma, so that the collision rate is of order unity. Since the AD field decouples below that temperature, ζ is suppressed for $T \lesssim m_\phi$.

4.2.2 Dissipation

If the transfer of baryon charges around a Q-ball is not sufficiently fast, the chemical equilibrium is realized around the Q-ball. In this case, a dissipation rate determines the evaporation rate of Q-ball [79].

The dissipation equation is given by

$$\frac{\partial}{\partial t} n_B\left(r,t\right) = D\Delta n_B = D\frac{1}{r}\frac{\partial^2}{\partial r^2}\left(r n_B\right), \tag{4.44}$$

where D is the dissipation coefficient. For squarks, it is given by $D = A/T$ and $A = 4 - 6$. Assuming that the baryon density is constant in time around the Q-ball, i.e., $n_B(R,t) = n_B^{\rm eq}(R)$, we obtain the solution such as

$$n_B\left(r,t\right) = n_B^{\rm eq}\frac{R}{r}. \tag{4.45}$$

Thus the charge current is calculated from

$$j = -D\nabla n_B = D n_B^{\rm eq}\frac{R}{r^2}, \tag{4.46}$$

so that the evaporation rate of Q-ball is given by

$$\Gamma_{\rm diff} = \frac{{\rm d}Q}{{\rm d}t} = -\int j\left(R,t\right){\rm d}S \simeq -4\pi D R n_B^{\rm eq} \sim -4\pi D R \mu_Q T^2. \tag{4.47}$$

In the last equality, we use $n_B^{\rm eq} \simeq \mu_Q T^2$ for $T \gtrsim m_\phi$.

The evaporation rate of Q-ball is determined by the smaller rate between the evaporation and dissipation rates. Since their ratio is given by

$$\frac{\Gamma_{\rm diff}}{\Gamma_{\rm evap}} \sim \frac{A}{\zeta T R} \sim \frac{\omega_0}{\zeta T}, \tag{4.48}$$

we find that the dissipation rate determines the evaporation rate. Since ζ is suppressed for $T \lesssim m_\phi$, we should integrate Eq. (4.47) for $T \gtrsim m_\phi$.

4.2.3 Summary in this section

When $T_{\rm RH} \lesssim m_\phi$, we use Eq. (B.18) and obtain

$$\frac{{\rm d}T}{{\rm d}t} \simeq \frac{T}{4}\frac{\dot{H}}{H} = -\frac{3}{8}TH, \tag{4.49}$$

so that the solution is given by

$$-\delta Q \simeq 4\pi\,(R\omega_0)\,A\frac{8}{3}T_{\rm RH}^2 M_{\rm Pl}\frac{5}{m_\phi^3} \sim 8\times 10^{18}\left(\frac{T_{\rm RH}}{\rm TeV}\right)^2\left(\frac{m_\phi}{\rm TeV}\right)^{-3}. \tag{4.50}$$

On the other hand, when $T_{\rm RH} \gtrsim m_\phi$, the radiation dominated era contributes to the integral:

$$\frac{{\rm d}T}{{\rm d}t} \simeq -\left(\frac{\pi^2 g_*}{90}\right)^{1/2}\frac{T^3}{M_{\rm Pl}}. \tag{4.51}$$

Thus we obtain

$$-\delta Q \simeq 4\pi\,(R\omega_0)\,A\frac{90 M_{\rm Pl}}{\pi g_*^{1/2}}\frac{1}{m_\phi} \sim 5\times 10^{18}\left(\frac{m_\phi}{\rm TeV}\right)^{-1}. \tag{4.52}$$

In either case, Q-balls with charge smaller than 10^{18} disappear and dissipate into thermal plasma.

4.3 Decay of Q-ball

In this section, we explain the decay rate of Q-ball and calculate its decay temperature. Let us focus on a Q-ball which consists only of squarks for simplicity.

Numerical simulations have shown that almost all of the baryon charge of the AD field are transferred into Q-balls [25, 73]. As explained in the previous section, small Q-balls soon

dissipate into thermal plasma. When a typical charge of Q-balls is larger than about 10^{18}, it survives at low temperature. Then Q-balls decay and release their baryon charge into quarks if they are unstable. The AD field interacts (i.e., squarks) with quarks via gauge interactions and thus Q-balls lose their baryon charge by emitting quarks from their surfaces [27].[4] The condition for Q-ball decay is that the energy of the Q-ball per unit baryon charge, $\omega_0/|b|$, is larger than masses of baryons in the hadron phase, $m_b \simeq 1\,\mathrm{GeV}$. This is satisfied for Q-balls in gravity-mediated SUSY breaking models. On the other hand, in gauge-mediated SUSY breaking models, this condition can be rewritten as

$$Q \lesssim 10^{29} k^2 c^2 |q|^{-4} \left(\frac{m_{3/2}}{1\ \mathrm{MeV}}\right)^2, \tag{4.53}$$

where k and c are parameters defined in Eqs. (3.13) and (4.38), respectively.

4.3.1 Decay of Q-ball into quarks

The baryon charge density inside a Q-ball is so large that a naive rate estimated by squark decay exceeds an upper limit by the Pauli blocking effect around the Q-ball surface. The rate of (massless) particle emission from the Q-ball surface is therefore determined by the Pauli blocking effect on its surface and is given as [27]

$$\frac{\mathrm{d}N}{\mathrm{d}t} \simeq \sum_i 4\pi \tilde{R}^2 \boldsymbol{n}\cdot\boldsymbol{j_i}, \tag{4.54}$$

$$\begin{aligned} \boldsymbol{n}\cdot\boldsymbol{j_i} &\simeq 2\int \frac{\mathrm{d}^3k}{(2\pi)^3}\theta\left(E_i/2-|\boldsymbol{k}|\right)\theta\left(\boldsymbol{k}\cdot\boldsymbol{n}\right)\hat{\boldsymbol{k}}\cdot\boldsymbol{n} \\ &= \frac{E_i^3}{96\pi^2}, \end{aligned} \tag{4.55}$$

where n is the outward-pointing normal vector, $\boldsymbol{j}$ is particle flux, and $\tilde{R}$ is the effective radius of the Q-ball given by $\phi(\tilde{R}) \sim \omega_0$ [34]. The interaction energy E_i is given by the energy of the Q-ball per unit charge, ω_0, when the relevant elementary process is squark decay, such as (squark) $\to$ (quark) + (gaugino). In addition, the baryon charge density inside the Q-ball is so large that the scattering process via gaugino (and/or Higgsino) exchange (squark) + (squark) $\to$ (quark) + (quark) occurs efficiently. It has been shown that the rate of this process is also saturated by the Pauli blocking effect, and the interaction energy E_i is

[4] Far inside Q-balls, field values of squarks are large and hence gauginos and quarks are heavy. Therefore, Q-balls cannot decay into them.

given by $2\omega_0$ in this case [34].[5] The rate of Q-ball decay is dominated by the latter process and thus its lifetime Γ_Q^{-1} is given by

$$\Gamma_Q^{-1} \simeq \left(\frac{1}{Q}\frac{\mathrm{d}N}{\mathrm{d}t}\right)^{-1}, \tag{4.56}$$

$$\simeq \left(8n_q\frac{\tilde{R}^2\omega_0^3}{24\pi Q}\right)^{-1}, \tag{4.57}$$

where n_q is the number of species for quarks interacting with the AD field and is typically $\mathcal{O}(10)$.

4.3.2 Decay of Q-ball into SUSY particles

Q-balls decay into SUSY particles if the decay process is kinematically allowed. From kinematics and the conservation of baryon charge, Q-ball can decay only into particles lighter than the energy of the Q-ball per unit charge, ω_0. Since ω_0 is less than the mass of the AD field [see Eq. (4.8)], Q-balls cannot decay into the AD field itself. This is another explanation of the stability of Q-ball. On the other hand, Q-balls decay into gauginos and/or Higgsinos if they interact with the Q-balls and their masses are less than ω_0. However, in contrast to the case of quarks, gauginos and Higgsinos cannot be produced through a scattering process like (squark) + (squark) $\to$ (gaugino) + (gaugino) due to the conservation of baryon charge. Thus if we could neglect their masses, their production rate from Q-ball decay is given by Eq. (4.55) with $E_i = \omega_0$.

Here, let us take into account nonzero masses of gaugeinos and higgsinos [35]. While flux of a massless particle at the Q-ball surface is calculated as in Eq. (4.55), that of a massive particle is suppressed by its mass. Here we consider the Q-ball decay through an elementary process (squark) $\to$ (quark) + (particle χ). We denote the mass of χ as m_χ. Since the total energy of this process is given by the energy of the Q-ball per unit charge, ω_0, the particle χ obtains energy in the range of $[m_\chi, \omega_0]$ and the quark obtains energy in the range of $[0, \omega_0 - m_\chi]$. Their flux is determined by the following procedure. Due to conservation of energy and angular momentum, quark flux with the energy of E have to coincide with χ flux with the energy of $\omega_0 - E$. Since either of them cannot exceed upper bound on their flux due to the Pauli blocking effect, their flux is determined by the severer bound. The quark flux with the energy of E is proportional to $\mathrm{d}p_{\mathrm{quark}} = \mathrm{d}E$, while the χ flux with the energy of

[5] It has been shown that the rates of N (≥ 3) body scattering processes are not saturated by the Pauli blocking effect and we can neglect these processes.

$\omega_0 - E$ is proportional to $v_\chi \times \mathrm{d}p_\chi = p_\chi/E \times E/p_\chi \mathrm{d}E = \mathrm{d}E$, where we use $p_\chi^2 = (\omega_0 - E)^2 - m_\chi^2$. We obtain their flux at the Q-ball surface as

$$\boldsymbol{n} \cdot \boldsymbol{j_\chi} \simeq \frac{1}{8\pi^2} \int_0^{\omega_0 - m_\chi} \mathrm{d}E \min\left[E^2, (\omega_0 - E)^2 - m_\chi^2\right]. \tag{4.58}$$

This integral can be performed analytically and we obtain the following correction to the flux given in Eq. (4.55):

$$\boldsymbol{n} \cdot \boldsymbol{j}_\chi \simeq \frac{\omega_0^3}{96\pi^2} \times f(m_\chi/\omega_0), \tag{4.59}$$

$$f(x) \equiv \begin{cases} 1 - 6x^2 + 8x^3 - 3x^4 & \text{for } 0 \le x \le 1 \\ 0 & \text{for } 1 < x. \end{cases} \tag{4.60}$$

The fluxes of massive gauginos and/ro higgsinos are given by this formula.

4.3.3 Decay temperature

Q-balls completely lose their charge and energy when the condition $\Gamma_Q \sim H$ is satisfied. The decay temperature of Q-ball is thus determined as

$$T_{\mathrm{decay}} \simeq \begin{cases} T_{\mathrm{RH}} \left(\sqrt{\frac{30}{\pi^2 g_*}} \frac{\Gamma_Q M_{\mathrm{Pl}}}{T_{\mathrm{RH}}^2} \right)^{1/4} & \text{for } T_{\mathrm{decay}} > T_{\mathrm{RH}}, \\ \left(\frac{90}{4\pi^2 g_*} \right)^{1/4} \sqrt{\Gamma_Q M_{\mathrm{Pl}}} & \text{for } T_{\mathrm{decay}} < T_{\mathrm{RH}}, \end{cases} \tag{4.61}$$

where the first line is the case where Q-balls decay before reheating completes while the second one is the case where Q-balls decay after reheating completes. In the latter case, the energy density of Q-balls may dominate the Universe. Since Q-balls are localized lumps much smaller than the horizon scale, their energy density decreases as a^{-3}, where a is a scale factor. Thus the energy density of Q-balls never dominate that of the Universe when the following condition is satisfied:

$$1 \gtrsim \left. \frac{\rho_Q}{\rho_{\mathrm{rad}}} \right|_{T = T_{\mathrm{decay}}} \simeq \left. \frac{\rho_Q}{\rho_{\mathrm{rad}}} \right|_{T = T_{\mathrm{RH}}} \left(\frac{T_{\mathrm{RH}}}{T_{\mathrm{decay}}} \right), \tag{4.62}$$

$$\simeq \left. \frac{\rho_Q}{\rho_{\mathrm{inf}}} \right|_{\mathrm{osc}} \left(\frac{T_{\mathrm{RH}}}{T_{\mathrm{decay}}} \right) \simeq \frac{\phi_{\mathrm{osc}}^2}{3M_{\mathrm{Pl}}^2} \left(\frac{T_{\mathrm{RH}}}{T_{\mathrm{decay}}} \right), \tag{4.63}$$

where ρ_Q, ρ_{rad}, and ρ_{inf} are the energy densities of Q-balls, radiation, and inflaton, respectively.

Here we write a typical decay temperature of Q-balls. In gravity-mediated SUSY breking models, it is given by

$$T_{\rm decay} \simeq 2\,{\rm GeV}\left(\frac{\omega_0}{10^3\,{\rm GeV}}\right)^{1/2}\left(\frac{Q}{10^{23}}\right)^{-1/2}, \tag{4.64}$$

where we assume $n_q = 10$, $\tilde{R} = 20/\omega_0$, and $T_{\rm RH} > T_{\rm decay}$. In gauge-mediated SUSY breking models, it is given by

$$\begin{aligned} T_{\rm decay} &\simeq 0.1\,{\rm GeV}\left(\frac{\omega_0}{100\,{\rm GeV}}\right)^{1/2}\left(\frac{Q}{10^{23}}\right)^{-1/2} & (4.65)\\ &\simeq 0.08\,{\rm GeV}k^{3/4}\left(\frac{m_{3/2}}{1\,{\rm MeV}}\right)^{1/4}\left(\frac{Q}{10^{23}}\right)^{-5/8}, & (4.66)\end{aligned}$$

where we assume $n_q = 10$, $c = 6$, and $T_{\rm RH} > T_{\rm decay}$, and use $\tilde{R} = \pi/\omega_0$. These low decay temperatures imply that the decay of Q-balls can be a non-thermal source of DM.

Chapter 5

Co-genesis from Q-ball decay

This chapter is based on the work done by the author [30]. As explained in Chap. 2, the observed baryon and DM densities are equal up to a factor of 5, which indicates that the baryon asymmetry and DM have a common origin. In this chapter, we provide a scenario that explains the coincidence in gravity-mediated SUSY breaking models including the CMSSM, where the baryons and DM are generated simultaneously through the late-time decay of Q-balls. In particular, the scenario can be naturally realized in chaotic inflation models as shown in the next chapter.

5.1 Scenario for co-genesis from Q-ball decay

As explained in Chap. 2, the observed energy densities of baryon and DM are equal to each other up to a factor of 5. This coincidence is a mystery known as the baryon-DM coincidence problem.

In this section, we provide a scenario for co-genesis of baryon and DM to overcome the baryon-DM coincidence problem in models of gravity-mediated SUSY breaking [24]. The baryon asymmetry is generated in the early Universe as a form of squark ($\tilde{q}$) condensation by ADBG, which then fragments into Q-balls (see Chap. 4) [24, 26, 22, 23, 25]. Although Q-balls are very long-lived, they decay before the Big Bang Nucleosynthesis epoch through baryon-number-conserving elementary processes, such as the decay of squark into quark (q) and gaugino ($\tilde{g}$) (see Sec. 4.3) [27]. Since the gaugino subsequently decays into the LSP DM, the baryon (quark) and DM (LSP) are generated simultaneously by the decay of Q-balls. In the original work of the scenario for the co-genesis proposed in Ref. [24], they focused on the process of squark decay into quark and gaugino, which implies that the number of quarks is the same as that of the LSP due to the R-parity conservation. To explain the

baryon-DM coincidence problem, they concluded that the mass of DM has to be $\mathcal{O}(1)$ GeV. Since this is excluded by the collider experiments, alternative scenarios have been proposed in Refs. [28, 80, 81, 82]. However, as we see in Sec. 4.3, we should take into account the annihilation of squarks inside Q-balls. As a result, we find that the branching ratio into SUSY particles is of order 0.01 and the resulting baryon-to-DM ratio is naturally of order unity for the LSP with mass of $\mathcal{O}(100)$ GeV [35, 30].

In this section, we generically consider gravity-mediated SUSY breaking models, where the mass of the AD field $m_\phi(|\phi|)$ logarithmically depends on $|\phi|$ due to the renormalization group running of squark masses. In many cases, the strong interaction dominates quantum corrections for a typical flat direction, and we obtain $K < 0$ and $|K| \sim 0.01 - 0.1$ [24] [see Eq. (4.14)], which satisfies the condition for Q-ball formation in Eq. (4.8).

Since we are interested in the non-thermal production of DM from Q-ball decay, it has to be generated from Q-ball after DM freezes out for the pair annihilation of LSPs to be ineffective. This implies that the Q-ball decay temperature of Eq. (4.64) is much smaller than the mass of DM. This indicates that the charge of Q balls should be $Q \gtrsim 10^{26}$ and thus the magnitude of the scalar field at the onset of oscillation is given by $\phi_0 \gtrsim 10^{13} m_\phi(\phi_0)$.

As we have explained in Sec. 4.3, the decay rate of Q-ball is saturated and determined by the Pauli blocking effect. While SUSY particles are produced from the Q-ball surface only through elementary decay process like (squark) $\to$ (quark) + (gaugino), quarks are dominantly produced through scattering process via gaugino or Higgsino exchange like (squark) + (squark) $\to$ (quark) + (quark) [34]. Thus, the ratio of the Q-ball decay into sparticles and quarks is calculated as

$$\frac{\mathrm{Br}(Q\text{−ball} \to (\text{gauginos}))}{\mathrm{Br}(Q\text{−ball} \to (\text{quark}))} \simeq \frac{n_s}{8 n_q}, \tag{5.1}$$

where a factor of 8 is due to the difference of the elementary processes. The factor n_s is the effective number of sparticles into which Q-balls can decay. Since the flux of massive particles from a Q-ball surface is smaller than that of massless particles, there is a correction due to non-zero sparticle masses [see Eq. (4.60)]. Thus we obtain

$$n_s = \sum_s g_s f(m_s/\omega_0), \tag{5.2}$$

where m_s is the mass of the sparticle s, g_s is the number of species for the sparticle and f is a function given in Eq. (4.60). For example, $g_s = 1$, 3, and 8 for the bino, wino, and gluino, respectively.[1] However, Q-balls can decay only into particles lighter than the energy of the

[1] Note that g_s also depends on the flat direction. In the case of $\bar{u}\bar{d}\bar{d}$ flat direction, Q-balls do not decay into winos, $g_{\mathrm{wino}} = 0$, because they consists of only right-handed squarks [35].

Q-ball per unit charge, ω_0, which is approximately equal to the mass of squarks at the energy scale of $|\phi|$ ($\sim 10^{15}$ GeV). In a typical model of gravity mediation, a mass of squarks at the energy scale of 10^{15} GeV is mostly smaller than the mass of the gluino and larger than that of the bino (LSP). Thus in the typical models Q-balls can decay into binos, and not into gluino.[2] Depending on a model, Q-balls can also decay into winos and Higgsinos. Hereafter, we assume Q-balls can not decay into Higgsinos, for simplicity.

Since all sparticles eventually decay into binos,[3] we obtain the following formula for the baryon-to-DM ratio:[4]

$$\frac{\Omega_{\rm DM}}{\Omega_b} = \frac{m_{\tilde{b}}}{|b|\, m_p} \frac{n_s}{8 n_q}, \tag{5.3}$$

$$\simeq \frac{m_{\tilde{b}}}{|b|\, m_p} \frac{\sum_s f(m_{\rm s}/\omega_0)}{8 n_q}. \tag{5.4}$$

We should emphasize that this ratio is independent of the reheating temperature and the charge of Q-balls. As an illustration, let us calculate two asymptotic solutions. When $m_s \ll \omega_0$, the function f approaches 1 [see Eq. (4.60)] and $n_s \simeq 12$, where we have included contributions from gauginos. On the other hand, if $m_{\tilde{b}} \to \omega_0$ with other particles mass larger than ω_0, a combination of $m_{\tilde{b}} n_s/\omega_0$ approaches $4(1 - m_{\tilde{b}}/\omega_0)^3 \ll 1$. Thus we obtain two asymptotic solutions for the bino mass, which yields the correct ratio of DM and baryon density;

$$m_{\tilde{b}} \approx \begin{cases} 0.7 n_q\, |b|\, m_p \frac{\Omega_{\rm DM}}{\Omega_b} \simeq 10 \text{ GeV} & (\omega_0 \gg m_s) \\ \omega_0 \left[1 - \left(2 n_q\, |b|\, \frac{\Omega_{\rm DM}}{\Omega_b} \frac{m_p}{\omega_0} \right)^{1/3} \right] & (m_{\tilde{b}} \to \omega_0), \end{cases} \tag{5.5}$$

where we assume $n_q = 10$ and $b = 1/3$ in the first line. The bino mass of 10 GeV is unrealistic for ordinary models in gravity mediation. We conclude that we can explain the observed baryon-to-DM ratio if the bino mass is close to below ω_0.

In Fig. 5.1, we show the constraint on ω_0 and $m_{\tilde{b}}$. On the boundary of and inside the blue shaded region, the DM density produced by the decay of Q-balls is equal and larger than the observed value respectively. Here, we have assumed the grand unified theory (GUT) relation, where the masses of the wino and gluino are two and six times larger than that of the bino

[2] Even in this case Eq. (5.2) is valid since $f(x > 1) = 0$.

[3] For the case of the axino LSP, see Refs. [81].

[4] We do not include the quarks from the process of (squark) $\to$ (quark) + (bino), because the quarks production rates are determined by the Pauli exclusion principle and the phase space of the quarks produced by the squark decay is a subset of that of the quarks produced by the squark annihilation.

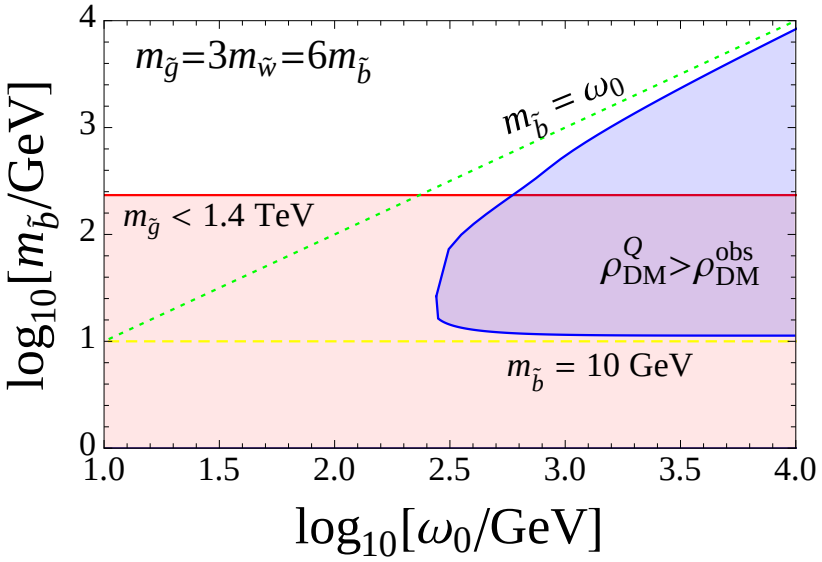

Figure 5.1: Exclusion plot in a model of gravity mediation with Q-ball formation. We assume that the number of quarks interacting with Q-ball, n_q, is 10 and baryon charge of the AD field, b, is $-1/3$. We also assume that the masses of the wino and gluino are two and six times larger than that of the bino, which is a typical case in gravity mediation with the grand unified theory relation. The abundance of DM produced from Q-ball decay is larger than that observed in the blue shaded region. In the red shaded region, the gluino mass is smaller than 1.4 TeV and excluded by the gluino search at the ATLAS Collaboration [83]. The green-dotted and yellow-dashed lines indicate the limit of $m_{\tilde{b}} \to \omega_0$ and $m_{\tilde{b}} \to 10$ GeV, respectively.

(see Appendix A.1.2). Under the GUT relation, the red shaded region is already excluded by the gluino search at the ATLAS Collaboration [83].

5.2 Application to the CMSSM

In this section, we apply the scenario explained in the previous section to the CMSSM, which is defined by only five parameters at the GUT scale ($\simeq 2 \times 10^{16}$ GeV) and is one of the simplest SUSY extended Standard Models. The discovery of the 125-GeV Higgs boson by the LHC experiment [1, 2] and theoretical 3-loop calculations of Higgs mass implies that the masses of SUSY particles are $\mathcal{O}(1)$ TeV [84, 85].

We assume a reheating temperature lower than the LSP freeze-out temperature to dilute the thermal relic density of the LSP. Note that since we consider a scenario for non-thermal production of DM, the phenomenological aspects are different from those of conventional

bino thermal relic scenarios. In conventional scenarios, the bino LSP and the stau have to be nearly degenerate in mass and their mass has to be smaller than about 1 TeV to obtain the required annihilation cross section. On the other hand, co-genesis mitigates the required degeneracy and allows heavier SUSY particles. It follows that our scenario is compatible with both the discovery of 125 GeV Higgs boson and null-detection of SUSY particles. The abundance of DM produced through the reheating process is negligible for a sufficiently low reheating temperature $T_{\rm RH} \lesssim \mathcal{O}(100)\,\text{MeV}$ and a sufficiently large inflaton mass [86]. Such a low reheating temperature is also favoured in light of baryonic isocurvature constraints as shown in Sec. 3.5 [65, 66, 58, 29]. Hereafter, we take the reheating temperature as a free parameter less than $\mathcal{O}(1)$ GeV.

If the beta function of the mass for the AD field K is negative, it leads to an instability of the homogeneous solution of the AD field. This results in the formation of Q-balls [24, 26, 22, 23, 25]. We have calculated beta functions for the mass of flat directions using the code `SOFTSUSY 3.3.6` [87] and have found that the beta function is indeed negative in most of the parameter space in which the co-genesis scenario can be realized (see Figs. 5.2 and 5.3).

Q-balls decay during inflaton-oscillation (matter-dominated) era in the relevant CMSSM parameter region (shown in Figs. 5.2 and 5.3). Thus we define the Q-ball decay temperature $T_{\rm d}$ by the first line in Eq. (4.61). In the CMSSM, Q-balls can decay solely into binos among SUSY particles via the squark decay[5]

$$\frac{\Omega_{\rm DM}}{\Omega_B} \simeq \frac{3m_{\tilde{b}}}{m_p}\frac{f(m_{\tilde{b}}/\omega_0)}{8n_q}, \tag{5.6}$$

where $m_{\tilde{b}}$ and m_p are the bino mass and the proton mass, respectively. We should emphasize that the resulting baryon-to-DM ratio Eq. (5.6) depends only on the masses of SUSY particles except for n_q, which is typically $\mathcal{O}(10)$. This simple ratio illustrates that our co-genesis scenario can be realized not only in the CMSSM but also in a wide class of SUSY models. Note that the resulting baryon-to-DM ratio of Eq. (5.6) naturally results in $\mathcal{O}(1)$ when the mass of the LSP $m_{\rm LSP}$ is $\mathcal{O}(1)$ TeV and the function f is $\mathcal{O}(0.1)$.

The annihilation of LSPs produced via Q-ball decay might spoil the baryon-to-DM ratio of Eq. (5.6).[6] Here we check its efficiency. One might wonder that the spatial distribution of LSPs is localized around the Q-balls. However, the spatial distribution of LSPs becomes

[5]The decays into the other gauginos and higgsinos are kinematically forbidden for the parameter set in which the following co-genesis scenario is realized and the Higgs mass is consistent with the observation, though we correctly take into account these decay channels in our analysis.

[6]If we consider the case that the pair annihilation is effective, the resultant LSP density is determined by the mass of LSP, the pair annihilation rate of LSP, and the decay temperature of the Q ball [28, 80]. Thus, the branching ratios of the Q-ball decay do not affect the ratio of the baryon to LSPs.

homogeneous due to their free streaming before its thermalization and annihilation become effective [24]. The annihilation is ineffective when $n_{\rm DM}\langle\sigma v\rangle \lesssim H$ is satisfied at the time of Q-ball decay. We estimate the annihilation cross section $\langle\sigma v\rangle$ as follows. First, we check whether the LSPs kinematically thermalized due to elastic interactions with the thermal plasma or not. Since the LSP is mostly bino, the elastic scattering through sfermion exchange is in charge of losing their energy. The energy-loss rate is given as

$$-\frac{{\rm d}E_{\tilde{b}}}{E_{\tilde{b}}{\rm d}t} = \sum_i \frac{31\pi^3}{5120} g_1^4 \frac{T^6}{m_{\tilde{b}}^6} E_{\tilde{b}} \left(1-\frac{m_{\tilde{b}}^2}{E_{\tilde{b}}^2}\right)\left(6\frac{E_{\tilde{b}}^2}{m_{\tilde{b}}^2}-1\right) \times \left\{\left(\frac{Y_L^2}{m_{\tilde{f}_L}^2/m_{\tilde{b}}^2-1}\right)^2 + \left(\frac{Y_R^2}{m_{\tilde{f}_R}/m_{\tilde{b}}^2-1}\right)^2\right\}, \tag{5.7}$$

with $g_1 = \sqrt{5/3}g_Y$, left/right-handed sfermion masses $m_{\tilde{f}_{L/R}}$, $Y_L = -1/2, 1/6$ for leptons and quarks, and $Y_R = -1, 2/3, -1/3$ for charged leptons, up- and down-type quarks. The summation is taken for all relativistic particles. We average the energy-loss rate over non-thermal distribution, that is, we integrate it in terms of the energy of the bino $E_{\tilde{b}}$ with the weight given by the flux of bino at the surface of Q-ball. If the energy-loss is larger than the Hubble expansion rate, we use the thermally averaged annihilation cross section. Otherwise, we adopt the non-thermal annihilation cross section. The sfermion exchange dominates the annihilation of LSPs, whether the produced LSPs are thermalised or not. For the thermally averaged annihilation cross section, we consider s- and p-wave contributions [88]. When we calculate the non-thermal annihilation cross section, we ignore the fermion masses and average it over non-thermal distribution determined by the Q-ball decay.

Note that the Q-ball decay temperature $T_{\rm d}$ is proportional to $Q^{-1/4}T_{\rm RH}^{1/2}$ and hence is proportional to $T_{\rm RH}^{3/4}$ [see Eqs. (3.66), (4.12), and (4.64)]. This implies that when we consider a sufficiently high reheating temperature, the energy-loss rate Eq. (5.7) is so large that the bino-like LSP is thermalized. If the LSP is thermalized (high $T_{\rm RH}$), its annihilation cross section is so small that its annihilation can be neglected. If the LSP is not thermalized (low $T_{\rm RH}$), its annihilation cross section is independent of $T_{\rm RH}$ and is sizable. Here, noting that at the time of Q-ball decay $n_{\rm DM} \propto T_{\rm d}^8/T_{\rm RH}^5$ and $H \propto T_{\rm d}^4/T_{\rm RH}^2$ [see Eq. (4.61)], we find that $n_{\rm DM}/H$ is independent of $T_{\rm RH}$. It follows that the efficiency of the annihilation $n_{\rm DM}\langle\sigma v\rangle/H$ at $T = T_{\rm d}$ is independent of $T_{\rm RH}$ once the LSP is not thermalized. Therefore, there should be a region in which the annihilation can be neglected independently on $T_{\rm RH}$ (see the light green lines in Figs. 5.2 and 5.3).

We explicitly calculate the baryon-to-DM ratio of Eq. (5.6) in the CMSSM, where all

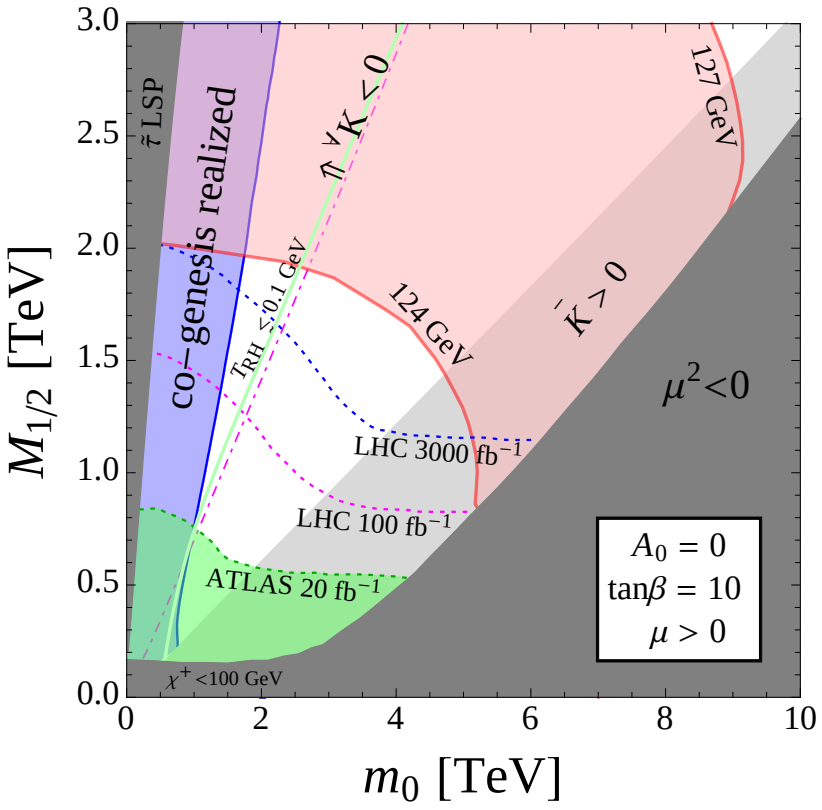

Figure 5.2: Allowed contours consistent with observations in two $(m_0, M_{1/2})$ planes of the CMSSM, with $\tan\beta = 10$ and $A_0 = 0$ with $\mathrm{sign}[\mu] = +1$. We can account for the baryon-to-DM ratio as well as baryon density in the blue shaded region, where we use $n_q \leq 36$. The red lines represent contours for the mass of the Higgs boson. The annihilation of the LSP is ineffective above the light green lines, which is plotted in the case of $T_{\rm RH} \lesssim 0.1\,\mathrm{GeV}$. Above the magenta dot-dashed line, $K < 0$ for all squarks. In the light gray region, the averaged value of K is positive. The dark gray shaded areas are excluded either because the LSP is charged, there is no consistent electroweak vacuum, or the mass of chargino is less than 100 GeV. The light green regions are excluded by the ATLAS search. The 14 TeV LHC with 100 fb^{-1} and 3000 fb^{-1} would probe the parameter space below the magenta and blue dotted line, respectively. We assume that the top quark pole mass as $m_t^{\rm pole} = 173.3\,\mathrm{GeV}$.

parameters are defined at the GUT scale ($\simeq 2 \times 10^{16}$ GeV); the universal scalar mass (m_0), the universal gaugino mass ($M_{1/2}$), the universal trilinear scalar coupling (A_0), the ratio of the VEV of the two Higgs fields ($\tan\beta$), and the sign of the higgsino mass parameter ($\mathrm{sign}[\mu]$). Low scale SUSY parameters, especially mass spectrum used in Eq. (5.6), are obtained by solving renormalization group equations. To this end, we use `SOFTSUSY 3.3.6` [87].

Let us summarize our procedure. Given a reheating temperature $T_{\rm RH}$, we obtain the

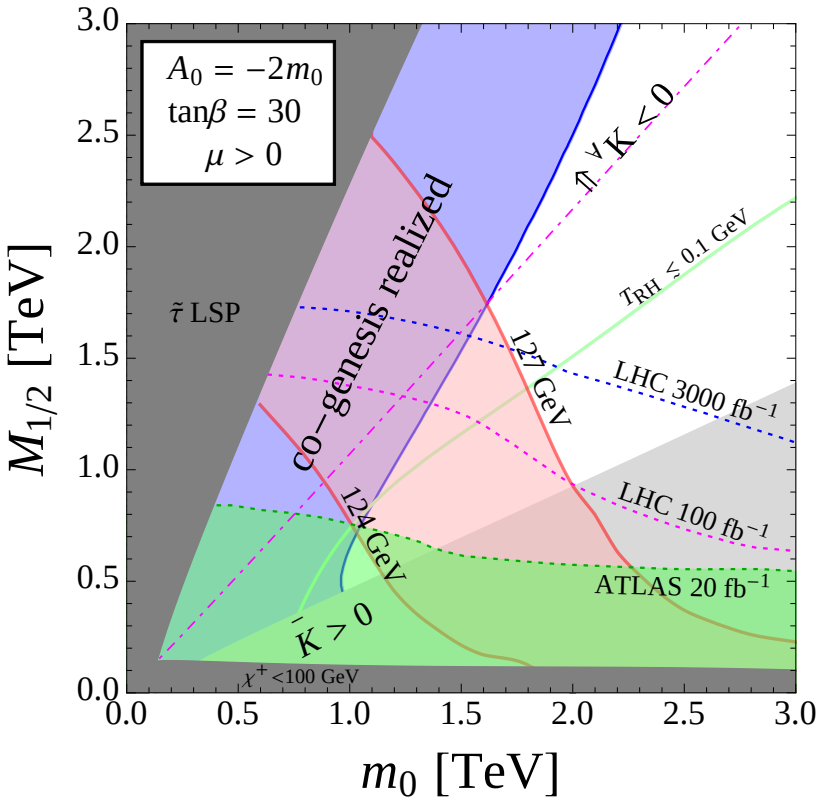

Figure 5.3: Same as Fig. 5.2 but with $\tan\beta = 30$ and $A_0 = -2m_0$.

VEV of the flat direction $\phi_{\rm osc}$ from Eq. (3.66), which then determines the charge of Q-balls from Eq. (4.12). For each CMSSM parameter set, we obtain the beta function K and the mass of the flat direction m_ϕ and bino $m_{\tilde{b}}$ by solving the renormalization group equations numerically with the code `SOFTSUSY 3.3.6` [87]. Here we take the parameters K and m_ϕ as averages of beta functions and masses over all squarks at the energy scale of ϕ_0. Then we can calculate the baryon-to-DM ratio from Eq. (5.6). Figure 5.2 is the result for the case of relatively small $\tan\beta$ and A_0, which require relatively large stop mass to explain the 125-GeV Higgs boson. Figure 5.3 is the result for the case of relatively large $\tan\beta$ and large mixings in the stop sector (i.e., $A_0/m_0 \sim \pm 2.5$), where relatively small stop mass can be consistent with the 125-GeV Higgs boson. The figures show that the baryon-to-DM ratio and their absolute abundance can be consistent with the observed values in the blue shaded region. The result implies the relation $m_0 \sim M_{1/2}$ to realize the co-genesis scenario. This is because the function f in Eq. (4.60) has to be suppressed for bino mass of $\mathcal{O}(1)$ TeV, that is, $m_{\tilde{b}} \simeq \omega_0$ ($\simeq m_0$). Note that the result is insensitive to the value of reheating temperature $T_{\rm RH}$ because ω_0 in Eq. (5.6) depends on $T_{\rm RH}$ only logarithmically.

We have checked whether or not the beta function of the mass for the flat direction K is negative, which is a condition for Q-ball formation. Above the magenta dot-dashed line in Figs. 5.2 and 5.3, the beta functions of all squarks are negative, which means that Q-balls are always formed after the Affleck-Dine baryogenesis. In the light gray region, the averaged value of K is positive and Q-balls cannot be formed unless the flat direction consists mainly of first and second family squarks. One can see that Q-balls actually form after ADBG in most of the blue shaded regions.

The annihilation of the LSP is ineffective above the light green lines in Figs. 5.2 and 5.3, where we assume $T_{\rm RH} \lesssim 0.1\,{\rm GeV}$. For higher reheating temperature, the annihilation of the LSP is less effective, as long as the reheating temperature is sufficiently lower than the mass of the LSP such that the thermal relic density of the LSP can be ignored. This is because for a higher reheating temperature, LSP's are well thermailzed and its annihilation cross section is p-wave suppressed. One can see that the annihilation effect is irrelevant in most of the blue shaded regions and Eq. (5.6) is justified.

In Figs. 5.2 and 5.3, the red curves are contours of Higgs mass calculated with the numerical code `FeynHiggs 2.10.0` [89, 90, 91, 92, 93]. Note that there are uncertainties in the predicted Higgs mass coming mainly from the uncertainties in the top mass and higher loop corrections. We have found that the co-genesis scenario can be consistent with the observed 125 GeV Higgs mass.

The light green regions are excluded by the ATLAS search for $\not{E}_T$ events with 20 fb^{-1} of

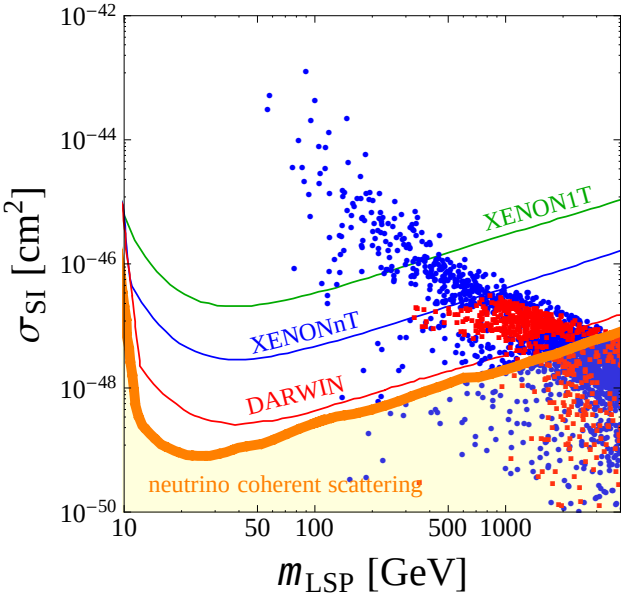

Figure 5.4: Spin-independent cross sections for the interactions of the LSP on nucleons as a function of LSP mass, and sensitivities of future DM direct detection experiments [98]. The green, blue, and red curves are the future sensitivities for XENON1T [99], XENONnT, and DARWIN [100], respectively. The yellow region is experimentally unaccessible due to irreducible neutrino backgrounds [101]. The blue dots correspond to sets of CMSSM parameters for the co-genesis scenario, while the red ones correspond to those realizing the observed Higgs mass as well as the co-genesis scenario.

data at 8 TeV [85], which has been shown to be independent of $\tan\beta$ and A_0 [94]. The 14 TeV LHC with 100 fb^{-1} and 3000 fb^{-1} would probe the parameter space below the magenta and blue dotted line, respectively [84, 95, 96]. Our results with the observed 125-GeV Higgs boson is consistent with the ATLAS results and would be partially tested by future LHC experiments.

We also use the code `micrOMEGAs 3.6.9` to calculate the spin-independent interactions of the LSP on nucleons [97]. The CMSSM parameters are generated randomly in the ranges $m_0 = 0$ - 10 TeV, $M_{1/2} = 0$ - 10 TeV, $A_0 = (-3m_0)$ - $(3m_0)$, $\tan\beta = 1$ - 60, and sign$[\mu] = \pm 1$ with a flat distribution. The results are plotted as blue dots in Fig. 5.4 when the co-genesis scenario is realized, while they are plotted as red dots when the Higgs mass, baryon density, and DM density are consistent with the observations. We find that XENONnT and DARWIN [100] can test a significant part of the parameter region for the co-genesis scenario consistent with the 125 GeV Higgs boson.

Chapter 6

Inflation and ADBG

This chapter is based on the works done by the author [29, 32]. In this chapter, we investigate the relation between ADBG and inflation. We focus on three typical models of inflation in SUSY theories: F-term hybrid, D-term hybrid, and chaotic inflation.

As we can see from Eq. (3.66), the baryon asymmetry generated via ADBG may depend on reheating temperature $T_{\rm RH}$. To determine it, we consider the decay of inflaton for each inflation model.

Since the AD field obtains a large VEV during inflation, we may need to take into account its effect on inflaton dynamics via supergravity effects.[1] In fact, there are many works revealing that a constant term in superpotential and a scalar field with a large VEV may affect inflaton dynamics [104, 105, 106, 107]. These effects may rescue the F-term hybrid and chaotic inflation models, which themselves are somewhat inconsistent with the observations of CMB temperature anisotropies. We investigate the backreaction of ADBG to inflaton dynamics in the F-term and D-term hybrid and chaotic inflation models in supergravity. Focusing on LH_u flat direction, we determine the lightest neutrino mass in these models so that the predictions of spectral index, tensor-to-scalar ratio, and baryon abundance are consistent with observations.

6.1 F-term hybrid inflation

In this section, we consider the simplest model of F-term hybrid inflation [59, 60]. We first explain its model and the reheating process. Then we discuss the backreaction of the AD field to inflaton dynamics.

[1] See Refs. [102, 103] for the case that the AD field also plays the role of inflaton.

6.1.1 Model

The superpotential of the inflaton sector is given by

$$W^{(\mathrm{inf})} = \kappa S\left(\psi\bar{\psi} - \mu^2\right), \tag{6.1}$$

where κ is a coupling constant, S is inflaton, and ψ and $\bar{\psi}$ are superfields that are charged under a U(1) gauge symmetry. Since the D-term potential gives a D-flat condition of $|\psi| = \left|\bar{\psi}\right|$, we write a flat direction called a waterfall field such as $\psi_+ = (\psi + \bar{\psi})/\sqrt{2}$ and its minimal VEV as $\langle\psi_+\rangle_{\mathrm{min}} \equiv v = \sqrt{2}\mu$. The F-term potentials are given as

$$V_{\mathrm{inf}}|_{\mathrm{tree}} = \kappa^2 \left|\frac{\psi_+^2}{2} - \mu^2\right|^2 + \kappa^2 |S|^2 |\psi_+|^2 . \tag{6.2}$$

When the inflaton S has a sufficiently large VEV, the fields ψ and $\bar{\psi}$ obtain large effective masses of $\kappa\langle S\rangle$ and thus stay at the origin of the potential. Then the F-term of S is nonzero and drives inflation, where the energy scale of inflation is given by

$$\begin{aligned} H_{\mathrm{inf}} &\simeq \frac{\kappa\mu^2}{\sqrt{3}M_{\mathrm{Pl}}} && (6.3)\\ &\simeq 2.4\times 10^8\ \mathrm{GeV}\left(\frac{\kappa}{10^{-3}}\right)\left(\frac{\mu}{10^{15}\ \mathrm{GeV}}\right)^2 . && (6.4) \end{aligned}$$

The inflaton s ($\equiv |S|/\sqrt{2}$) slowly rolls toward the origin due to the 1-loop Coleman-Weinberg potential:

$$\begin{aligned} V_{\mathrm{inf}}|_{1-\mathrm{loop}} &= \frac{\kappa^4\mu^4}{32\pi^2}\left[\left(x^2+1\right)^2 \ln\left(x^2+1\right) + \left(x^2-1\right)^2 \ln\left(x^2-1\right) - 2x^4 \ln x^2 - 3\right] && (6.5)\\ &\simeq \frac{\kappa^4\mu^4}{16\pi^2}\ln x^2, && (6.6) \end{aligned}$$

where we define $x \equiv |S|/\mu \equiv s/v$ and use $x \gg 1$ in the second line. The inflaton s slowly rolls down to the origin of the potential until its VEV reaches the critical value of $s_{\mathrm{cr}} \equiv v$. The COBE normalization requires [15, 6]

$$\mu \simeq \left(\frac{3A_s}{4\mathcal{N}_*}\right)^{1/4} \simeq 5.7\times 10^{15}\ \mathrm{GeV}, \tag{6.7}$$

where we assume $\mathcal{N}_* = 50$ in the second equality. The e-folding number, slow-roll parameters, and spectral index are given by

$$\mathcal{N}_* \simeq \frac{8\pi^2}{\kappa^2} s_*^2 \tag{6.8}$$

$$\epsilon_s \simeq \frac{1}{2}\left(\frac{\kappa^2}{16\pi^2}\right)^2 \frac{1}{s_*^2} \tag{6.9}$$

$$\eta_s \simeq -\frac{\kappa^2}{16\pi^2}\frac{1}{s_*^2} \simeq -\frac{1}{2\mathcal{N}_*} \tag{6.10}$$

$$n_s \simeq 1 - 1/\mathcal{N}_* \simeq 0.98, \tag{6.11}$$

where s_* is the field value at the e-folding number of $\mathcal{N}_*$ and $\mathcal{N}_*$ (≈ 55) is the e-folding number at the horizon exit of the pivot scale (see Appendix B). When the inflaton s reaches a critical VEV of $s_{\rm cr}$, the waterfall field and inflaton start to oscillate about their global minimum and inflation ends. Around the minimum of the potential, the masses of inflaton and waterfall field are given by $\sqrt{2}\kappa\mu$.

Since U(1) symmetry is spontaneously broken by the VEV of waterfall field, cosmic strings form after inflation. In the F-term hybrid inflation model, the energy density of cosmic string per unit length $\mu_{\rm CS}$ is calculated as (see, e.g., Ref. [108])

$$\mu_{\rm CS} = 2\pi B(\kappa^2/e^2)\mu^2 \tag{6.12}$$

$$B(x) \simeq \begin{cases} 1.04x^{0.195} & \text{for } \ 10^{-2} < x \ll 1 \\ 2.4\ln^{-1}(2/x) & \text{for } \ x < 10^{-2}, \end{cases} \tag{6.13}$$

where e is U(1) gauge coupling constant. They contribute to the spectrum of CMB temperature anisotropies, so that their energy density is bounded above by observations [109]:

$$G\mu_{\rm CS} \lesssim 3.2 \times 10^{-7}, \tag{6.14}$$

where $G \equiv 1/(8\pi M_{\rm Pl}^2)$.

Pulsar timing arrays put a constraint on the energy density of stochastic gravitational-wave background, which can be recast into a constraint on the string tension because cosmic strings emit gravitational waves via decaying string loops. The recent results from the North American Nanohertz Observatory for Gravitational Waves (NANOGrav) collaboration put a conservative bound such as [110]

$$G\mu_{\rm CS} \lesssim 3.3 \times 10^{-8}, \tag{6.15}$$

where they allow loop size to be a free parameter. The Square Kilometre Array (SKA) telescope will improve this constraint by one or two order of magnitudes [111].

In this simplest model, the spectral index is predicted as $n_s \simeq 0.98$ [see Eq. (6.11)], which is inconsistent with the observed value more than 2 sigma level: $n_s^{(\rm obs)} = 0.963 \pm 0.008$ [109]. The tension of the cosmic string Eq. (6.13) is also inconsistent with the constraint by the CMB observation. However, some modifications can make them consistent with the observed value and constraint [112, 113]. In Sec. 6.1.3 we also show that the backreaction of the AD field on the inflaton dynamics can make the spectral index and tension of cosmic string consistent with the constraint.

6.1.2 Reheating temperature

As we can see from Eq. (3.66), the resulting baryon asymmetry may depend on reheating temperature $T_{\rm RH}$. Here we consider the decay of inflaton, which determines the reheating temperature. There is a lower bound on the reheating temperature because the inflaton decays into the MSSM particles via supergravity effects. The fields ψ and $\bar{\psi}$ can be written as

$$\psi_\pm \equiv \frac{\psi \pm \bar{\psi}}{\sqrt{2}}. \tag{6.16}$$

The ψ_+ is the waterfall field, which starts to oscillate after inflation, while ψ_- does not because of D-term. Thus around the minimum of the potential, the superpotential is reduced to be Eq. (B.25) with $m_{\rm inf} = \sqrt{2}\kappa\mu$ and the replacements of $S \to \psi_+$ and $X \to S$. Thus we can use the results in Appendix with $K_S = \sqrt{2}\mu$. From Eq. (B.29), the lower bound on the reheating temperature is given by [114]

$$T_{\rm RH}^{(\rm min)} \simeq 3 \times 10^3 \text{ GeV} \, |y_t| \left(\frac{\mu}{10^{15} \text{ GeV}}\right) \left(\frac{m_{\rm inf}}{10^{12} \text{ GeV}}\right)^{3/2}. \tag{6.17}$$

If there is an interaction between the inflaton and Higgs fields such as

$$W \supset y S H_u H_d, \tag{6.18}$$

then the inflaton decay rate and the reheating temperature are estimated as

$$\Gamma_{\rm inf} = \frac{y^2}{4\pi} m_\phi \tag{6.19}$$

$$T_{\rm RH} \simeq 2 \times 10^{10} \text{ GeV} \left(\frac{y}{10^{-4}}\right) \left(\frac{m_{\rm inf}}{10^{12} \text{ GeV}}\right)^{1/2}. \tag{6.20}$$

Note that the coupling constant y should be smaller than κ so as not to affect the Coleman-Weinberg potential of Eq. (6.6). Thus the reheating temperature cannot be higher than that of Eq. (6.20) with $y \approx \kappa$.

We have to take into account the constraint on $T_{\rm RH}$ from gravitino overproduction problems. The inflaton decays also into gravitinos via supergravity effects. Its production rate is given by Eq. (B.34). The resulting gravitino-to-entropy ratio from this contribution is given by

$$Y_{3/2}^{(\rm decay)} \simeq \frac{3}{2}\left(\frac{90}{g_*\pi^2}\right)^{1/2}\frac{\Gamma_{3/2}M_{\rm Pl}}{m_{\rm inf}T_{\rm RH}}. \tag{6.21}$$

Gravitinos are also produced from scatterings in the thermal plasma after reheating completes. Its abundance is given by [115, 116, 117, 118]

$$Y_{3/2}^{(\rm thermal)} \simeq 0.26\frac{\rho_c}{m_{3/2}s_0}\left(\frac{T_{\rm RH}}{10^{10}\ {\rm GeV}}\right)\left[0.13\left(\frac{m_{3/2}}{100\ {\rm GeV}}\right)+\left(\frac{100\ {\rm GeV}}{m_{3/2}}\right)\left(\frac{m_{\tilde g}}{1\ {\rm TeV}}\right)^2\right], \tag{6.22}$$

where s_0 ($\simeq 2.9\times10^3\ {\rm cm}^{-3}$) and ρ_c ($\simeq 1.052\times10^{-5}h^2\ {\rm GeV/\ cm}^3$) are the present entropy density and critical energy density, respectively. The parameter $m_{\tilde g}$ is gluino mass and h is the present Hubble parameter in the unit of 100 ${\rm km\,s^{-1}\ Mpc^{-1}}$. Stringent bounds on the reheating temperature are obtained when we assume that the gravitino is the lightest SUSY particle (LSP) and is stable. In this case, its abundance should not exceed the observed DM abundance:

$$m_{3/2}\left(Y_{3/2}^{(\rm decay)}+Y_{3/2}^{(\rm thermal)}\right) \le \frac{\rho_c}{s_0}\Omega_{\rm DM} \simeq 0.4\ {\rm eV}, \tag{6.23}$$

where $\Omega_{\rm DM}h^2$ ($\simeq 0.12$) is the DM relic density.[2] For example, in the case of $m_{3/2}=100$ GeV, the reheating temperature is bounded such as

$$2\times10^7\ {\rm GeV}\left(\frac{\mu}{10^{15}\ {\rm GeV}}\right)^2\left(\frac{m_{\rm inf}}{10^{12}\ {\rm GeV}}\right)^2 \lesssim T_{\rm RH} \lesssim 9\times10^9\ {\rm GeV}, \tag{6.24}$$

where we use $h\simeq0.67$ [7].

From Eq. (3.66), we can see that an extremely large value of λ is required to be consistent with the lower bound on reheating temperature. In the case of such a large value of λ, the thermal log potential has to be taken into account even for $n=6$ [see Eq. (3.94)]. In Sec. 6.1.3, we focus on LH_u flat direction, which corresponds to the case of $n=4$.

[2] If the gravitino mass is about 1 TeV and it is unstable, its decay products interact with the light elements and destroy them at the time of BBN epoch. Then the gravitino abundance is bounded above by about four order of magnitude severer than the bound of Eq. (6.23) [49]. Here we assume gravitino to be stable. In this case, the next to lightest SUSY particle may decay in the epoch of Big Bang nucleosynthesis and may destroy light elements. This problem can be avoided when sneutrino is the next to lightest SUSY particle [49]. This constraint is highly model dependent, so that we use a conservative bound such that the gravitino abundance is below the observed DM abundance.

Here we briefly comment on the isocurvature constraint explained in Sec. 3.5. It can be easily satisfied because the energy scale of inflation is relatively small in F-term hybrid inflation models [see Eq. (6.4)].

6.1.3 Backreaction

Since the AD field obtains a large VEV during inflation, we should take into account its effect on inflaton dynamics via supergravity effects. Here we focus on the LH_u flat direction.

In supergravity, the potential of scalar fields is determined by Eq. (A.29). When we consider the total superpotential $W = W^{(\mathrm{AD})} + W^{(\mathrm{inf})}$, the terms of $W_S K^{\bar{S}\phi} W_{\bar{\phi}} + \mathrm{c.c.} - 3\,|W|^2$ give a linear potential of inflaton such as [119, 105]

$$V_{\mathrm{BR}} \simeq a' \frac{\kappa v^2}{M_{\mathrm{Pl}}^2} \left\langle W^{(\mathrm{AD})} \right\rangle S + \mathrm{c.c.}, \tag{6.25}$$

where a' is an $O(1)$ constant determined by higher dimensional Kähler potentials and $\left\langle W^{(\mathrm{AD})} \right\rangle$ is determined by Eqs. (3.30) and (3.39). Hereafter we assume $a' = 1$ for simplicity.

The effect of the linear term in the F-term hybrid inflation model has been studied in Ref. [105]. They have found that the linear term affect the inflaton dynamics when the slope of the linear term is the same order with that of the Coleman-Weinberg potential. They introduce a parameter to describe the relative importance of the two contributions to the slope:

$$\xi \equiv \frac{2^{9/2}\pi^2}{\kappa^3 \ln 2} \frac{\left\langle W^{(\mathrm{AD})} \right\rangle}{v M_{\mathrm{Pl}}^2}, \tag{6.26}$$

which should be smaller than unity so that the inflaton can rolls towards the critical value. When ξ is of order but below unity, the linear term is efficient for the inflaton dynamics. We define a critical value of coupling constant for the AD field [see Eq. (3.30] such as

$$\lambda_c \equiv 2.2 \frac{v^3}{\kappa}, \tag{6.27}$$

where we use $H_{\mathrm{inf}}^2 = \kappa^2 v^4 / 12 M_{\mathrm{Pl}}^2$. When λ is near the critical value, ξ is close to unity and the backreaction of the AD field to inflaton dynamics is efficient. Note that λ should not larger than λ_c so that the inflaton can rolls towards the critical value and inflation can end.

Since the linear term breaks R-symmetry, under which the inflaton S is charged, we need to investigate the inflaton dynamics in its complex plane as done in Ref. [105].[3] We read their

[3] A CP-odd component of inflaton is excited via this dynamics, which also provide another scenario of baryogenesis [120].

result of Fig. 9, where desired values of $\langle W^{(\mathrm{AD})} \rangle$ can be read from the contours of gravitino masses by the relation of $m_{3/2} M_{\mathrm{Pl}}^2 \leftrightarrow \langle W^{(\mathrm{AD})} \rangle$.[4] The result is shown in Fig. 6.1, where the spectral index as well as the baryon asymmetry can be consistent with the observed values in the colored region. Here, we assume that the final phase of the inflaton is larger than $\pi/32$ to avoid a fine-tuning of initial condition. Above the red-dashed curves for each case of gravitino mass, we can neglect the effect of a linear term arising from low energy SUSY breaking, which is investigated in the original work of Ref. [105]. If there is only the effect of a linear term arising from low energy SUSY breaking, the spectral index can be consistent with the observation on the red-dashed curve for each case of gravitino mass. Thus we can explain the observation on and above the red-dashed curve for each case of gravitino mass in our model.[5]

We set reheating temperature such that the gravitino abundance generated from inflaton decay [114] and scattering in the thermal plasma [115, 116, 117] is minimized. The upper-right regions (above the upper green dot-dashed line for $m_{3/2} \leq 100$ GeV and the lower one for $m_{3/2} = 1$ TeV) are excluded by the overproduction of gravitinos if they are stable. Note that if gravitino is unstable, the bound is much severer than the case of stable gravitino. For the cases of stable gravitino with mass heavier than a few TeV, we find that there is no viable region because of the gravitino problem [105].

The regions above the green lines are excluded by the cosmic string bound from the observations of CMB temperature anisotropies [see Eq. (6.14)] [109] and pulsar timing array (PTA) [see Eq. (6.15)] [110]. The Square Kilometre Array (SKA) telescope will improve the sensitivity of PTA by about one order of magnitude in terms of the parameter v [111], so that we can search whole parameter region for the case of $m_{3/2} \gtrsim 100$ GeV.

Since the value of superpotential of the AD field is determined at each point in Fig. 6.1, we can determine its coupling constant λ. Then we can use Eq. (3.76) to calculate the baryon abundance. For the case of $m_{3/2} = 100$ GeV, we can explain the baryon abundance by taking $\tilde{\epsilon}$ properly. On the other hand, for the case of $m_{3/2} = 100$ MeV, the baryon asymmetry cannot be produced efficiently below the blue-doted curve even if $\tilde{\epsilon}$ is as large as unity.[6] Using Eq. (3.31), we predict lightest neutrino mass m_ν as given in the contour plot. Since the coupling constant in the superpotential of the AD field is roughly determined by

[4] The dynamics of the phase direction of the AD field can be neglected for the case of $\lambda \ll \kappa$, which is actually satisfied in our case, so that the dynamics of inflaton is basically equivalent to the one in Ref. [105].

[5] We neglect an $\mathcal{O}(1)$ uncertainty arising near the red-dashed curve that comes from the phase difference between two linear terms.

[6] When the coefficient of A-term a in Eq. (3.3.1) is much larger than unity, $\tilde{\epsilon}$ can be larger than unity and the bound of the blue curve disappear.

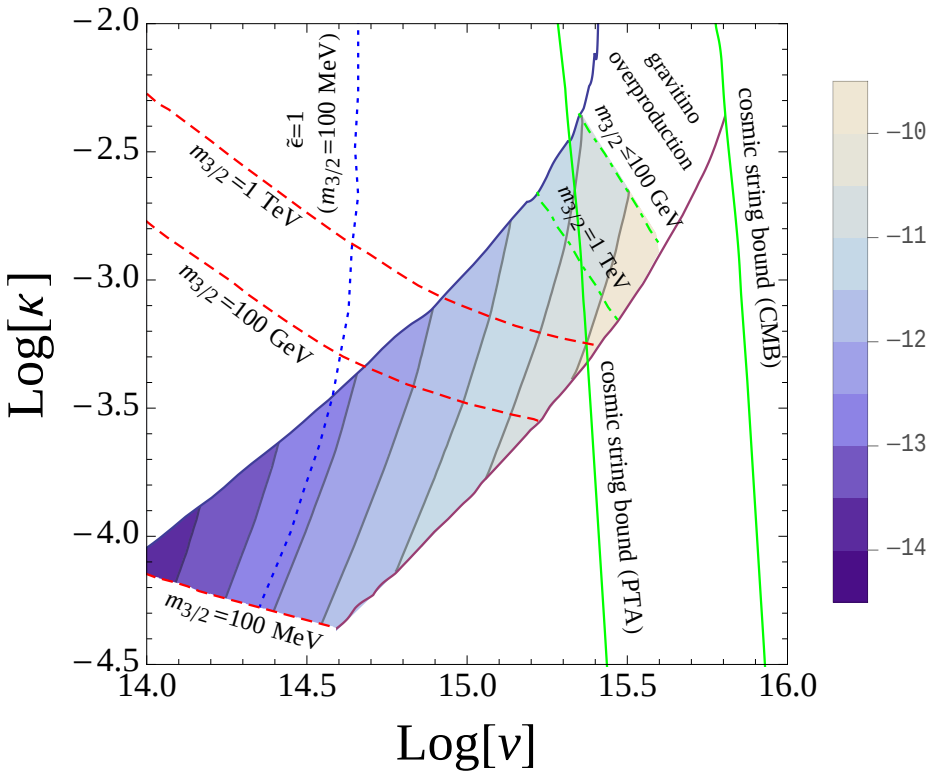

Figure 6.1: Contour plot of Log[m_ν] in the unit of eV in Log[v]-Log[κ] plane. For the case of $m_{3/2} = 100$ GeV, the spectral index as well as the baryon abundance can be consistent with the observations above the corresponding red-dashed curve in the colored region, while for the case of $m_{3/2} = 100$ MeV, they can above the corresponding red-dashed curve and blue-dotted curve in the colored region.

Eq. (6.27) to affect the inflaton dynamics, m_ν is larger for larger v and smaller κ. From the figure, we can see that m_ν can be as large as 10^{-10} eV for the case of $m_{3/2} = 100$ GeV, while it is at most 10^{-13} eV for the case of $m_{3/2} = 100$ MeV.

6.2 D-term hybrid inflation

In this section, we consider the simplest model of D-term hybrid inflation [63, 64]. We first explain its model and the reheating process. Then we discuss the baryonic isocurvature problem and backreaction of the AD field to inflaton dynamics.

6.2.1 Model

D-term inflation models are motivated by the so-called η-problem. If inflation is driven by a nonzero F-term potential energy, supergravity effects induce masses of order the Hubble parameter to all scalar fields, including inflaton. However, the Hubble-induced mass for inflaton spoils the flatness of its potential and results in an $\mathcal{O}(1)$ slow roll parameter $\eta \sim 1$. Since Hubble-induced masses come only from nonzero F-term potential energy, the η problem is absence in the case of D-term inflation, in which inflation is driven by nonzero D-term potential energy. Although the following simple model of D-term inflation predicts the spectral index relatively blue tilted compared with the observation of CMB temperature anisotropies and is also excluded by the cosmic string constraint, we use it as an illustration. Note that there are variants of D-term inflation models which predict the spectral index consistent with the observed value [121, 122], and the results in the next subsection can be applied to those models, too.[7]

We introduce a U(1) gauge symmetry with a Fayet-Ilipoulos (FI) term ξ and consider superfields S, ψ_-, and ψ_+ with U(1) gauge charges as 0, -1, and 1, respectively. The D-term potential is written as

$$V_D = \frac{g^2}{2}\left(|\psi_+|^2 - |\psi_-|^2 - \xi\right)^2, \tag{6.28}$$

where g is the U(1) gauge coupling constant. We introduce a superpotential given as

$$W^{(\mathrm{inf})} = \lambda S \psi_+ \psi_-, \tag{6.29}$$

where λ is a coupling constant.

The field s ($\equiv |S|/\sqrt{2}$) plays the role of inflaton. Suppose that the inflaton s has a VEV larger than the critical value of $s_{\rm cr} \equiv g\sqrt{\xi}/(\sqrt{2}\lambda)$. The fields ψ_- and ψ_+ obtain large effective masses from the VEV of the inflaton and stays at the origin of the potential. In this regime, the nonzero D-term potential of $V_0 = g^2\xi^2/2$ drives inflation. The Coleman-Weinberg potential for the inflaton lifts its potential above the critical point as Eq. (6.6) with the replacement of $\kappa^2\mu^2 \to g^2\xi$. Thus, the inflaton slowly rolls down to the origin of the potential. The COBE normalization requires [15, 6]

$$\sqrt{\xi} \simeq \left(\frac{3A_s}{\mathcal{N}_*}\right)^{1/4} \simeq 8.1 \times 10^{15}\ \mathrm{GeV}, \tag{6.30}$$

[7] The results are not applicable to the inflation model considered in Ref. [123] because a F-term potential drives inflation with a sizable e-folding number in that scenario.

where we assume $\mathcal{N}_* = 50$ in the second equality. This leads to the Hubble parameter during inflation such as

$$H_{\rm inf} \simeq \frac{g\xi/\sqrt{2}}{\sqrt{3}M_{\rm Pl}} \simeq 5.7 \times 10^{12}\ {\rm GeV} \left(\frac{g}{0.5}\right) \left(\frac{\sqrt{\xi}}{8.2 \times 10^{15}\ {\rm GeV}}\right)^2 . \tag{6.31}$$

The e-folding number, a slow roll parameter, and spectral index are calculated as

$$\mathcal{N}_* \simeq \frac{2\pi^2}{g^2}\frac{s_*^2}{M_{\rm Pl}^2}, \tag{6.32}$$

$$\eta_s \simeq -\frac{g^2}{4\pi^2}\frac{M_{\rm Pl}^2}{s_*^2} \simeq -\frac{1}{2\mathcal{N}_*} \tag{6.33}$$

$$n_s \simeq 1 - \frac{1}{\mathcal{N}_*} \simeq 0.98, \tag{6.34}$$

where the subscript $_*$ denotes values corresponding to the pivot scale $k_* = 0.05\ {\rm Mpc}^{-1}$. The slow roll condition fails (i.e., $\eta_s = 1$) at the VEV around $s \simeq g/(2\pi)M_{\rm Pl}$, which is larger than the critical value $s_{\rm cr}$ for the case of $\lambda = \mathcal{O}(1)$. Thus, slow roll inflation ends at the VEV around $s \simeq g/(2\pi)M_{\rm Pl}$ and soon after that the waterfall field ψ_+ starts to oscillate around the low energy minimum of $\sqrt{\xi}$.

The scalar spectral index deviates from the observation by about 2σ. Let us emphasize that the results in the next section can be applied to other variants of D-term inflation models, including the ones which predict the spectral index consistent with the observed value within a 1σ level [121, 122]. In Sec. 6.2.4 we also show that the backreaction of the AD field on the inflaton dynamics can make the spectral index consistent with the observation.

In order to obtain a sufficiently large e-folding number, say, $\mathcal{N}_* \gtrsim 60$, the initial VEV of the inflaton s has to be as large as $\mathcal{N}_* \frac{g^2}{2\pi^2} M_{\rm Pl} \simeq 0.8 M_{\rm Pl}$ for $g = 0.5$. which is of order the Planck scale. Planck-scale physics may affect the potential of the inflaton at such a high energy scale and may spoil its flatness. Hereafter, we just assume the above potential for simplicity. In Sec. 8.2, we provide a model to avoid this problem.

Since U(1) symmetry is spontaneously broken by the VEV of waterfall field, cosmic strings form after inflation. They contribute to the spectrum of CMB temperature anisotropies, so that their energy density is bounded above by the CMB observation as Eq. (6.14) [109]. In the D-term hybrid inflation model, the energy density of cosmic string per unit length $\mu_{\rm CS}$ is calculated by Eq. (6.13) with $B = 1$, so that it is written as

$$G\mu_{\rm CS} \simeq 2.9 \times 10^{-6} \left(\frac{\xi}{8.2 \times 10^{15}\ {\rm GeV}}\right) . \tag{6.35}$$

Therefore, the cosmic string bound of Eq. (6.14) is inconsistent with the value of ξ required by the COBE normailzation. To avoid the cosmic string constraint, we may have to modify the D-term inflation model (see, e.g., Ref. [121, 122, 123]).

6.2.2 Reheating temperature

After inflation ends, the inflaton S and waterfall field ψ_+ start to oscillate around the minima and the energy density of the Universe is dominated by these oscillations. When some MSSM fields carry nonzero U(1) charge, the field ψ_+ immediately decays into the MSSM fields through the interaction in the D-term potential. Even if the MSSM fields have no U(1) charge, the kinetic mixings between the U(1) and $\mathrm{U}(1)_Y$ makes the field ψ_+ decay into the MSSM fields relatively fast [67]. Thus, the reheating temperature of the Universe is determined by the relatively late-time decay of the inflaton S, which dilutes the relics produced from the decay of ψ_+.

Thus around the minimum of the potential, the superpotential is reduced to be Eq. (B.25) with $m_{\rm inf} = \lambda\sqrt{\xi}$ and the replacements of $X \to \psi_-$. However, since $K_{\psi_-} = K_S = 0$, non-thermal production process of gravitinos is absent in this model. If there is an interaction between the inflaton and Higgs fields such as

$$W \supset y S H_u H_d, \tag{6.36}$$

then the inflaton decay rate and the reheating temperature are estimated as

$$\Gamma_{\rm inf} = \frac{y^2}{4\pi} m_\phi \tag{6.37}$$

$$T_{\rm RH} \simeq 2 \times 10^{10}\ {\rm GeV} \left(\frac{y}{10^{-4}}\right) \left(\frac{m_{\rm inf}}{10^{12}\ {\rm GeV}}\right)^{1/2}. \tag{6.38}$$

The gravitino overproduction problem puts the upper bound on the reheating temperature as explained in the previous section. Note that the lower bound is absent because $K_{\psi_-} = K_S = 0$.

6.2.3 Baryonic isocurvature constraint

The isocurvature constraint explained in Sec. 3.5 implies that the coupling constant λ should be smaller than 10^{-3} for $n = 4$ and 0.1 for $n = 6$ when we assume $H_{\rm inf} = 6 \times 10^{12}$ GeV [see Eq. (6.31)]. Note that for $n = 4$ the coupling constant λ has to be smaller than of order 10^{-4} to explain the observed amount of baryon asymmetry [see Eq. (3.76)], so that the baryonic isocurvature constraint is satisfied. For the case of $n = 6$, the upper bound on λ implies an upper bound on $T_{\rm RH}$ of order 10^{2-3} GeV via the relations of Eqs. (3.66) and (3.70).

6.2.4 Backreaction

In order to discuss the backreaction of the AD field to the dynamics of inflaton, we need to estimate the VEV of the AD field during inflation. When we consider D-term inflaton models, the Hubble-induced mass term is absent during inflation [65, 66]. In this case, there is no reason that the AD field stays at the origin because the potential of the AD field is extremely flat compared with the Hubble parameter. To estimate the VEV of the AD field during D-term inflation, we solve the equation of motion of the AD field [66]:

$$3H_{\rm inf}\dot{\phi} + V'_\phi \simeq 0, \tag{6.39}$$

where we assume the slow roll of the AD field and neglect a second derivative term. Assuming a sufficiently large initial VEV of the AD field, we obtain its VEV at the time of horizon exit of the pivot scale such as

$$\langle|\phi|\rangle_{\rm inf} \simeq \left(\frac{1}{2\sqrt{\delta\mathcal{N}}}\frac{H_{\rm inf}M_{\rm Pl}}{\lambda}\right)^{1/2}, \tag{6.40}$$

where $\delta\mathcal{N}$ is the difference of e-folding number from the beginning of primordial inflation to the time of horizon exit of the pivot scale. Although the resulting VEV of Eq. (6.40) is slightly different from the one in the case of F-term inflation models [see Eq. (3.39)], the resulting baryon asymmetry are the same with the ones in F-term inflation (see footnote 3).

Here we consider the backreaction. In the case of D-term inflation, no linear potential can be induced by the backreaction of the AD field because the superpotential of the inflaton sector vanishes during inflation. However, a Hubble-induced mass term of inflaton comes from the higher dimensional Kähler potential, which is necessary to realize the Affleck-Dine mechanism [104]:

$$\begin{aligned} V &\supset c'_H H^2 |S|^2 && (6.41)\\ c'_H &= (1-c)\frac{V_F}{H^2 M_{\rm Pl}^2} && (6.42)\\ &= \frac{(1-c)}{4N}\langle|\phi|\rangle_{\rm inf}^2, && (6.43) \end{aligned}$$

where we use Eqs. (3.34) and (6.40). Note that we have assumed $(1-c) < 0$ to realize the Affleck-Dine mechanism, so that it gives a negative contribution to the curvature of inflaton potential. As a result, the slow roll parameter η is smaller than the case without the backreaction such as

$$\eta \simeq -\frac{c'_H}{3}\left[1 + \left(1 - e^{-2/3c'_H\mathcal{N}}\right)\right], \tag{6.44}$$

where $\mathcal{N}$ is the e-folding number. The spectral index can be consistent with the observed value ($n_s^{(\rm obs)} = 0.963 \pm 0.008$) within 1 sigma level for the case of $0.009 < -c'_H < 0.024$. In addition, the slow roll epsilon parameter is also smaller, so that the energy scale of inflation is lower. This implies that the FI parameter ξ and $G\mu$ are smaller such as

$$\sqrt{\xi} \simeq 8.2 \times 10^{15}\ \text{GeV} \times \left(\frac{2c'_H N}{3} \frac{e^{-4/3c'_H N}}{1 - e^{-2/3c'_H N}} \right)^{1/4} \tag{6.45}$$

$$G\mu \simeq 2.9 \times 10^{-6} \times \left(\frac{2c'_H N}{3} \frac{e^{-4/3c'_H N}}{1 - e^{-2/3c'_H N}} \right)^{1/4}. \tag{6.46}$$

Unfortunately, the correction to the energy density per unit length μ is at most about a factor of 0.5, which is not enough to avoid the cosmic string constraint of Eq. (6.14). To avoid the cosmic string constraint, we may have to modify the D-term inflation model (see, e.g., Ref. [121, 122, 123]).

Next, let us identify the AD field as LH_u flat direction. We determine the VEV of the AD field during inflation to predict the lightest neutrino mass. Note that the VEV of inflaton at the time of horizon exit of pivot scale is just below or of order the Planck scale, so that the total e-folding number of inflation could not be much larger than $\mathcal{O}(10)$. For example, if the initial VEV of inflaton is the Planck scale, the total e-folding number of D-term inflation is at most 52 (62) for $c'_H = 0.017$ (0.024). Thus we take $(1 - c)/(4N) = -0.1$ in Eq. (6.43) to determine c'_H. This result implies that the coefficient of the Hubble induced mass of inflaton can be of order 0.01 when the VEV of the AD field is just below the Planck scale. Therefore, the lightest neutrino mass is given by $m_\nu \approx 10^{-11}$ eV for $c'_H = \mathcal{O}(0.01)$.

6.3 Chaotic inflation

In this section, we consider a chaotic inflation model in supergravity [125]. We first explain its model and the reheating process. Then we discuss the baryonic isocurvature problem and backreaction of the AD field to inflaton dynamics.

6.3.1 Model

We consider a chaotic inflation model in supergravity where an inflaton superfield I has shift symmetry in the Kähler potential [125]:

$$K_{\rm inf} = c_0 M_{\rm Pl} (I + I^*) + \frac{1}{2} (I + I^*)^2 + |X|^2 - \frac{c_3}{4} \frac{|X|^4}{M_{\rm Pl}^2}, \tag{6.47}$$

where X is a stabiliser field. Note that c_0 is an order parameter of Z_2 symmetry, under which the fields I and X are odd, so that we take c_0 as a free parameter that may be smaller than unity. We include the $|X|^4$ term in the Kähler potential, which cannot be suppressed by any symmetries. The other higher dimensional terms do not change our discussion qualitatively, so that we neglect them in the following analysis.

The imaginary part of its scalar component $\eta \equiv (I - I^*)/\sqrt{2}$ is identified with inflaton. The shift symmetry is explicitly broken by a superpotential of

$$W^{(\mathrm{inf})} = m_{\mathrm{inf}} I X, \tag{6.48}$$

where m_{inf} is inflaton mass. When the inflaton has a large VEV, the stabiliser field obtains a large effective mass and stays at the origin. The inflaton potential is then given by the quadratic potential via the F-term of the stabiliser field. Thanks to the shift symmetry in the Kähler potential, the VEV of inflaton can be larger than the Planck scale and quadratic chaotic inflation can be realized in this model.

The real component of I obtains a Hubble-induced mass and stays at a VEV of $\mathrm{Re}[I] \simeq -c_0/2$ [125]. When the VEV of the inflaton decreases down to the Planck scale, the real component of I as well as the inflaton start to oscillate around the origin of the potential and inflation ends. The dynamics is illustrated in Fig. 6.2, where we numerically solve the equation of motion of the field I and plot its trajectory for the case of $c_0 = 1$. The field I slowly rolls along the imaginary axis during inflation, where $\mathrm{Re}[I] = -c_0/2$ is approximately satisfied. We denote the imaginary part of I as η, which has a quadratic potential such as

$$V_{\mathrm{inf}} \simeq \frac{1}{2} m_{\mathrm{inf}}^2 \eta^2. \tag{6.49}$$

Thus the energy scale of inflation is given by

$$H_{\mathrm{inf}} \simeq \frac{m_{\mathrm{inf}} \eta}{\sqrt{6} M_{\mathrm{Pl}}}. \tag{6.50}$$

The COBE normalization implies that the mass of the inflaton is given by

$$m_{\mathrm{inf}} \simeq \left(\frac{24\pi^2 A_s}{4\mathcal{N}_*^2} \right)^{1/2} \simeq 1.6 \times 10^{13}\ \mathrm{GeV}, \tag{6.51}$$

where we assume $\mathcal{N}_* = 55$ in the last equality. The e-folding number, slow roll parameters,

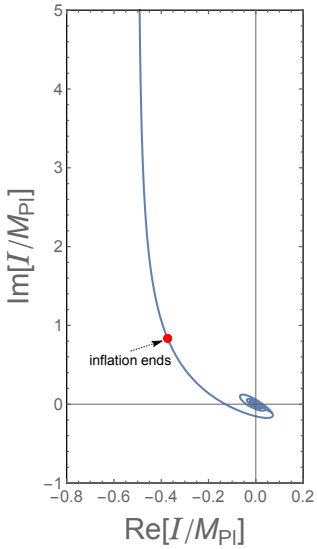

Figure 6.2: Dynamics of the field I in the complex plane in the chaotic inflation model. We set $c_0 = 1$. The field I slowly rolls along the line of $\mathrm{Re}[I] = -c_0/2$ during inflation. After it reaches the red point, inflation ends and it starts to oscillate and rotate around the origin.

and spectral index are calculated as

$$N_* \simeq \frac{\eta_*^2}{4M_{\rm Pl}^2} \tag{6.52}$$

$$\epsilon_s \simeq \frac{2}{\eta^2} \simeq \frac{1}{2\mathcal{N}_*} \tag{6.53}$$

$$\eta_s \simeq \frac{2}{\eta^2} \simeq \frac{1}{2\mathcal{N}_*} \tag{6.54}$$

$$n_s \simeq 1 - \frac{2}{\mathcal{N}_*} \simeq 0.96. \tag{6.55}$$

Inflation ends when the slow roll parameters reaches unity. The Hubble parameter at the end of inflation is given by

$$H_{\rm inf,end} \simeq \frac{m_{\rm inf}}{\sqrt{3}}. \tag{6.56}$$

In Fig. 6.2, inflation ends when the field I reaches the red point. After inflation ends, it starts to oscillate and rotate around the origin.

The stabiliser field X obtains a Hubble-induced mass via the higher dimensional Kähler potential such as

$$V \supset c_3 m^2 \frac{|I|^2}{M_{\rm Pl}^2} |X|^2 \simeq 3c_3 H^2 |X|^2 . \tag{6.57}$$

This implies that the dynamics of X is qualitatively different from the case with $c_3 = 0$. We should include them because the higher dimensional Kähler potential cannot be suppressed by any symmetries, To realize chaotic inflation, we assume $c_3 > 0$. Then the field X stays at the origin.

6.3.2 Reheating temperature

The inflaton can decay into the MSSM particles via supergravity effects when the Z_2 breaking parameter is nonzero. Its decay rate is calculated in Sec. B.4.1 and is given by Eq. (B.29) with $K_S = c_0$, which implies that there is a lower bound on reheating temperature given by

$$T_{\rm RH} \simeq 2 \times 10^8 \text{ GeV} c_0 \left|y_t\right| \left(\frac{m_{\rm inf}}{10^{13} \text{ GeV}}\right)^{3/2}. \tag{6.58}$$

Note that there may be a renormalizable coupling such as

$$W \supset y X H_u H_d. \tag{6.59}$$

If c_0 is sufficiently small, the decay rate is determined by this term and is given by

$$T_{\rm RH} \simeq 6 \times 10^8 \text{ GeV} \left(\frac{y}{10^{-6}}\right) \left(\frac{m_{\rm inf}}{10^{13} \text{ GeV}}\right)^{1/2}. \tag{6.60}$$

However, the coupling constant y should be suppressed by a factor of $m_{\rm inf}/M_{\rm Pl}$ not to affect the inflaton potential, so that the reheating temperature is at most 10^9 GeV [126].

The Z_2 breaking term makes the inflaton decay into gravitinos efficiently via supergravity effects and its decay rate is the same order with that of Eq. (B.29) as shown in Eq. (B.34). Therefore, there is a gravitino problem from inflaton decay as explained in Sec. 6.1.2. For example, in the case of $m_{3/2} = 100$ GeV, the reheating temperature is bounded such as

$$10^6 \text{ GeV} \left(\frac{c_0}{10^{-5}}\right)^2 \left(\frac{m_{\rm inf}}{10^{13} \text{ GeV}}\right)^2 \lesssim T_{\rm RH} \lesssim 9 \times 10^9 \text{ GeV}. \tag{6.61}$$

Here we assume that the inflaton decays into the MSSM particles via Eq. (6.59) and write the resulting temperature as $T_{\rm RH}$.

6.3.3 Baryonic isocurvature constraint

The isocurvature constraint explained in Sec. 3.5 implies that the VEV of the AD field should be as large as the Planck scale in chaotic inflation models, where $H_{\rm inf}$ is as large as 10^{14} GeV. This means that the higher-dimensional operator in the superpotential should

be suppressed; $\lambda \lesssim H_{\rm inf}/M_{\rm Pl} \approx \mathcal{O}(10^{-4})$ [see Eq. (3.39)]. Note that for the case of $n = 4$ the coupling constant λ should be smaller than 10^{-4} to account for the observed amount of baryon asymmetry [see Eq. (3.76)], so that the baryonic isocurvature constraint is usually satisfied.

When the VEV of the AD field is as large as the Planck scale, we have to take into account higher-dimensional terms V_K coming from a Kähler potential. Let us consider the following Kähler potential as an illustration for the origin of V_K:

$$K \sim |X|^2 \frac{\phi^{n'}}{M_{\rm Pl}^{n'}} + \text{c.c.}, \tag{6.62}$$

where X is a field which has a non-zero F-term during inflation (i.e. $|F_X|^2 = 3H_{\rm inf}^2 M_{\rm Pl}^2$). This operator gives the AD field a potential as

$$V_K = \left(\frac{-a_{H^2}}{n' M_{\rm Pl}^{n'-2}} H^2 \phi^{n'} + c.c. \right) + \dots, \tag{6.63}$$

where "$\cdots$" denotes higher-dimensional Planck-suppressed terms. The parameter a_{H^2} is an $\mathcal{O}(1)$ constant. Curvature of the phase direction of AD field, θ, is dominantly given by V_K;

$$m_\theta^2 \equiv \frac{1}{2|\phi_{\rm inf}|^2} \frac{\partial^2 V_K}{\partial \theta^2}, \tag{6.64}$$

$$\simeq \frac{n'|a_{H^2}|}{2} H_{\rm inf}^2 \left(\frac{|\phi_{\rm inf}|}{M_{\rm Pl}} \right)^{n'-2}. \tag{6.65}$$

Note that the curvature is highly suppressed compared with $H_{\rm inf}^2$ for $|\phi_{\rm inf}| \lesssim M_{\rm Pl}$, that is, for $\lambda \gtrsim 10^{-4}$. [see Eqs. (6.50) and (3.39)]. Therefore, the phase direction of the AD field obtains a mass of the order of the Hubble parameter during inflation [see Eq. (6.65)].[8] In this case, the baryonic isocurvature fluctuation is absent from the beginning. To summarize, in order to avoid a sizable baryonic isocurvature fluctuation, the VEV of the AD has to be as large as the Planck scale, in which case baryonic isocurvature fluctuation is absent due to the potential originated from a Kähler potential.

Let us discuss the implication of the baryonic isocurvature constraint on the reheating temperature. Since the VEV of the AD field at the beginning of its oscillation is related with that during inflation via $|\phi_{\rm osc}| = (H_{\rm osc}/H_{\rm inf})^{1/(n-2)} |\phi_{\rm inf}|$, a large VEV during inflation results in a relatively large VEV at the onset of its oscillation, and then the AD field tends

[8] In contrast, if $\lambda = \mathcal{O}(1)$, the lower bound in Eq. (3.93) requires about 1% and 10% tuning on the initial phase θ for $n = 4$ and $n = 6$ flat directions, respectively. This tuning would not be explained by the anthropic principle because human life would be able to exist whether or not baryonic isocurvature fluctuation exists.

to dominate the Universe. Therefore, in order to account for today's baryon-to-entropy ratio without additional entropy production except for the decay of inflaton, the reheating temperature tends to be small to dilute the AD field successfully. From Eq. (3.39), the VEV of the AD field at the beginning of its oscillation is given by

$$|\phi_{\rm osc}| \simeq \begin{cases} 3\times 10^{15}\ {\rm GeV}\left(\frac{\lambda}{10^{-4}}\right)^{-1/4}\left(\frac{H_{\rm osc}}{1\ {\rm TeV}}\right)^{1/4} & \text{for } n=6, \\ 3\times 10^{16}\ {\rm GeV}\left(\frac{\lambda}{10^{-4}}\right)^{-1/6}\left(\frac{H_{\rm osc}}{1\ {\rm TeV}}\right)^{1/6} & \text{for } n=8, \end{cases} \tag{6.66}$$

where $H_{\rm osc}$ is the Hubble parameter at the oscillation time. Thus the observed baryon density requires the reheating temperature of the Universe as

$$T_{\rm RH} \simeq \begin{cases} 0.8\ {\rm GeV}\ \epsilon^{-1}\left(\frac{\lambda}{10^{-4}}\right)^{1/2}\left(\frac{H_{\rm osc}}{1{\rm TeV}}\right)^{1/2} & \text{for } n=6, \\ 9\ {\rm MeV}\ \epsilon^{-1}\left(\frac{\lambda}{10^{-4}}\right)^{1/3}\left(\frac{H_{\rm osc}}{1{\rm TeV}}\right)^{2/3} & \text{for } n=8, \end{cases} \tag{6.67}$$

where we have used $Y_B \simeq 8.7\times 10^{-11}$ for the observed baryon-to-entropy ratio [7], and assumed $b=-1/3$. We should emphasize that the tight constraint on the baryonic isocurvature perturbation requires that $\lambda \lesssim 10^{-4}$ and puts a severe upper bound on the reheating temperature.

6.3.4 Backreaction

The isocurvature constraint requires that the AD field has a VEV of order the Planck scale during inflation. Such a large VEV may affect the inflaton potential via supergravity effects. In this subsection, we investigate the backreaction of the AD field to the inflaton dynamics.

The full supergravity potential for the inflaton η and the AD field ϕ is given by

$$\begin{aligned} V &= e^{|\phi|^2/M_{\rm Pl}^2}\left[\frac{1}{2}m^2\eta^2\frac{1}{1+c_3\,|\phi|^2/M_{\rm Pl}^2}\right. \\ &\qquad \left. +\lambda^2\left(\frac{|\phi|^6}{M_{\rm Pl}^2}+\frac{5}{16}\frac{|\phi|^8}{M_{\rm Pl}^4}+\frac{1}{16}\frac{|\phi|^{10}}{M_{\rm Pl}^6}\right)\right], \end{aligned} \tag{6.68}$$

where we assume $c_0=0$ and $n=4$ for simplicity. The constant c_3 is the parameter in the Kähler potential [see Eq. (6.47)]. This potential implies that the effect of the AD field is relevant when its VEV is as large as the Planck scale. Since $H_{\rm inf}\sim 10m$ in the chaotic inflation model, the VEV of the AD field is as large as the Planck scale for the case of

$$\lambda \sim \lambda_c \equiv 10\sqrt{c-1}\frac{m}{M_{\rm Pl}}, \tag{6.69}$$

[see Eq. (3.39)].

We numerically solve the equations of motion of the inflaton η and the AD field ϕ and calculate the tensor-to-scalar ratio r and spectral index n_s. We show the result in Fig. 6.3, where we take the parameters c_3 and λ randomly within the intervals of $[1, 10]$ and $[0, 100m/M_{\rm Pl}]$, respectively. The red, green, and blue dots represent the results at e-folding numbers of 50, 55, and 60, respectively. As a result, the tensor-to-scalar ratio can be as small as 0.14, 0.13, and 0.12 at the e-folding number of 50, 55, and 60, respectively, which is marginally consistent with the present upper bound within 2σ. We plot the results as the light dots for the case of $\lambda/\lambda_c < 0.5$, $5 < \lambda/\lambda_c$, or $c_3 < 5$, which clarifies that the tensor-to-scalar ratio can be smaller only for the case of $0.5 < \lambda/\lambda_c < 5$ and $c_3 > 5$. This requires that the coupling constant in the superpotential is of order $10m/M_{\rm Pl} \sim 10^{-4}$. When we identify the AD field as LH_u flat direction, the lightest neutrino mass is predicted to be of order 10^{-9} eV. Note that the resulting baryon asymmetry of Eq. (3.76) is naturally consistent with the observation when gravitino mass is of order 100 GeV $-$ 1 TeV.

Finally, we also perform numerical calculations including higher dimensional Kähler potentials of

$$K \supset d\frac{1}{M_{\rm Pl}^2}|\phi|^4 + d'\frac{1}{M_{\rm Pl}^4}|\phi|^6 + c'\frac{1}{M_{\rm Pl}^4}|X|^2|\phi|^4\,, \tag{6.70}$$

and find that the tensor-to-scalar ratio can not be smaller than about 0.11 at the e-folding number of 60 even in this case.[9] This is in contrast with the result of Ref. [107], where they have investigated the effect of an additional scalar field to chaotic inflation in a non-SUSY model and found that the tensor-to-scalar ratio can be much smaller than 0.1. This is because the exponential factor in the supergravity potential of Eq. (6.68) makes the VEV of the AD field smaller and its backreaction to the inflaton dynamics smaller in supergravity.

6.3.5 Realization of co-genesis scenario

Here we comment on the relation to the scenario for the co-genesis explained in Chap. 5. Suppose that Q-balls form after ADBG in the chaotic inflation model. A typical charge of Q-ball formed after the Affleck-Dine baryogenesis is given by Eq. (4.33) in gravity-mediated SUSY breaking models, where we should substitute Eq. (6.66) for the value of $\phi_{\rm osc}$. The decay rate of the Q-ball is calculated from Eq. (4.57) with $\tilde{R} \simeq R(2\log(\phi_0/\sqrt{2}\omega_0))^{1/2} \simeq 7R$.

[9] We also take into account kinetic couplings between the inflaton and AD field due to the higher-dimensional Kähler potential of $c''|\phi|^2(I+I^*)^2/2M_{\rm Pl}^2$. However, we find that their effect is also very limited.

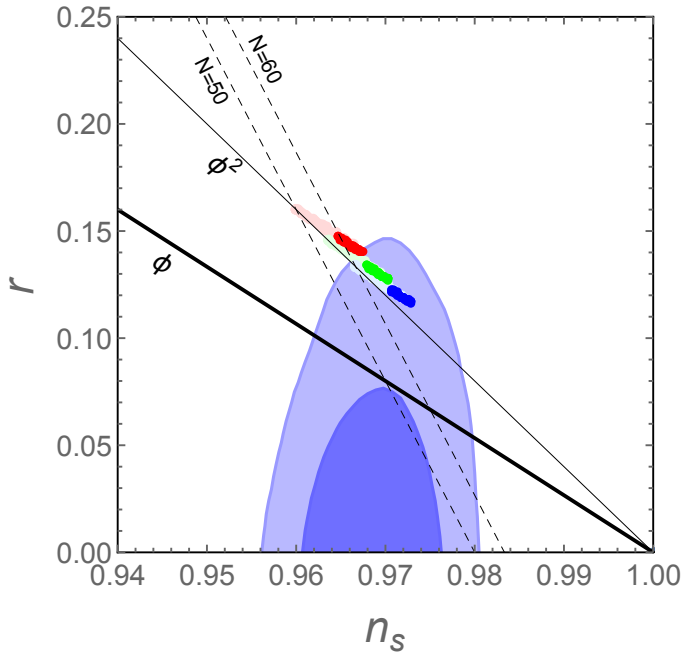

Figure 6.3: Spectral index n_s and tensor-to-scalar ratio r in the chaotic inflation model with the backreaction of the AD field. The red, green, and blue dots represent our results at e-folding numbers of 50, 55, and 60, respectively. We randomly take 100 points for the parameters c_3 and λ within the intervals of $[1, 10]$ and $[0, 100m/M_{\rm Pl}]$, respectively. We plot the results as the light dots for the case of $\lambda/\lambda_c < 0.5$, $5 < \lambda/\lambda_c$, or $c_3 < 5$. The blue regions are the 1σ (deep colored regions) and 2σ (pale colored regions) constraints of the Planck experiment [6]. For comparison with standard results, we plot the predictions in the chaotic inflation models with linear and quadratic potentials without the backreaction as the black thin and thick lines, respectively, where the results are given as intersection points of black lines and dashed lines for corresponding e-folding numbers.

For $n = 6$ and $n = 8$, the Q-ball decays just before the reheating such as

$$T_{\rm decay} \simeq \begin{cases} 2\ {\rm GeV} \left(\frac{\lambda}{10^{-4}}\right)^{3/8} \left(\frac{H_{\rm osc}}{1\ {\rm TeV}}\right)^{1/8} \left(\frac{m_\phi}{1\ {\rm TeV}}\right)^{3/4}, & \text{for } n = 6, \\ 60\ {\rm MeV} \left(\frac{\lambda}{10^{-4}}\right)^{1/4} \left(\frac{H_{\rm osc}}{1\ {\rm TeV}}\right)^{1/4} \left(\frac{m_\phi}{1\ {\rm TeV}}\right)^{3/4}, & \text{for } n = 8, \end{cases} \tag{6.71}$$

where we assume that the effective number of relativistic degrees of freedom at the decay time g_* is 10.75. We find that Q-balls decay after DM freezes out for $n = 6$ and $n = 8$. Thus, we can realize the scenario of baryon and DM co-genesis from Q-ball decay as explained in Chap. 5.

Chapter 7

New scenario of ADBG

This chapter is based on the work done by the author [33]. In this chapter, we propose a new scenario of the Affleck-Dine baryogenesis where a flat direction in the MSSM generates $B-L$ asymmetry just after the end of inflation. The resulting amount of baryon asymmetry is independent of low-energy supersymmetric models but is dependent on inflation models. We consider the hybrid and chaotic inflation models and find that reheating temperature is required to be higher than that in the conventional scenario of ADBG, which is explained in Chap. 3. In particular, non-thermal gravitino-overproduction problem is naturally avoided in the hybrid inflation model. Our results imply that ADBG can be realized in a broader range of SUSY and inflation models than expected in the literature.

7.1 Introduction

As mentioned in Chap 3, the AD field obtains a Hubble-induced mass due to the finite energy density of the Universe during and after inflation. In the conventional scenario of ADBG, the sign of the Hubble-induced mass term is assumed to be negative during and after inflation. However, the sign of the Hubble-induced mass term can change after inflation because the source of the energy density of the Universe generically changes after inflation. In this chapter, we investigate a new scenario that the AD field obtains a negative Hubble-induced mass term during inflation while it obtains a positive one after inflation.[1] In this case, the AD field starts to oscillate around the origin of the potential due to the positive Hubble-induced

[1]The opposite case, where the Hubble-induced mass term is positive during inflation and is negative after inflation, has been considered in Refs. [127, 128] (see Refs. [129, 130] for earlier works). Although $B-L$ asymmetry cannot be generated via the dynamics of the flat direction, topological defects form after inflation and emit gravitational waves.

mass term just after the end of inflation. At the same time, its phase direction is kicked by an A-term and $B-L$ asymmetry is generated. We calculate the produced amount of baryon asymmetry and show that it can be consistent with that observed.

The whole scenario is much simpler than the conventional scenario of ADBG. This is because the dynamics of the AD field is determined only by the Hubble-induced terms and the low-energy potential of the AD field [e.g., $V_{\rm soft}$ in Eq. (3.35)] does not affect the resulting $B-L$ asymmetry. This means that the scenario and our calculations in this chapter can be applied to many SUSY models, including gravity-mediated and gauge-mediated SUSY breaking models. In particular, the scenario does not result in the formation of Q-balls even in gauge-mediated SUSY breaking models. In addition, thermal effect on the dynamics of the AD field can be neglected in our scenario because it starts to oscillate before thermal plasma grows. This is the case even for LH_u flat direction. However, the resulting $B-L$ asymmetry depends on the energy scale of inflation because the dynamics of the AD field is determined by Hubble-induced terms. In particular, the A-term depends on inflation models, so that we need to calculate $B-L$ asymmetry for each inflation model. Since the resulting $B-L$ asymmetry depends on parameters in inflaton sector, we could check the consistency of the scenario by observing predictions of inflation models, such as the spectral index and tensor-to-scalar ratio.

In the next section, we briefly overview our scenario of ADBG. Then we apply it to the hybrid inflation model in Sec. 7.3 and the chaotic inflation model in Sec. 7.4. Finally, we consider a similar scenario in the D-term hybrid inflation model, where the Hubble-induced mass term is absent during inflation and appears with a positive coefficient after inflation.

7.2 Affleck-Dine baryogenesis just after inflation

In this section, we overview a new scenario of ADBG where the AD field starts to oscillate around the origin of the potential just after the end of inflation. In general, this scenario is realized when the Kähler potential is give by

$$K = |\phi|^2 + |S|^2 + |\psi|^2 + \frac{c_1}{M_{\rm Pl}^2}|\phi|^2|S|^2 - \frac{c_2}{M_{\rm Pl}^2}|\phi|^2|\psi|^2 , \tag{7.1}$$

where S is the field whose F-term drives inflation and ψ is the field whose oscillation energy dominates the Universe after inflation. Here, we assume that the fields S and ψ are different fields, which is actually the case in F-term hybrid and chaotic inflation models as shown in the subsequent sections.

During inflation, the AD field acquires the Hubble-induced mass via the F-term potential of the field S as Eq. (3.17). After inflation ends, the Hubble-induced mass comes also from higher-dimensional kinetic interactions between ϕ and ψ as Eq. (3.24). Therefore, the Hubble induced mass term for the AD field ϕ is given by

$$V_H = c_H H^2(t) |\phi|^2 \tag{7.2}$$

$$c_H = \begin{cases} -3(c_1 - 1) & \text{during inflation} \\ 3\left(-(1-r)c_1 + rc_2 + \frac{1}{2}\right) & \text{after inflation,} \end{cases} \tag{7.3}$$

where r $(0 \leq r \leq 1)$ is the fraction of the energy density of ψ to the total energy after inflation. Therefore the sign of the Hubble-induced mass term can change after inflation. If its sign continues to be negative after inflation, the conventional scenario of ADBG is realized as we explain in Chap. 3. On the other hand, when the coefficient is negative during inflation and is positive after inflation, the AD field starts to oscillate around the origin of the potential just after the end of inflation.

In the above scenario, the dynamics of the AD field is determined by the potential of

$$V(\phi) = c_H H^2(t) |\phi|^2 + \lambda^2 \frac{|\phi|^{2n-2}}{M_{\rm Pl}^{2n-6}} + V_A(\phi), \tag{7.4}$$

where $c_H < 0$ during inflation and $c_H > 0$ after inflation. The A-term potential of V_A depends on inflation models and is explicitly derived in the subsequent sections. The low-energy soft terms of Eq. (3.9) are irrelevant for the dynamics of the AD field. This makes our calculation simple and independent of low-energy SUSY models. In particular, the resulting $B-L$ asymmetry is independent of how SUSY breaking effect is mediated to the visible sector.

Since we consider the case that $c_H < 0$ during inflation and $c_H > 0$ after inflation, the AD field starts to oscillate around the origin just after the end of inflation. At the same time, its phase direction is kicked by the A-term. The origin of A-term depends on inflation models and thus the resulting $B-L$ asymmetry does. Here we just write generated $B-L$ asymmetry as

$$\frac{a^3(t)}{a^3(t_{\rm osc})} n_{B-L}(t) \equiv q\epsilon H_{\rm osc} |\phi|^2_{\rm osc}\,, \tag{7.5}$$

and derive ϵ in the subsequent sections. The resulting baryon-to-entropy ratio is thus written as

$$Y_b \simeq \left. \frac{8}{23} \frac{3T_{\rm RH} n_{B-L}}{4\rho_{\rm inf}} \right|_{\rm osc} \tag{7.6}$$

$$\simeq \frac{8}{23} \frac{\epsilon q T_{\rm RH}}{4H_{\rm osc}} \left(\frac{\phi_{\rm osc}}{M_{\rm Pl}} \right)^2 . \tag{7.7}$$

This is the same with Eq. (3.66) but $H_{\rm osc}$ is not given by Eqs. (3.59) and (3.71). Since the AD field starts to oscillate just after the end of inflation in this scenario, $H_{\rm osc}$ is given by the Hubble parameter at the end of inflation. Here, let us emphasise differences from the conventional scenario of ADBG. The Hubble parameter at the time of beginning of oscillation $H_{\rm osc}$ is determined by the energy scale of inflation, not by either m_ϕ nor $T_{\rm RH}$ [see Eqs. (3.59) and (3.72)]. This is because the flat direction starts to oscillate just after the end of inflation due to the positive Hubble-induced mass term. In addition, $\phi_{\rm osc}$ depends only on $H_{\rm osc}$ and λ via Eq. (3.50). Therefore, the resulting $B-L$ asymmetry is independent of parameters in low-energy SUSY models, such as m_ϕ and $m_{3/2}$.

There are some advantages in this scenario. First, as we explained above, the resulting $B-L$ asymmetry is independent of the masses of the AD field and gravitino. The result is also independent of how SUSY breaking effect is mediated to the visible sector. Secondly, Q-balls may not form (or dissipate soon if they form as discussed in the next section) in our scenario. This makes the discussion much simpler. Thirdly, the thermal effect on the AD field can be neglected because the AD field starts to oscillate just after the end of inflation and before the thermal plasma grows sufficiently [131]. This also makes calculations simpler. In particular, the thermal log potential can be neglected even for LH_u flat direction. Finally, our results imply that ADBG works in broader range of parameter space. Since the sign of the Hubble-induced mass term cannot be determined by underlying physics, it is equally possible that the sign becomes positive after inflation. In addition, viable parameter regions for some parameters, e.g., the reheating temperature, are different from the ones in the conventional scenario of ADBG. These fact imply that the Affleck-Dine mechanism works well in more cases than expected in the literature.

One might wonder if the energy density of the AD field dominates that of the Universe in the case that its initial VEV is as large as the Planck scale. This may be true in the case of conventional scenario of ADBG. However, the energy density of the AD field never dominates the Universe in the above scenario because it decreases faster than that of radiation. Just after inflation, the AD field starts to oscillate around the origin due to the positive Hubble-induced mass term. Then, its number density decreases with time as a^{-3} due to the expansion of the Universe. This means that its energy density decreases as $a^{-9/2}$ because its effective mass is of order the Hubble parameter, which decreases as $a^{-3/2}$. When the Hubble parameter decreases down to the mass of the AD field, that is, when $H(t) \simeq m_\phi$, its energy fraction to

the total energy density is given as

$$\left.\frac{\rho_{\rm AD}}{\rho_{\rm tot}}\right|_{H\simeq m_\phi} \simeq \left(\frac{m_\phi}{H_I}\right)\left.\frac{\rho_{\rm AD}}{\rho_{\rm tot}}\right|_{H\simeq H_I} \simeq 10^{-11}\left(\frac{\phi_{\rm osc}}{M_{\rm Pl}}\right)^2\left(\frac{m_\phi}{\rm TeV}\right)\left(\frac{H_I}{4\times 10^{12}\ {\rm GeV}}\right)^{-1}. \tag{7.8}$$

Thus, the energy density of AD field is negligible and the result of Eq. (7.7) is applicable to the case of $\phi_{\rm osc} \simeq M_{\rm Pl}$.

7.2.1 Comments on Q-ball formation

In this subsection, we comment on Q-ball formation. If the potential of the AD field is shallower than the quadratic potential, its coherent oscillation is unstable and fragments into Q-balls [26]. In the case considered in this chapter, the AD field starts to oscillate by the positive Hubble-induced mass term. When the beta function for the Hubble-induced mass of the AD field is positive, Q-ball does not form. The beta function has positive contributions from Yukawa interactions while it has negative ones from gauge interactions (see Sec. A.1.2). The former positive contributions are roughly proportional to the squared masses of squarks and sleptons, and the latter negative ones are roughly proportional to the squared masses of gauginos. Here, since the Hubble-induced mass for gauginos is absent or 1-loop suppressed, the positive contributions from Yukawa interactions are usually dominant. Therefore, the beta function for the Hubble-induced mass of the AD field is usually positive and Q-balls may not form in our scenario. However, if the AD field consists only of the first and second family squarks and/or sleptons, the positive contributions from Yukawa interactions are suppressed by small Yukawa couplings. In this case, Q-balls might form. We estimate the typical charge of Q-balls as

$$Q \sim \beta\left(\frac{\phi_{\rm osc}}{m_{\phi,{\rm eff}}}\right)^2, \tag{7.9}$$

where $m_{\phi,{\rm eff}}$ is the effective mass and β ($\sim 10^{-4} - 10^{-2}$) is a numerical factor obtained from simulations of Q-ball formation [see Eqs. (4.34) and (4.42)]. Here, we should substitute the Hubble-induced mass into the effective mass, and so the typical charge of Q-balls is at most 10^8. Such small Q-balls soon evaporate into thermal plasma via interactions with the thermal plasma (see Sec. 4.2).[2] Therefore, the subsequent cosmological scenario and the calculation

[2]The evaporation is efficient during the inflaton oscillation era. In addition, since the energy per unit charge for these Q-balls is given by the Hubble parameter, their energy density decreases with time as $a^{-9/2}$. Thus, the energy density of the Q-balls never dominate that of the Universe.

of the baryon asymmetry does not change.

Even if Q-balls do not form just after the end of inflation, they may form at the time of $H(t) \simeq m_\phi$. After that time, the potential of the AD field is dominated by its soft mass term. If the beta function of the soft mass is negative, the AD field becomes to fragment into Q-balls at that time. Since $n_b \propto H(t)\phi^2(t) \propto a^{-3} \propto H(t)^2$ until the Hubble parameter decreases down to the soft mass, the amplitude of the AD field at $H(t) \simeq m_\phi$ is given as

$$\phi|_{H(t)\simeq m_\phi} \simeq \left(\frac{m_\phi}{H_{\rm inf}}\right)^{1/2} \phi_{\rm osc}. \tag{7.10}$$

Here we implicitly assume that $m_\phi \gtrsim H_{\rm RH}$. This implies that a typical charge of Q-balls is given as

$$Q \simeq \beta \left(\frac{\phi|_{H(t)\simeq m_\phi}}{m_\phi}\right)^2 \simeq \beta \left(\frac{\phi_{\rm osc}^2}{m_\phi H_{\rm inf}}\right). \tag{7.11}$$

This is at most 10^{18} for typical parameters. Such small Q-balls are evaporate into thermal plasma. Even if Q-balls survive, they may be so small as to decay into quarks before the BBN epoch. However, they may decay after the electroweak phase transition [27, 34]. Since the sphaleron process is decoupled at that time, the AD field has to carry a nonzero baryon charge (not $B - L$) to generate the baryon asymmetry. In that case, the resulting baryon asymmetry is given by Eq. (7.7) without the factor of 8/23.

7.3 F-term hybrid inflation

In this section, we consider the new scenario of ADBG in the simplest hybrid inflation model [59, 60] and calculate $B - L$ asymmetry.

7.3.1 Dynamics of the AD field

The inflaton S is identified with the field S in Eq. (7.1) and the waterfall fields ψ and $\bar{\psi}$ play the role of the field ψ in Eq. (7.1). Thus the coefficient of the Hubble-induced mass c_H can change after inflation. In this subsection, we consider the dynamics of the AD field in the hybrid inflation model and calculate $B - L$ asymmetry.

Let us first consider the dynamics of the phase direction of the AD field. Using Eq. (A.29) with the total superpotential of $W^{(\rm AD)} + W^{(\rm inf)}$, we find that there is an A-term potential

coming from

$$W_S^{(\rm inf)} K^{\bar{S}\phi} W_{\bar{\phi}}^{(\rm AD)} + K_\phi W^{(\rm inf)} \left(W_\phi^{(\rm AD)}\right)^* \tag{7.12}$$

$$+K_S W^{(\rm AD)} \left(W_S^{(\rm inf)}\right)^* - 3W^{(\rm inf)} \left(W^{(\rm AD)}\right)^* + \text{c.c.} \tag{7.13}$$

The A-term is written as

$$V_A = -\left(1 - c_1 - \frac{2}{n}\right) \frac{\kappa \mu^2 \lambda}{M_{\rm Pl}^{n-1}} S^* \phi^n + \text{c.c.} \tag{7.14}$$

$$= -a \frac{H_{\rm inf}^2}{M_{\rm Pl}} |S| \, |\phi|^2 \cos\left(\theta_S - n\theta_\phi\right), \tag{7.15}$$

$$a \equiv -2\left(c_1 - 1 + \frac{2}{n}\right) \sqrt{\frac{3\,|c_H|}{n-1}}, \tag{7.16}$$

where θ_S and θ_ϕ are the complex phases of the fields S and ϕ, respectively. We use Eq. (3.39) and $H_{\rm inf}^2 = \kappa^2 \mu^4 / 3 M_{\rm Pl}^2$ in the second line. This is a linear term of the inflaton S, so that the slope of the potential should not be larger than that of the Coleman-Weinberg potential [119, 113, 105]. Otherwise the inflaton cannot reach the critical VEV and inflation cannot terminate unless we allow a fine-tuning of the initial phase of inflaton. Referring to Ref. [105] or Eq. (6.26), we introduce a parameter to describe the relative importance of the two contributions to the slope of the potential:

$$\xi \equiv \frac{1}{2}\left(1 - c_1 - \frac{2}{n}\right) \frac{16\pi^2}{\kappa^3 \ln 2} \frac{\langle |\phi| \rangle^n}{\mu M_{\rm Pl}^{n-1}} \tag{7.17}$$

$$\simeq \frac{8\pi^2 a}{3 \ln 2} \frac{\mu \langle |\phi| \rangle^2}{\kappa^2 M_{\rm Pl}^3}, \tag{7.18}$$

which should be smaller than unify so that the inflaton can roll towards the critical value without the fine-tuning. When the VEV of the AD field is so large that the parameter ξ becomes of order unity (but below unity), the A-term of Eq. (7.15) affects inflaton dynamics and the spectral index can be consistent with the observed value as explained in Sec. 6.1.3.

In the above minimal setup, there is no other term than Eq. (7.15) that affects the dynamics of the phase directions. Therefore, there is only one massive phase during inflation. For simplicity, let us assume that the inflaton and the AD field have approximately constant VEVs and $(\theta_S - n\theta_\phi) \ll 1$. In this case, the unitary matrix to diagonalise the squared mass matrix for the phase directions is given by

$$\frac{1}{\sqrt{n^2 |S|^2 + |\phi|^2}} \begin{pmatrix} |\phi| & -n\,|S| \\ n\,|S| & |\phi| \end{pmatrix}, \tag{7.19}$$

in the $(|S|\,\theta_S/\sqrt{2}, |\phi|\,\theta_\phi/\sqrt{2})^T$ basis. Thus, the massive direction denoted by $f_m\theta_m$ can be written as

$$f_m\theta_m = \frac{\sqrt{2}\,|S|\,|\phi|}{\sqrt{n^2\,|S|^2 + |\phi|^2}}\,(\theta_S - n\theta_\phi)\,, \tag{7.20}$$

and its mass m_{θ_m} is given by

$$m_{\theta_m} = \sqrt{\frac{aH^2}{2}\frac{|\phi|}{M_{\rm Pl}}\left(\frac{|\phi|}{|S|} + n^2\frac{|S|}{|\phi|}\right)}. \tag{7.21}$$

If the curvature of the phase direction is larger than the Hubble parameter during inflation, it stays at the minimum of the A-term, i.e., $\theta_m = 0$, and the phase direction cannot be kicked in the complex plane after inflation. In this case, $B-L$ asymmetry cannot be generated. Thus, we require $m_{\theta_m} \ll H_{\rm inf}$, which can be rewritten as

$$a\,|\phi|^2 \;\ll\; |S|\,M_{\rm Pl}, \tag{7.22}$$

$$an^2\,|S| \;\ll\; M_{\rm Pl}, \tag{7.23}$$

in order that the phase direction can stay at a different phase from the minimum due to the Hubble friction effect. We denote the initial phase as $\theta_m^{\rm ini}$.

After inflation ends, the AD field acquires a positive Hubble-induced mass term and starts to oscillate around the origin of the potential. At the same time, the massive phase direction is kicked by the above A-term. Since the radial direction decreases with time due to the Hubble expansion, the A-term is relevant just after the beginning of oscillation. Thus we can estimate the angular velocity of massive phase direction such as

$$\dot\theta_m \approx \frac{m_{\theta_m}^2}{H}\theta_m^{\rm ini}, \tag{7.24}$$

[see Eq. (3.41)]. Using the inverse of the unitary matrix of Eq. (7.19), we obtain the angular velocity of the phase of the AD field such as

$$\dot\theta_\phi = \frac{-n\,|S|}{\sqrt{n^2\,|S|^2 + |\phi|^2}}\frac{f_m}{\sqrt{2}\,|\phi|}\dot\theta_m \tag{7.25}$$

$$\approx \frac{m_{\theta_m}^2}{H}\frac{-n\,|S|}{\sqrt{n^2\,|S|^2 + |\phi|^2}}\frac{f_m\theta_m^{\rm ini}}{\sqrt{2}\,|\phi|} \tag{7.26}$$

$$= \frac{m_{\theta_m}^2}{H}\frac{-n\,|S|}{\sqrt{n^2\,|S|^2 + |\phi|^2}}\frac{|S|}{\sqrt{n^2\,|S|^2 + |\phi|^2}}\,(\theta_S - n\theta_\phi)^{\rm ini} \tag{7.27}$$

$$= -\frac{an}{2}\frac{|S|}{M_{\rm Pl}}H\,(\theta_S - n\theta_\phi)^{\rm ini}\,. \tag{7.28}$$

Thus we obtain

$$\frac{a^3(t)}{a^3(t_{\rm osc})} n_{B-L}(t) = 2\dot{\theta}_\phi \left|\phi\right|^2 \Big|_{\rm osc} \tag{7.29}$$

$$\equiv \epsilon q H_{\rm osc} \phi^2 \tag{7.30}$$

$$\epsilon \equiv \tilde{\epsilon} \frac{S_{\rm cr}}{M_{\rm Pl}} \tag{7.31}$$

$$\tilde{\epsilon} \simeq (0.1 - 0.2) an \sin\left(n\theta_\phi - \theta_S\right)_{\rm osc}, \tag{7.32}$$

where we define $\tilde{\epsilon}$ which is expected to be of order unity. The numerical factor of $(0.1 - 0.2)$ is determined from our numerical calculations explained below. Note that the resulting ellipticity parameter ϵ is consistent with a naive estimation of $\epsilon \sim V'_A/\phi H^2_{\rm osc}$.[3] The ellipticity parameter ϵ, which describes the efficiency of baryogenesis, is much smaller than unity because of the condition of Eq. (7.23). This is because the phase direction of the AD field is kicked by the A-term that is suppressed by the VEV of the inflaton.

After the oscillations begins, the amplitude of the radial direction of the inflaton S decreases with time as $|S| \propto a^{-3/2}$. That of the AD field does as $|\phi| \propto a^{-3/4}$ so that its number density $(H(t)\left|\phi\right|^2/2)$ decreases as $\propto a^{-3}$. Since the A-term, i.e., the $B-L$ number violating interaction, is a higher dimensional term, it is turned off soon after the AD field starts to oscillate after inflation. The generated $B-L$ asymmetry is then conserved in a comoving volume and thus $n_{B-L} \propto a^{-3}$ for $t > t_{\rm osc}$.

We have numerically solved the equations of motion together with the Friedmann equation, where the waterfall fields are collectively described by a real scalar field $\tilde{\psi}$ such as $\psi = \bar{\psi} \equiv \tilde{\psi}/\sqrt{2}$. We assume $\left|S\right|^2/M^2_{\rm Pl}$, $\left|\phi\right|^2/M^2_{\rm Pl}$, $\tilde{\psi}^2/M^2_{\rm Pl} \ll 1$ and take into account next-to-leading order terms in terms of them. We use the full kinetic terms for S and ϕ [see Eq. (A.30)], while we assume a canonical one for $\tilde{\psi}$ for simplicity. One of the results is shown in Fig. 7.1, where the generated $B-L$ asymmetry is consistent with Eq. (7.60). Taking parameters such as $n = 4, 6$, $\kappa = 0.02 - 0.5$, $\mu = 0.0004 - 0.02$, $\lambda = 0.01 - 100$, and $\theta^{\rm ini}_\phi = 0.001 - 0.1$, we confirm the above parameter dependences and obtain the numerical uncertainty of $(0.1 - 0.2)$ in Eq. (7.32). We assume $c_H = -1$ and $c_2 = 0$ in our calculations, but we check that nonzero values of c_2 ($= \mathcal{O}(1)$ and ≥ 0) does not change our results even quantitatively.

[3] We implicitly assume that $(S_{cr}/M_{\rm Pl}) \gtrsim m_{3/2}/H_{\rm osc}$ so that we can neglect an A-term of $m_{3/2}W_\phi$ [see Eq. (3.9)]. Otherwise ϵ may be of order $m_{3/2}/H_{\rm osc}$.

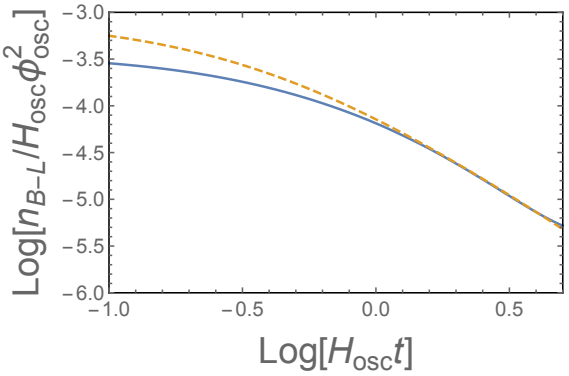

Figure 7.1: Evolution plot for $B-L$ number after hybrid inflation. The dashed curve is our prediction of Eq. (7.32) with a numerical factor of 0.2. We assume $\lambda = 1$, $n = 6$, $c_H = -1$, $c_2 = 0$, $\kappa = 0.05$, $\mu = 0.001$, and $\theta_\phi^{\rm ini} = 0.01$.

7.3.2 Baryon asymmetry

The AD field starts to oscillate just after inflation and generate $B-L$ asymmetry. The oscillating AD field decays and dissipates into radiation [68] and the sphaleron effect relates the $B-L$ asymmetry to the baryon asymmetry [20, 21]. Using Eq. (7.60), we can calculate the baryon-to-entropy ratio Y_b such as

$$Y_b \simeq \frac{8}{23}\frac{\epsilon q T_{\rm RH}}{4H_{\rm osc}}\left(\frac{\phi_{\rm osc}}{M_{\rm Pl}}\right)^2 \tag{7.33}$$

$$\simeq \begin{cases} 0.05\sqrt{|c_H|}q\frac{\epsilon}{\lambda}\frac{T_{\rm RH}}{M_{\rm Pl}} & \text{for} \quad n=4 \\ 0.06\,|c_H|^{1/4}\,q\frac{\epsilon}{\lambda^{1/2}}\frac{T_{\rm RH}}{\sqrt{H_{\rm osc}M_{\rm Pl}}} & \text{for} \quad n=6. \end{cases} \tag{7.34}$$

Since $\epsilon \equiv \tilde{\epsilon} S_{\rm cr}/M_{\rm Pl}$, $S_{\rm cr} = \mu$, and $H_{\rm osc}^2 \simeq \kappa^2\mu^4/(3M_{\rm Pl}^2)$, this is rewritten as

$$Y_b \simeq \begin{cases} 0.05\frac{\mu T_{\rm RH}}{\lambda M_{\rm Pl}^2} & \text{for} \quad n=4 \\ 0.08\frac{T_{\rm RH}}{\sqrt{\kappa\lambda}M_{\rm Pl}} & \text{for} \quad n=6, \end{cases} \tag{7.35}$$

where we assume $|c_H| = 1$, $q = 1$, and $\tilde{\epsilon} = 1$. For typical parameters, it is given by

$$Y_b \simeq \begin{cases} 9\times10^{-11}\left(\frac{\mu}{10^{15}\ {\rm GeV}}\right)\left(\frac{T_{\rm RH}}{10^{9}\ {\rm GeV}}\right)\left(\frac{\lambda}{10^{-4}}\right)^{-1} & \text{for} \quad n=4 \\ 1\times10^{-10}\lambda^{-1/2}\left(\frac{\kappa}{10^{-3}}\right)^{-1/2}\left(\frac{T_{\rm RH}}{10^{7}\ {\rm GeV}}\right) & \text{for} \quad n=6. \end{cases} \tag{7.36}$$

We check that the constraints of Eqs. (7.22) and (7.23) and $\xi \leq 1$ [see Eq. (7.18)] are satisfied for the above reference parameters. Thus, we can explain the observed baryon asymmetry of $Y_b^{\rm obs} \simeq 8.6\times10^{-11}$ [7] in this scenario.

As we can see in Eq. (7.36), the resulting baryon asymmetry depends on reheating temperature $T_{\rm RH}$. Here we need to take into account the constraint on $T_{\rm RH}$ from gravitino overproduction problem. For example, in the case of $m_{3/2} = 100$ GeV, the reheating temperature is bounded as Eq. (6.24). We can see that the reference parameters used in Eq. (7.36) are consistent with that bound.

Note that for the case of $n = 4$, the coupling constant in the superpotential of the AD field cannot be much larger than 10^{-4} because of the upper bound on the reheating temperature. For the case of $n = 6$, we can naturally explain the observed baryon asymmetry for $\lambda = \mathcal{O}(1)$ with a reheating temperature consistent with the gravitino problem. This is in contrast to the result in the conventional scenario of ADBG [see Eq. (3.66)], where an extremely large value of λ is required to be consistent with the lower bound on reheating temperature.

Since a linear combination of phase directions is massless during inflation, our scenario predicts nonzero baryonic isocurvature fluctuations as explained in Sec. 3.5. However, the energy scale of hybrid inflation can be lower than the constraint of Eq. (3.93). In fact, for the above reference parameters, our scenario is consistent with the present upper bound on the isocurvature fluctuations.

7.4 Chaotic inflation

In this section, we consider the new scenario of ADBG in the chaotic inflation model with a shift symmetry in supergravity [61, 62].

7.4.1 Dynamics of the AD field

Taking into account the AD field, we consider the Kähler potential of

$$K = K_{\rm inf} + |\phi|^2 + c_1 |X|^2 |\phi|^2 - \frac{c_2}{2} (I + I^*)^2 |\phi|^2 , \tag{7.37}$$

where $K_{\rm inf}$ is given by Eq. (6.47). Although we introduce a shift symmetry for the field I, the fields X and I basically correspond to the fields S and ψ in Eq. (7.1), respectively. The AD field acquires the Hubble-induced mass term from the F-term of X during inflation. After inflation ends, the Hubble-induced mass term partially comes from kinetic interactions. In fact, the Kähler potential of $-c_2/2(I + I^*)^2 |\phi|^2$ induces a kinetic interaction of

$$\mathcal{L} \supset -c_2 \frac{1}{M_{\rm Pl}^2} |\phi|^2 |\partial_\mu I|^2 . \tag{7.38}$$

We obtain the effective Hubble-induced mass term of $(3c_2/2)H^2(t)\,|\phi|^2$ from this kinetic interaction. To sum up, the Hubble-induced mass term is given by

$$V_H = c_H H^2(t)\,|\phi|^2 \tag{7.39}$$

$$c_H = \begin{cases} -3(c_1-1) & \text{during inflation} \\ \frac{3}{2}(c_2 - c_1 + 1) & \text{after inflation,} \end{cases} \tag{7.40}$$

where the other terms than the one proportional to c_2 come from the potential energy. Thus we can consider the case that the coefficient c_H is negative during inflation and is positive after inflation.

There is also an A-term such as

$$V_A = \frac{1}{n}(n(1-c_1)-2)\frac{\lambda m_{\rm inf}}{M_{\rm Pl}^{n-1}} I X (\phi^*)^n + \text{c.c.} \tag{7.41}$$

$$= \frac{2}{n}(n(1-c_1)-2)\frac{\lambda m_{\rm inf}}{M_{\rm Pl}^{n-1}} |I|\,|X|\,|\phi|^n \cos(\theta_I + \theta_X - n\theta_\phi) \tag{7.42}$$

$$\simeq -aH^2(t)\frac{|X|}{M_{\rm Pl}}|\phi|^2 \cos(\theta_I + \theta_X - n\theta_\phi), \tag{7.43}$$

where we use Eq. (3.39) and $H(t) \simeq m_{\rm inf}\,|I|/\sqrt{3}M_{\rm Pl}$ in the last line and θ_I, θ_X, and θ_ϕ are the complex phases of the fields I, X, and ϕ, respectively. The coefficient a is given by

$$a = 2\sqrt{\frac{3\,|c_H|}{n-1}}\left(c_1 - 1 + \frac{2}{n}\right). \tag{7.44}$$

The A-term can be regarded as a linear term for X. Since the field X has a positive Hubble-induced mass term of Eq. (6.57), it stays at the following minimum during inflation:

$$\langle |X| \rangle \simeq \frac{a}{6c_3}\frac{1}{M_{\rm Pl}}|\phi|^2. \tag{7.45}$$

A linear combination of the phase directions has a mass of order the Hubble parameter due to the A-term, so that it stays at the following minimum during inflation:

$$\langle \theta_X - n\theta_\phi \rangle = -\langle \theta_I \rangle \simeq -\text{sign}[c_0]\frac{\pi}{2}, \tag{7.46}$$

where we use $\text{Re}[I] \ll \text{Im}[I]$ during inflation.

After inflation ends, the field I starts to rotate in the phase space as shown in Fig. 6.2 and its phase θ_I has a nonzero velocity. This implies that a linear combination of the phases θ_X and θ_ϕ obtains a nonzero velocity to follow its potential minimum. We perform numerical calculations to solve the equations of motion for the complex scalar fields I, X, and ϕ. We use

the full supergravity potential for I, X, and ϕ. The kinetic interactions are simplified such that I and X have canonical kinetic terms for simplicity. We take into account the kinetic interactions for ϕ associated with c_2, which is needed to change the sign of its Hubble-induced mass term. The parameters are taken in the intervals of $\lambda = 10^{-3} - 10^4$ and $c_0 = 10^{-5} - 1$ for $n = 4$ and 6. The $\mathcal{O}(1)$ coefficients in the Kähler potential are assumed to be $c_1 = 2$, $c_2 = 1$, and $c_3 = 1$. From our numerical calculations, we obtain the following results:

$$\frac{a^3(t)}{a^3(t_{\rm osc})} n_{B-L}(t) \equiv \epsilon q H_{\rm osc} \phi_{\rm osc}^2 \tag{7.47}$$

$$\epsilon \equiv \tilde{\epsilon} c_0 \tag{7.48}$$

$$\tilde{\epsilon} \simeq (0.01 - 0.1) a, \tag{7.49}$$

where the factor of $0.01 - 0.1$ is a numerical uncertainty. One example of our results is shown in Fig. 7.2, where we set $\lambda = 1$, $n = 6$, $c_0 = 0.5$, $c_1 = 2$, $|c_2| = 1$, and $c_3 = -1$. The blue curve represents the time evolution of the $B - L$ number after the end of inflation, while the orange dashed curve corresponds to Eq. (7.49) with a numerical factor of 0.01. The oscillation behaviour of $B - L$ number density may come from the effect of the oscillating inflaton through supergravity effects and is irrelevant for our discussion.[4] The c_0 dependence in our result of Eq. (7.48) comes from the ellipticity of the dynamics of the inflaton in the complex plane. This means that $B - L$ asymmetry cannot be generated for $c_0 = 0$, in which case no CP odd component of the field I is excited.

7.4.2 Baryon asymmetry

Using the results obtained in the previous subsection, we calculate the baryon-to-entropy ratio such as

$$Y_b \simeq \frac{2\tilde{\epsilon} q}{23} c_0 \frac{T_{\rm RH}}{H_{\rm osc}} \left(\frac{\phi_{\rm osc}}{M_{\rm Pl}} \right)^2 \tag{7.50}$$

$$\simeq \begin{cases} 0.005 c_0 \frac{T_{\rm RH}}{\lambda M_{\rm Pl}} & \text{for} \quad n = 4 \\ 0.006 c_0 \frac{T_{\rm RH}}{\sqrt{\lambda H_{\rm osc} M_{\rm Pl}}} & \text{for} \quad n = 6, \end{cases} \tag{7.51}$$

[4] It has been investigated that this supergravity effect can be used for another scenario of baryogenesis [120]. Note that we do not introduce a $B - L$ violating operator associated with the right-handed neutrino, so that the net $B - L$ asymmetry vanishes for this effect. Even if we introduce the $B - L$ violating operator, the resulting $B - L$ asymmetry generated from this effect is much smaller than that generated from ADBG.

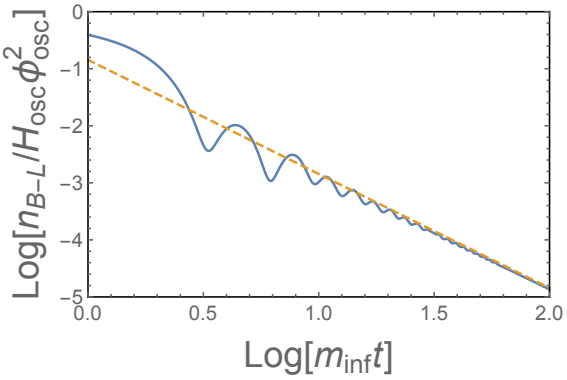

Figure 7.2: Evolution plot for $B-L$ number density in our scenario of ADBG in the chaotic inflation model. The dashed curve is our prediction of Eq. (7.49) with a numerical factor of 0.01. We take $\lambda = 1$, $n = 6$, $c_0 = 0.5$, $c_1 = 2$, $|c_2| = 1$, and $c_3 = -1$.

where we assume $\tilde{\epsilon} q = 0.1$ and $|c_H| = 1$ in the last line. For typical parameters, it is given by

$$Y_b \simeq \begin{cases} 2 \times 10^{-10} \left(\frac{c_0 T_{\rm RH}}{10^7 \text{ GeV}}\right) \left(\frac{\lambda}{10^{-4}}\right)^{-1} & \text{for } n = 4 \\ 1 \times 10^{-10} \left(\frac{c_0 T_{\rm RH}}{10^6 \text{ GeV}}\right) \left(\frac{\lambda}{10^{-4}}\right)^{-1/2} & \text{for } n = 6, \end{cases} \tag{7.52}$$

where we use $H_{\rm osc} \simeq m_{\rm inf} \approx 10^{13}$ GeV. Thus, we can explain the observed baryon asymmetry of $Y_b^{\rm obs} \simeq 8.6 \times 10^{-11}$ [7].

Since the COBE normalisation of the amplitude of density perturbations requires that the energy scale of chaotic inflation is given by $H_{\rm inf} \simeq 10^{14}$ GeV, the baryonic isocurvature constraint of Eq. (3.93) is much severer than the case in the hybrid inflation. It requires that the parameter in the superpotential λ is smaller than about 10^{-4}. This means that the VEV of the AD field is as large as the Planck scale during inflation. In this case, the backreaction of the AD field to inflaton dynamics might be relevant as explained in Sec. 6.3.4. As a result, the tensor-to-scalar ratio can be consistent with the present constraint within 2σ [32]. Note that the number density of the AD field decreases with time as $\propto a^{-3}$ due to the expansion of the Universe. This means that its energy density decreases as $a^{-9/2}$ because its effective mass is of order the Hubble parameter, which decreases as $a^{-3/2}$. Thus its energy density never dominates that of the Universe and the result of Eq. (7.50) is applicable even for the case of $\phi_{\rm osc} \simeq M_{\rm Pl}$.

Note also that when the oscillation amplitude of the AD field is as large as the Planck scale as indicated by the baryonic isocurvature constraint, higher-dimensional Kähler potential may affect the dynamics of inflaton. In particular, the phase direction of the AD field may be kicked by some Kähler potentials as we explain in Sec. 7.5 [see Eq. (7.57)]. In this case,

the epsilon parameter is typically of order unity.

In order to kick the phase direction and generate $B-L$ asymmetry, we may need a nonzero value of Z_2 breaking parameter c_0. However, the Z_2 breaking term makes the inflaton decay into gravitinos efficiently via supergravity effects and it leads to the gravitino overproduction problem as explained in Sec. 6.3.2. We can avoid the problem by assuming that the gravitino is sufficiently heavy ($m_{3/2} \gtrsim 100$ TeV) so as to decay before the BBN epoch and the R-parity is violated for the LSP not to overclose the Universe. Or, we can assume that gravitino is sufficiently light ($m_{3/2} \lesssim 2$ keV), in which case its thermal abundance do not overclose the Universe. The former possibility might be well motivated partly because the observed 125 GeV Higgs mass favours a heavy squark mass of order 100 TeV for a small $\tan\beta$ [132, 133]. However, since we need a VEV of order the Planck scale to avoid the baryonic isocurvature constraint, the AD field may be kicked by higher-dimensional Kähler potential. In this case, we can generate baryon asymmetry without introducing the Z_2 breaking term in the inflaton sector and we can set $c_0 = 0$. Then we can avoid the gravitino problem.

7.5 D-term inflation

In this section, we investigate a similar scenario to the one explained in the previous sections, where the AD field starts to oscillate just after the end of inflation [134, 31]. This is realized in D-term inflation when the AD field obtains a positive Hubble-induced mass term after inflation.

7.5.1 Dynamics of the AD field

In the case of D-term inflation, the superpotential in the inflaton sector is absent during and after inflation because ψ_- in Eq. (6.29) has a vanishing VEV throughout the history of the Universe. Thus the A-term of the AD field may come only from the low-energy SUSY breaking effect, which may be too small to explain the observed baryon asymmetry in our scenario. However, there is another source of $B-L$ violating operator as shown below when the VEV of the AD field is as large as the Planck scale. Thus, in this section, we assume that the superpotential of the AD field is absent or sufficiently small so that the initial VEV of the AD field $\phi_{\rm osc}$ can be as large as the Planck scale ($\phi_{\rm osc} \simeq M_{\rm Pl}$). Such a large VEV is favoured to avoid the baryonic isocurvature constraint as shown in Sec. 6.2.3. Note that owing to the exponential term in the supergravity potential the VEV of the AD field is restricted below the Planck scale. Since the curvature of the phase direction is absent (or at least much less

than the Hubble parameter), the phase of the flat direction also stays at a certain phase during inflation. We denote the initial phase of the AD field as $\theta_{\rm ini}$.

After inflation, the energy density of the Universe is dominated by that of oscillating inflaton. Since the F-term of ψ_- is given by $\lambda S\psi_+$, the flat direction obtains Hubble-induced terms through supergravity effects [19]:

$$V_H = 3\frac{|\phi|^2}{M_{\rm Pl}^2}\left|\lambda S\psi_+\right|^2, \tag{7.53}$$

for the minimal Kähler potential. Using $\psi_+ = \sqrt{\xi}$ and taking average with respect to time, we obtain the Hubble-induced mass term of

$$\begin{aligned} V_H &= c_H H^2(t)\,|\phi|^2 & (7.54)\\ c_H &= \frac{3}{2}. & (7.55) \end{aligned}$$

Introducing a higher-dimensional Kähler potential of

$$K^{(H)} = c_S\,|S|^2\,\frac{|\phi|^2}{M_{\rm Pl}^2}, \tag{7.56}$$

we allow the coefficient c_H to be an arbitrary $\mathcal{O}(1)$ parameter.

In addition to the Hubble-induced mass term, the flat direction obtains higher-dimensional terms from non-renormalizable Kähler potentials. If we assign R-charges as, for example, $R(Q) = R(L) = R(e^c) = R(u^c) = R(d^c) = 0$ and $R(H_u) = R(H_d) = 2$, we can write nonrenormalizable Kähler potentials of[5]

$$\begin{aligned} & \frac{2}{3}a_H\int {\rm d}^2\theta{\rm d}^2\bar\theta\,|S|^2\,\frac{\phi^n}{nM_{\rm Pl}^n} + {\rm c.c.} \\ \simeq\ & -\frac{2}{3}a_H\,|\partial_\mu S|^2\,\frac{\phi^n}{nM_{\rm Pl}^n} + {\rm c.c.} \\ \simeq\ & -a_H H^2(t)\left(\frac{\phi^n}{nM_{\rm Pl}^{n-2}} + {\rm c.c.}\right), \end{aligned} \tag{7.57}$$

where n is an integer depending on flat directions. For example, $n = 3, 6, 9, \ldots$ for $u^c d^c d^c$ flat direction. In the last line, we take average with respect to time and use the relation

[5] The R-symmetry has to be broken to obtain nonzero gaugino and higgsino masses and to set the vacuum energy (almost) zero. Its symmetry breaking order parameter is proportional to the SUSY breaking scale, so that R-symmetry breaking terms are suppressed by a factor of $m_\phi^2/M_{\rm Pl}^2$. Since this is much smaller than the energy scale of inflation, such breaking terms can be neglected in the following discussion. Therefore, it is reasonable to consider that R-symmetry may suppress the superpotential for the flat direction.

of $\langle(\partial_0 S)^2\rangle \simeq 3H^2(t)M_{\rm Pl}/2$, which comes from the virial theorem. Note that this term has a nonzero phase which is different from the phase of the flat direction $\theta_{\rm ini}$ during inflation. We can redefine the phase of the flat direction to eliminate the phase of a_H. After the elimination, we redefine the initial phase of the flat direction as $\theta_{\rm ini}$ without loss of generality. The discrepancy between the initial phase of the flat direction and the phase of the above $U(1)$ breaking term is essential to generate the baryon asymmetry.

In summary, the AD field obtains the following potential after inflation:

$$V(\phi) = c_H H^2(t)\,|\phi|^2 - a_H H^2(t)\left(\frac{\phi^n}{nM_{\rm Pl}^{n-2}} + {\rm c.c.}\right) + \ldots, \tag{7.58}$$

where c_H and a_H are positive $\mathcal{O}(1)$ parameters. The dots represents higher-dimensional terms which restrict the AD field below the Planck scale. Since the flat direction starts to oscillate due to the Hubble-induced mass, we can neglect usual soft mass and A-terms for the AD field.

7.5.2 Baryon asymmetry

In this subsection, we calculate the baryon asymmetry generated from the AD field with the potential (7.58). The initial VEV and phase are $\phi_{\rm osc}$ and $\theta_{\rm ini}$, respectively. For $c_H > 0$, the flat direction starts to oscillate around the origin of the potential just after the end of inflation. At the same time, the flat direction is kicked in the phase direction due to the second term in Eq. (7.58). The $B-L$ asymmetry is generated through this dynamics:

$$\frac{a^3(t)}{a^3(t_{\rm osc})} n_{B-L}(t) \equiv \epsilon q H_{\rm osc}\phi_{\rm osc}^2 \tag{7.59}$$

$$\epsilon \simeq (3-4)\times\frac{8}{3n-6} a_H \sin\left(-n\theta_{\rm ini}\right)\left(\frac{\phi_{\rm osc}}{M_{\rm Pl}}\right)^{n-2}, \tag{7.60}$$

where we have used $\phi \propto a^{-3/4}$. We have numerically solved the equations of motion for ϕ and S with the Friedmann equation and have obtained the numerical factor of $(3-4)$ for $\epsilon \lesssim 1$. The amplitude of the flat direction decreases as time evolves due to the Hubble expansion and the $B-L$ breaking effect is absent soon after the oscillation. Thus, the generated $B-L$ asymmetry is conserved soon after the AD field starts to oscillate.

We can calculate the resulting baryon-to-entropy ratio Y_b as

$$\begin{aligned} Y_b &\simeq \frac{8}{23}\frac{\epsilon q T_{\rm RH}}{4H_I}\left(\frac{\phi_{\rm osc}}{M_{\rm Pl}}\right)^2 \\ &\simeq 8.7\times 10^{-11}\epsilon q \left(\frac{T_{\rm RH}}{4\times 10^3\ {\rm GeV}}\right)\left(\frac{H_I}{4\times 10^{12}\ {\rm GeV}}\right)^{-1}\left(\frac{\phi_{\rm osc}}{M_{\rm Pl}}\right)^2. \end{aligned} \tag{7.61}$$

This can be consistent with the observed baryon asymmetry when $T_{\rm RH}$ is of order 10^{3-4} GeV.

Chapter 8

Solutions to the coincidence problem in the new scenario

This chapter is based on the work done by the author [31]. In this chapter, we apply the scenario explained in the previous chapter and provide another scenario to account for the baryon-DM coincidence problem.

8.1 Introduction

In this chapter, we propose another scenario that predicts an $\mathcal{O}(1)$ ratio of baryon and DM densities. The inflaton sector is constructed such that the inflaton and waterfall fields decay into gravitinos with an $\mathcal{O}(1)$ branching ratio. The gravitino is assumed to be as heavy as 100 TeV so that it decays into the MSSM particles before the BBN epoch. The decay of those gravitinos is a source of non-thermal production of LSP DM and the resulting DM abundance is proportional to the reheating temperature and inversely proportional to the inflaton mass. When the AD field has a VEV as large as the Planck scale, the resulting amount of the baryon asymmetry has similar parameter dependences to that of DM. As a result, the baryon and DM densities are related with each other through the energy scale of inflation. The resulting baryon and DM densities are naturally of order unity when the scenario applies to F- term and D-term hybrid inflation models.[1]

[1] Another scenario for co-genesis of baryon and DM has been proposed in Ref. [135] where they introduce an additional heavy field to generate both of them.

8.2 Models

In this section, we provide models that realise the scenario to account for the coincidence problem explained in the subsequent sections.

The AD field is assumed to start to oscillate around the minimum just after inflation as we explain in the previous chapter. We require that its superpotential is absent or highly suppressed so that its oscillation amplitude is as large as the Planck scale. This is actually required in chaotic inflation models to avoid the isocurvature constraint. It is also required in D-term inflation models to kick the AD field in the complex plane by higher-dimensional Kähler potentials. In the hybrid inflation model, the superpotential should be highly suppressed so that the backreaction of the AD field to the inflaton can be neglected for such a large initial VEV of the AD field. In any cases, when the oscillation amplitude of the AD field is as large as the Planck scale, the AD field is kicked by higher-dimensional Kähler potentials and the ellipticity parameter is of order unity. The resulting baryon asymmetry is then given by Eq. (7.7) with $\phi_{\rm osc} \simeq M_{\rm Pl}$ and $\epsilon \approx 1$.

We also require that gravitinos are produced with an $\mathcal{O}(1)$ branching ratio in the reheating epoch. This is naturally realized when inflaton (and/or waterfall fields if there exist) decays only through the supergravity effects as explained in Sec. B.4.1. This is naturally realized in F-term hybrid inflation model when we suppress the interaction of Eq. (6.18). In this case, the branching into gravitino is of order unity and the reheating temperature is given by Eq. (6.17). In the chaotic inflation model, we suppress the interaction of Eq. (6.59) so that the inflaton decays mainly into gravitinos. The reheating temperature is determined by Eq. (6.58), which depends on the Z_2 breaking parameter c_0.

As for D-term inflation models, we modify it by introducing a shift symmetry and an approximate Z_2 symmetry for the inflaton field S [61]. Under these symmetries, S transforms as $S \to S + i\alpha$ (α:real) and $S \to -S$, respectively. Then, the Kähler potential is written as

$$K = c_0 \left(S + S^*\right) + \frac{1}{2}\left(S + S^*\right)^2 + \left|\psi_-\right|^2 + \left|\psi_+\right|^2 , \tag{8.1}$$

where c_0 ($\ll 1$) is an order parameter for the Z_2 symmetry breaking effect. The superpotential of Eq. (6.29) explicitly breaks the shift symmetry, which is required to ensure a graceful exit of inflation. In this model, we should replace $|S|^2$ with $(S + S^*)^2/2$ for the calculations in Sec. 7.5, though the results are unchanged. We introduce Z_2 breaking terms in the Kähler potential so that the field S efficiently decays into gravitinos [114], whose decay is a source of non-thermal production of LSP DM. There is an advantage to impose the shift symmetry to the inflaton. In order to obtain a sufficiently large e-folding number, say, $N_* \gtrsim 60$, the initial

VEV of the inflaton S has to be as large as $N_* \frac{\sqrt{2}g^2}{4\pi^2} M_{\rm Pl} \simeq 0.5 M_{\rm Pl}$. which is of order the Planck scale. This implies that the Planck-scale physics may affect the potential of the inflaton and spoil its flatness. However, the shift symmetry ensures the flatness of the inflaton potential above the Planck scale.

As explained in Sec. 6.2.2, the field ψ_+ decays into the MSSM fields much faster than the inflaton S, so that the reheating temperature of the Universe is determined by the relatively late-time decay of the inflaton S [67]. After the field ψ_+ decays completely, the effective superpotential can be rewritten as Eq. (B.25) with $m_{\rm inf} = \lambda\sqrt{\xi}$ and the replacements of $X \to \psi_-$. Thus we can use the results derived in Appendix B.4.1.

8.3 Reheating process

In this section, we investigate the reheating process and calculate the DM abundance in the models introduced in the previous section. At the minimum of potential, the models reduce to the one considered in Appendix B.4.1, so that we use the same notation with the one used in Sec B.4.1.

The Z_2 breaking term in the Kähler potential or the nonzero VEV of water fall fields result in their decay through supergravity effects [114]. The branching ratio of inflaton decay into gravitinos is given by Eq. (B.35). Since $d/c = \mathcal{O}(1)$ and $y_t = \mathcal{O}(1)$, the branching ratio is almost unity. This means that the energy density of the Universe is dominated by that of the gravitinos after the fields $\Phi_\pm$ decay completely.[2]

Since the fields $\Phi_\pm$ are much heavier than gravitino, the produced gravitinos are highly relativistic. The Lorentz factor for the gravitinos at a time $H^{-1}(t)$ is given as

$$\gamma(t) = \left[\left(\frac{m_{\rm inf}}{m_{3/2}}\right)^2 \frac{H(t)}{\Gamma_{\rm inf}} + 1\right]^{1/2} \simeq \frac{m_{\rm inf}}{m_{3/2}} \left(\frac{H(t)}{\Gamma_{\rm inf}}\right)^{1/2}. \tag{8.2}$$

The gravitinos decay into MSSM particles with a rate of

$$\Gamma_{3/2} \simeq \gamma^{-1}(t) \frac{1}{48\pi} \frac{\sum_i m_{\tilde{X}_i}^5}{m_{3/2}^2 M_{\rm Pl}^2}, \tag{8.3}$$

where the summation is taken for all MSSM particles $\tilde{X}_i$. When we consider a SUSY model with relatively light gauginos and relatively heavy squark and sleptons, we can roughly

[2]Note that since we consider relatively low reheating temperature $\sim 10^{3-4}$ GeV as explained in the next section, we can neglect the thermal production of gravitinos [116, 117].

estimate the numerator as $24m_{3/2}^5$. This implies that the gravitino decays into radiation at the temperature of

$$\begin{aligned} T_{3/2} &\simeq \left(\frac{90}{g_*\pi^2}\right)^{1/4}\sqrt{\Gamma_{3/2}M_{\rm Pl}} \\ &\simeq 1.1\ {\rm MeV}\left(\frac{T_{\rm RH}}{4\times10^3\ {\rm GeV}}\right)^{1/3}\left(\frac{m_{\rm inf}}{5\times10^{15}\ {\rm GeV}}\right)^{-1/3}\left(\frac{m_{3/2}}{400\ {\rm TeV}}\right)^{4/3}, \end{aligned} \tag{8.4}$$

where g_* ($\simeq 10.75$) is the effective number of degrees of freedom at the decay time. We require that the mass of gravitino is of order 10^{2-3} TeV or larger so that its decay completes before the BBN epoch, that is, $T_{3/2} \gtrsim 1$ MeV. Otherwise the decay particles interact with the light elements and spoil the success of the BBN [49]. The gravitino decay temperature $T_{3/2}$ is much smaller than the mass of the LSP, so that the decay of gravitino is a source of its nonthermal production. Since the energy density of the Universe is dominated by that of gravitino before they decay, the thermal relic density of the LSP is diluted by the entropy production from the gravitino decay. Therefore, the LSP abundance is determined by the nonthermal production from the gravitino decay. The produced number density of the LSPs is equal to that of the gravitinos due to the R-parity conservation. Note that the annihilation of the produced LSP is usually inefficient in such a low temperature.

The Lorentz factor of the gravitino is of order 10^3 for the reference parameters shown in Eq. (8.4). This implies that the scale factor of the Universe continues to decrease as a^{-4} from the time of reheating by the decay of $\Phi_\pm$. Although the LSPs are relativistic at the time they are produced from gravitino decay, they lose their energy through interactions with the thermal plasma and soon become to non-relativistic particles [136, 137, 138]. Therefore, the LSP DM is cold even though they are produced non-thermally in this scenario.

Here we comment on the hierarchy of gravitino mass and other SUSY particles. Such a heavy gravitino is well motivated in a class of SUSY models with a split spectrum [139, 140, 141, 50]. In these models, the masses of gravitino as well as squarks and sleptons are of order (or larger than) 10^{2-3} TeV while those of gauginos are of order 1 TeV. This hierarchy can be realized when gauginos acquire one-loop suppressed soft masses through the anomaly mediated SUSY breaking effect [142, 143]. When the Higgs μ-term is of order the gravitino mass, the Higgsino threshold correction is important and the wino mass can be as small as $10^{-3}m_{3/2}$. Note that neutral higgsino can also be the LSP when the Higgs μ-term is sufficiently small. The following discussion does not rely on the detailed properties of the LSP except for its mass. Hereafter, we assume that the mass of gravitino is $O(10^{2-3})$ TeV and that of the LSP is $O(10^{2-3})$ GeV.

8.3.1 DM density and baryon-DM coincidence

Let us summarize the scenario of non-thermal production of DM. First, the fields $\Phi_\pm$ (i.e., inflaton and/or waterfall fields) decay into gravitinos as well as the MSSM particles at $H(t) \simeq \Gamma_{\rm inf}$. Then the energy density of the Universe is dominated by the relativistic gravitinos and decreases as a^{-4}. The gravitinos decay into the MSSM particles just before the BBN epoch and the LSP DM is produced non-thermally. Since the thermal relic density of the LSP is diluted by the entropy production of gravitino decay, its abundance is determined by the gravitino decay. Thus, we can estimate the resulting DM abundance as

$$\begin{aligned} Y_{\rm DM} &\equiv \frac{n_{\rm LSP}}{s} \\ &\simeq \left.\frac{n_{3/2}}{s}\right|_{H=\Gamma_{3/2}} \\ &\simeq \left.\frac{3T_{3/2}}{4}\frac{n_{3/2}}{\rho_{3/2}}\right|_{H=\Gamma_{3/2}} \\ &\simeq \left.\frac{3T_{3/2}}{4}\left(\frac{\Gamma_{\rm inf}}{\Gamma_{3/2}}\right)^{1/2}\frac{n_{3/2}}{\rho_{3/2}}\right|_{H=\Gamma_S} \\ &\simeq \left.\frac{3T_{\rm RH}^{(\rm eff)}}{4}\frac{2{\rm Br}_{3/2}n_S}{\rho_S}\right|_{H=\Gamma_S} \\ &\simeq \frac{3T_{\rm RH}^{(\rm eff)}}{2m_{\rm inf}}, \end{aligned} \tag{8.5}$$

where we have used ${\rm Br}_{3/2} \simeq 1$ in the last line. We define the effective reheating temperature $T_{\rm RH}^{(\rm eff)}$ by Eq. (B.19) with the replacement of $g_*(T_{\rm RH}) \to g_*(T_{3/2})$ as

$$\begin{aligned} T_{\rm RH}^{(\rm eff)} &\simeq \left(\frac{90}{g_*(T_{3/2})\pi^2}\right)^{1/4}\sqrt{\Gamma_{\rm inf}M_{\rm Pl}} \\ &\simeq 1.5\times10^3\ {\rm GeV}\left(\frac{m_{\rm inf}}{5\times10^{15}\ {\rm GeV}}\right)^{3/2}\left(\frac{d}{10^{-10}}\right). \end{aligned} \tag{8.6}$$

In the chaotic inflation model and D-term inflation model, the reheating temperature is adjusted by the Z_2 symmetry order parameter d to obtain a desirable abundance of baryon asymmetry from Eq. (7.7) or DM from Eq. (8.5). On the other hand, in the F-term hybrid inflation model the reheating temperature is determined as Eq. (6.17), where we can realize $T_{\rm RH} = 10^{3-4}$ GeV for $\mu \simeq 10^{15}$ GeV and $m_{\rm inf} \simeq 10^{12}$ GeV.

Here we take into account the baryon asymmetry generated by ADBG. Once we replace the reheating temperature $T_{\rm RH}$ with the effective one $T_{\rm RH}^{(\rm eff)}$ defined by Eq. (8.6), the resulting

baryon asymmetry is still given by Eq. (7.7) even in this scenario. Combining Eqs. (7.7) and (8.5), we obtain the following simple relation for the baryon-to-DM ratio:

$$\frac{\Omega_b}{\Omega_{\rm DM}} \simeq \frac{4}{69}\epsilon q \frac{m_p}{m_{\rm LSP}} \frac{m_{\rm inf}}{H_{\rm osc}}, \tag{8.7}$$

where we assume $\phi_{\rm osc} \simeq M_{\rm Pl}$.

In chaotic inflation models, $H_{\rm osc} \simeq m_{\rm inf}$, so that the resulting baryon-to-DM ratio cannot be consistent with the observed value. On the other hand, in the F-term hybrid inflation model, substituting benchmark parameters and the proton mass $m_p \simeq 0.938$ GeV, we obtain

$$\begin{aligned} \frac{\Omega_b}{\Omega_{\rm DM}} &\simeq 0.11\epsilon q \left(\frac{m_{\rm LSP}}{500\ {\rm GeV}}\right)^{-1} \left(\frac{m_{\rm inf}}{10^{12}\ {\rm GeV}}\right) \left(\frac{H_I}{10^{9}\ {\rm GeV}}\right)^{-1}, \\ &\simeq 0.13\epsilon q \left(\frac{m_{\rm LSP}}{500\ {\rm GeV}}\right)^{-1} \left(\frac{v}{5\times 10^{15}\ {\rm GeV}}\right)^{-1}. \end{aligned} \tag{8.8}$$

These benchmark parameters result in the reheating temperature consistent with Eq. (8.6). In the D-term inflation model, we obtain

$$\begin{aligned} \frac{\Omega_b}{\Omega_{\rm DM}} &\simeq 0.22\epsilon q \left(\frac{m_{\rm LSP}}{400\ {\rm GeV}}\right)^{-1} \left(\frac{m_{\rm inf}}{6.6\times 10^{15}\ {\rm GeV}}\right) \left(\frac{H_I}{4\times 10^{12}\ {\rm GeV}}\right)^{-1}, \\ &\simeq 0.12\epsilon q \lambda g^{-1} \left(\frac{m_{\rm LSP}}{400\ {\rm GeV}}\right)^{-1} \left(\frac{\sqrt{\xi}}{6.6\times 10^{15}\ {\rm GeV}}\right)^{-1}. \end{aligned} \tag{8.9}$$

Those results are naturally of order unity and are consistent with the observed value of $\Omega_b^{\rm (obs)}/\Omega_{\rm DM}^{\rm (obs)} \simeq 0.2$ [7]. The scenario naturally explains the coincidence of their energy density, known as the baryon-DM coincidence problem. This is because both of them are related to the energy scale of inflation. The amount of baryon asymmetry is proportional to the reheating temperature of the Universe and inversely proportional to the Hubble parameter during inflation. That of DM is proportional to the reheating temperature and inversely proportional to the mass of inflaton. Since the Hubble parameter and the inflaton mass is related to each other, the resulting baryon and DM density is naturally of order unity.

Although the result has an $\mathcal{O}(1)$ uncertainty coming mainly from v or λ and ξ, the LSP with mass of $O(10^{2-3})$ GeV is favoured in our scenario. If the LSP DM is mostly wino or higgsino, the indirect detection experiments of DM puts lower bounds on DM mass. The wino DM with $m_{\tilde{w}} \leq 390$ GeV and 2.14 TeV $\leq m_{\tilde{w}} \leq 2.53$ TeV is excluded [144], while the higgsino DM with $m_{\tilde{h}} \leq 160$ GeV is excluded [145]. The future indirect detection experiments can detect the wino DM with $m_{\tilde{w}} \leq 1.0$ TeV and 1.66 TeV $\leq m_{\tilde{w}} \leq 2.77$ TeV [144].

Chapter 9

Conclusion

The origin of baryon asymmetry is an outstanding mystery in cosmology and particle physics. The BBN theory and observations of light element abundance imply that the baryon-to-entropy ratio is of order 10^{-10} at least at the temperature of 1 MeV. The Sakharov conditions clarify that it is difficult to generate baryon asymmetry, and in particular, we cannot generate enough baryon asymmetry in the SM of particle physics. The cosmological and astrophysical observations also reveal that there is DM in the Universe. Remarkably, the energy density of DM is almost equal to that of baryons within a factor of order unity, which is known as the baryon-DM coincidence problem. This coincidence may imply that the baryon and DM have a common origin in the early Universe.

In this thesis, we have investigated the Affleck-Dine mechanism to generate baryon asymmetry and to explain the baryon-DM coincidence problem in SUSY theories. It generates squark condensation in the early Universe via the dynamics of a baryonic flat direction called an AD field. The condensation subsequently decays into quarks and light SUSY particles. Since the LSP is a good candidate of DM, this scenario may be able to account for the coincidence between the energy densities of baryon and DM. In fact, we have provided two scenarios to account for the coincidence problem by using the Affleck-Dine mechanism.

The first scenario stands on the formation and decay of non-topological solitons called Q-balls. The squark condensation forms Q-balls after the ADBG in many SUSY models and they carry enormously large baryon charges. The Q-balls eventually decay into baryons and light SUSY particles before the BBN epoch. Therefore the Q-balls are the sources of baryon and DM in this scenario. The branchings of its decay are determined by the Pauli blocking effect and the ratio of LSP and quarks is of order 0.01. As a result, the LSP with mass of order the electroweak scale, which is expected in light of solution of hierarchy problem

in particle physics, can explain the baryon-DM coincidence problem. We have applied this scenario to the CMSSM, which is a typical example of SUSY models, and have determined a parameter region where the coincidence, baryon abundance, and the observed 125 GeV Higgs boson are simultaneously explained. We have shown that the future LHC experiment will search a part of parameter region and would test our scenario.

We have also investigated the relation between the ADBG and inflation models. In particular, we have shown that the backreaction of the AD field affects predictions of inflation models. In F-term hybrid and chaotic inflation models, we have revealed that the resulting spectral index and tensor-to-scalar ratio can be consistent with the observed values by the backreaction. As for the F-term hybrid inflation model, the SKA telescope would detect stochastic gravitational background emitted from cosmic strings and could check the consistency of our scenario. The ADBG predicts baryonic isocurvature density fluctuations that affect CMB temperature anisotropies. The observation thus puts a constraint on a parameter of the AD field. We have shown that the above co-genesis scenario is naturally realized in the chaotic inflation model avoiding the isocurvature constraint and predicting the consistent spectral index and tensor-to-scalar ratio.

Then we have provided a new scenario of ADBG, where the AD field starts to oscillate coherently just after the end of inflation. Our results imply that the ADBG can be realized and can explain the observed baryon asymmetry in a broader range of parameter space than expected in the literature. In fact, it can be realized in the simplest model of F-term hybrid inflation avoiding the gravitino overproduction problem. Based on this new scenario, we have explained the second scenario to solve the baryon-DM coincidence problem. We assume that the AD field has a Planck scale VEV during inflation and then starts to oscillate coherently just after inflation. When the inflaton does not directly interact with the MSSM particles, it mainly decays into gravitinos via SUGRA effects. The gravitinos decay into the MSSM particles before the BBN epoch when the gravitino mass is larger than 100 TeV. As a result, the baryon-to-DM ratio is written by a simple relation. This is because both of the resulting baryon and DM densities depend on parameters in inflaton sector. In particular, we have found that the resulting baryon-to-DM ratio is naturally of order unity in hybrid inflation models. We could check the scenario by detecting DM via the indirect and direct detection experiments of DM.

As a result of those studies, we conclude that ADBG is a promising mechanism to explain the baryon-DM coincidence problem as well as the baryon asymmetry. Those scenarios can be tested by the future LHC experiment and direct and indirect DM searches.

Acknowledgements

The author thanks his supervisor Masahiro Kawasaki for various instructive discussions and collaborations. He also thanks Ayuki Kamada, Keisuke Harigaya, and Kyohei Mukaida, who are collaborators for the studies of the main part of this thesis, for fruitful discussions and collaborations. He also thanks Wilfried Buchmüller for grateful discussions and comments and for kind hospitality at DESY during a part of his Ph. D. course, and Masahiro Ibe for invaluable comments.

This work is supported by World Premier International Research Center Initiative (WPI Initiative), MEXT, Japan, the Program for the Leading Graduate Schools, MEXT, Japan, and the JSPS Research Fellowships for Young Scientists, No. 25.8715.

Appendix A

Supersymmetry

A.1 Supersymmetry

In this Appendix, we briefly explain supersymmetry (SUSY), which is a symmetry that relates fermions and bosons. It is motivated in light of a solution to the hierarchy problem. It also achieves gauge coupling unification, which is required for grand-unified theories. The lightest SUSY particle (LSP) is a good candidate for DM, and the baryon asymmetry can be generated by the Affleck-Dine baryogenesis [17, 19], which is the main topic of this thesis.

A.1.1 MSSM

SUSY theories can be formulated by using superspace, where fermionic coordinates θ^α and $\bar{\theta}_{\dot{\alpha}}$ is added to the spacetime coordinates. The general renormalizable Lagrangian is written as

$$\mathcal{L} = \int \mathrm{d}^2\theta \mathrm{d}^2\bar{\theta} \Phi^{*i} \left(e^{2T^a V^a}\right)_i^j \Phi_j + \int \mathrm{d}^2\theta \left[W(\Phi_i) + \frac{1}{4g_a^2} \mathcal{W}^{a\alpha} \mathcal{W}^a_\alpha + \mathrm{c.c.} \right], \tag{A.1}$$

where Φ_i are chiral supermultiplets, g_a are gauge coupling constants, T^a are generators, V^a are vector supermultiplets, W is superpotential, and $\mathcal{W}^a_\alpha$ are field strength chiral superfield. The superscripts a runs over the adjoint representation of the gauge group. In the Wess-Zumino gauge, it is rewritten in terms of component fields such as

$$\begin{aligned}
\mathcal{L} &= -\nabla^\mu \phi^{*i} \nabla_\mu \phi_i + i\chi^{\dagger i} \bar{\sigma}^\mu \nabla_\mu \chi_i - \frac{1}{4} F^a_{\mu\nu} F^{\mu\nu a} + i\lambda^{\dagger a} \bar{\sigma}^\mu \nabla_\mu \lambda^a & \text{(A.2)} \\
&- \frac{1}{2} \left(W^{ij} \chi_i \chi_j + h.c. \right) + |F_i|^2 & \text{(A.3)} \\
&- \sqrt{2} g_a \left(\phi^{*i} T^a \chi_i \right) \lambda^a - \sqrt{2} g_a \lambda^{\dagger a} \left(\chi^{\dagger i} T^a \phi_i \right) + \sum_a \frac{1}{2} \left(D^a \right)^2, & \text{(A.4)}
\end{aligned}$$

where F-term and D-term are given by

$$|F_i|^2 = |W_i|^2 \tag{A.5}$$

$$\frac{1}{2}(D^a)^2 = \frac{1}{2}g_a^2\left(\phi^{*i}T^a\phi_i\right)^2. \tag{A.6}$$

We define $W_i = \partial W/\partial\phi_i$, and $W^i = (\partial W/\partial\phi_i)^*$, and $W^{ij} = (\partial^2 W/\partial\phi_i\partial\phi_j)^*$. The fields ϕ_i and χ_i are scalar and fermion components of chiral supermultiplets Φ_i, respectively, while the fields λ^a and $F^a_{\mu\nu}$ are fermion and vector components of vector supermultiplets, respectively.

In the minimal SUSY Standard Model (MSSM), the superpotential is given by

$$W^{(\mathrm{MSSM})} = y_u Q H_u u^c - y_d Q H_d d^c - y_e L H_d e^c + \mu H_u H_d, \tag{A.7}$$

within the renormalizable level, where we omit flavour indices for simplicity. Note that we need to introduce up-type and down-type Higgs fields because of the holomorphy of superpotential and the cancellation of anomaly. Here we implicitly assume R-parity conservation to avoid disastrous proton decay. As a result, the lightest SUSY particle (LSP) is stable and is a candidate of DM. Note that the squarks, which are superpartners of quarks, have baryon charge. Therefore we can generate baryon asymmetry via the dynamics of squarks. In fact, it can be naturally generated by the Affleck-Dine mechanism, which is the main topic of this thesis.

SUSY must be broken in a hidden sector so that all superpartners of the SM fields are sufficiently heavy to be consistent with the null results of collider experiments. As a result, there are additional terms called soft-SUSY breaking terms, which do not affect the cancellation of Higgs mass to solve the hierarchy problem. They are written as

$$\mathcal{L}_{\mathrm{soft}} = -\frac{1}{2}\left(M_3\tilde{g}\tilde{g} + M_2\tilde{w}\tilde{w} + M_1\tilde{b}\tilde{b} + \mathrm{h.c.}\right) \tag{A.8}$$

$$- \left(A_u Q H_u u^c - A_d Q H_d d^c - A_e L H_d e^c + \mathrm{c.c.}\right) \tag{A.9}$$

$$- m_Q^2 Q^\dagger Q - m_L^2 L^\dagger L - m_{u^c}^2 (u^c)^\dagger u^c - m_{d^c}^2 (d^c)^\dagger d^c - m_{e^c}^2 (e^c)^\dagger e^c \tag{A.10}$$

$$- m_{H_u}^2 H_u^* H_u - m_{H_d}^2 H_d^* H_d - \left(B H_u H_d + \mathrm{c.c.}\right), \tag{A.11}$$

where $\tilde{g}$, $\tilde{w}$, and $\tilde{b}$ are gauginos of $SU(3)$, $SU(2)$, and $U(1)_Y$, respectively. We denote scalar components of chiral supermultiplets by the same symbols as the superfields. The terms proportional to M_i $(i = 1, 2, 3)$ are gaugino mass terms, that to A_i $(i = u, d, e)$ are A-terms, that to m_i $(i = Q, L, u^c, d^c, e^c, H_u, H_d)$ are soft mass terms, and that to B is a B-term. The soft masses are assumed to be of order TeV scale or higher to be consistent with the null results of collider experiments.

A.1.2 Renormalization running equations

In SUSY theories, the couplings in the superpotential are not renormalized due to the supersymmetric non-renormalization theorem. This is the reason that the hierarchy problem between the electroweak scale and the Planck scale is solved in SUSY. The renormalization effects therefore come only from wavefunction renormalizations. For example, for particles with a superpotential of $W = y^{ijk}\Phi_i\Phi_j\Phi_k$, anomalous dimension matrices are calculated as

$$\gamma^i_j = \frac{1}{16\pi^2}\left[\frac{1}{2}y^{imn}y^*_{jmn} - 2g_a^2 C_a(i)\delta^i_j\right], \tag{A.12}$$

where $C_a(i)$ are the quadratic Casimir for the superfield Φ_i:

$$(T^a T^a)^j_i = C_a(i)\delta^j_i. \tag{A.13}$$

For a supermultiplet with a $U(1)$ charge q, $C_1(i) = q^2$, while for supermultiplets with fundamental representations for $SU(2)$ and $SU(3)$, $C_2(i) = 3/4$ and $C_3(i) = 4/3$.

When SUSY is softly broken, soft terms are also renormalized. Here we write the renormalization group equations of soft-masses of squark and sleptons and Higgs μ-parameter with canonical kinetic terms, which are particularly important to discuss Q-ball formation after the ADBG:

$$16\pi^2\frac{\mathrm{d}}{\mathrm{dlog}\mu}m^2_{Q_3} = X_t + X_b - \frac{32}{3}g_3^2|M_3|^2 - 6g_2^2|M_2|^2 - \frac{2}{15}g_1^2|M_1|^2 + \frac{1}{5}g_1^2 S, \tag{A.14}$$

$$16\pi^2\frac{\mathrm{d}}{\mathrm{dlog}\mu}m^2_{u^c_3} = 2X_t - \frac{32}{3}g_3^2|M_3|^2 - \frac{32}{15}g_1^2|M_1|^2 - \frac{4}{5}g_1^2 S, \tag{A.15}$$

$$16\pi^2\frac{\mathrm{d}}{\mathrm{dlog}\mu}m^2_{d^c_3} = 2X_b - \frac{32}{3}g_3^2|M_3|^2 - \frac{8}{15}g_1^2|M_1|^2 + \frac{2}{5}g_1^2 S, \tag{A.16}$$

$$16\pi^2\frac{\mathrm{d}}{\mathrm{dlog}\mu}m^2_{L_3} = X_\tau - 6g_2^2|M_2|^2 - \frac{6}{5}g_1^2|M_1|^2 - \frac{3}{5}g_1^2 S, \tag{A.17}$$

$$16\pi^2\frac{\mathrm{d}}{\mathrm{dlog}\mu}m^2_{e^c_3} = 2X_\tau - \frac{24}{5}g_1^2|M_1|^2 + \frac{6}{5}g_1^2 S, \tag{A.18}$$

$$16\pi^2\frac{\mathrm{d}}{\mathrm{dlog}\mu}\mu = \mu\left[3y_t^* y_t + 3y_b^* y_b + y_\tau^* y_\tau - 3g_2^2 - \frac{3}{5}g_1^2\right], \tag{A.19}$$

where

$$S \equiv \mathrm{Tr}\left[Y_j m^2_{\phi_j}\right] = m^2_{H_u} - m^2_{H_d} + \mathrm{Tr}\left[m^2_Q - m^2_L - 2m^2_{u^c} + m^2_{d^c} + m^2_{e^c}\right], \tag{A.20}$$

$$X_t = 2|y_t|^2\left(m^2_{H_u} + m^2_{Q_3} + m^2_{\bar{u}_3}\right) + 2|a_t|^2, \tag{A.21}$$

$$X_b = 2|y_b|^2\left(m^2_{H_d} + m^2_{Q_3} + m^2_{\bar{d}_3}\right) + 2|a_b|^2, \tag{A.22}$$

$$X_\tau = 2|y_\tau|^2\left(m^2_{H_d} + m^2_{L_3} + m^2_{\bar{e}_3}\right) + 2|a_\tau|^2. \tag{A.23}$$

The trace is taken over the flavour indices. The renormalization running equations for the first and second families are given by the same equations without X_i terms when we neglect their small Yukawa couplings.

We also write the renormalization group equations of gauge couplings for an $SU(N)$ gauge theory with F flavours:

$$16\pi^2 \frac{\mathrm{d}}{\mathrm{d}\log\mu} g = -bg^3 \tag{A.24}$$

$$b = 3N - F. \tag{A.25}$$

For the $U(1)_Y$ gauge theory, $b_1 = \sum_i 3Y_i^2/5$ when we normalize $U(1)_Y$ gauge coupling by $g_1 = \sqrt{5/3}g'$. Applying these to the SM gauge symmetries in SUSY, we obtain

$$(b_1, b_2, b_3) = (-33/5,\ -1,\ 3). \tag{A.26}$$

On the other hand, $(b_1, b_2, b_3) = (-41/10,\ 19/6,\ 7)$ without SUSY particles. As a result, the gauge couplings are unified at the energy scale of $M_{\rm GUT} \simeq 2 \times 10^{16}$ GeV in the MSSM. The renormalization group equations for gaugino masses are similar to those for gauge coupling constants within one-loop level:

$$\frac{\mathrm{d}}{\mathrm{d}\log\mu} M_a = -\frac{1}{8\pi^2} b_a g_a^2 M_a. \tag{A.27}$$

Thus we obtain

$$\frac{M_1}{g_1^2} = \frac{M_2}{g_2^2} = \frac{M_3}{g_3^2} = \frac{m_{1/2}}{g_{\rm GUT}^2}, \tag{A.28}$$

when we assume that gaugino masses as well as gauge couplings unify near the GUT scale. This relation implies that the bino is the lightest gaugino in the MSSM.

A.1.3 Supergravity

Supergravity is a theory with a local SUSY. To discuss the ADBG and gravity-mediated SUSY breaking effect, here we quote the scalar potential in supergravity (see, e.g., Refs. [146, 147] for detail).

In supergravity, scalar potentials are written in terms of superpotential, W, and Kähler potential, K. The potential of scalar fields is given by

$$V_{\rm SUGRA} = e^{K/M_{\rm Pl}^2} \left[(D_i W)\, K^{i\bar{j}}\, (D_j W)^* - \frac{3}{M_{\rm Pl}^2} |W|^2 \right], \tag{A.29}$$

where $D_i W \equiv W_i + K_i W/M_{\rm Pl}^2$. The subscripts represent the derivatives with respect to corresponding fields, e.g., $W_i = \partial W/\partial\phi_i$, and $K^{i\bar{j}}$ is defined by the inverse of $K_{i\bar{j}}$. The Kähler potential also determines kinetic terms such as

$$\mathcal{L}_{\rm kin} = K_{i\bar{j}}\partial_\mu\phi^i\partial^\mu\phi^{*j}. \tag{A.30}$$

The equations of motion of homogeneous scalar fields are thus given by

$$a^{-3}\frac{\mathrm{d}}{\mathrm{d}t}\left(a^3 K_{i\bar{j}}\dot{\phi}^i\right) - K_{i\bar{k}\bar{j}}\dot{\phi}^i\dot{\phi}^{*k} + \frac{V_{\rm SUGRA}}{\partial\phi^{*j}} = 0. \tag{A.31}$$

In supergravity, gravitino is introduced as a superpartner of graviton and its mass is given by $m_{3/2} = |W|\exp(K/2)$. Suppose that a field z has a nonzero F-term F_z to break SUSY, where $F_z \equiv -\exp(K/2)(W_z + K_z W)$. Since the vacuum energy (or cosmological constant) is almost vanish in our Universe, the condition of $V_{\rm SUGRA} = 0$ yields $|F_z|^2 = 3\exp(K)\,|W|^2$ and $m_{3/2} = |F_z|/\sqrt{3}$.

A.1.4 Gravity-mediated SUSY breaking models

Here we explain the Polonyi model as an example of SUSY breaking hidden sector:

$$W^{(\rm hidden)} = \mu^2 z + W_0 \tag{A.32}$$

$$K^{(\rm hidden)} = |z|^2, \tag{A.33}$$

where μ and W_0 are parameters. The vanishing vacuum energy determines the value of W_0. Using the potential of Eq. (A.29), we obtain

$$\left\langle W^{(\rm hidden)}\right\rangle = \mu^2 \tag{A.34}$$

$$\langle z\rangle = \sqrt{3} - 1 \tag{A.35}$$

$$m_{3/2}^2 = \frac{|F_z|^2}{3} = \mu^2\exp(\sqrt{3}-1). \tag{A.36}$$

Here we explain gravity-mediated SUSY breaking effect. Suppose that the field z has a nonzero F-term as Eq. (A.36). Assuming the Kähler potential of the field z as Eq. (A.33), we obtain the potential of other scalar fields ϕ_i from Eq. (A.29) such as

$$V_{\rm soft} = m_{3/2}^2\,|\phi|_i^2 + a m_{3/2} W^{(\rm visible)} + \text{c.c.} \tag{A.37}$$

$$a = n - 3 + \langle z^*\rangle\left(\langle z\rangle + \frac{\left\langle (W_z^{(\rm hidden)})^*\right\rangle}{\langle W^{(\rm hidden)}\rangle}\right), \tag{A.38}$$

where $W^{(\text{hidden})}$ and $W^{(\text{visible})}$ are superpotentials of hidden and visible sector, respectively. Here we rescale the superpotential by a factor of $\exp(|z|^2/2)$ and absorb it to the definition of W. For example, $a = n - \sqrt{3}$ in the Polonyi model. Note that there are $\mathcal{O}(1)$ factors in each term in Eq. (A.37) when we consider more generic Kähler potential. Therefore, scalar fields obtain masses of order gravitino mass via the supergravity effect. This is called gravity-mediated SUSY breaking effect.

Supergravity action contains a term

$$\mathcal{L} \supset \frac{1}{4}\exp(-K/2)\left(W_z + K_z W\right)\frac{\partial f^*_{\alpha\beta}}{\partial z^*}\lambda^\alpha\lambda^\beta \tag{A.39}$$

$$= -\frac{1}{4}F^*_z\frac{\partial f^*_{\alpha\beta}}{\partial z^*}\lambda^\alpha\lambda^\beta, \tag{A.40}$$

where $f_{\alpha\beta}$ is gauge kinetic function. When $\partial f^*_{\alpha\beta}/\partial z^*$ is of order unity, gauginos obtain masses of order gravitino mass. This is usually assumed in gravity-mediated SUSY breaking models.

The constrained minimal supersymmetric (SUSY) model (CMSSM) is widely used in the literature as a typical example of gravity-mediated SUSY breaking model. It is defined by only five parameters at the GUT scale ($\simeq 2\times 10^{16}$ GeV); the universal scalar mass m_0, the universal gaugino mass $M_{1/2}$, the universal A-term A_0, the ratio between the VEVs of up-type and down-type Higgses $\tan\beta$, and the sign of Higgs μ-term. The low energy spectrum can be obtained by solving renormalization running equations from the GUT scale. The μ-term and the B-term are determined by the 246 GeV Higgs VEV and the value of $\tan\beta$.

A.1.5 Gauge-mediated SUSY breaking models

Suppose that there is a spurion field S that has VEV of

$$\langle S\rangle = M_m + \theta^2 F_S, \tag{A.41}$$

and interacts with hidden fields Q and $\bar{Q}$ called messenger fields such as

$$W = ySQ\bar{Q}. \tag{A.42}$$

When Q and $\bar{Q}$ are charged under the SM gauge symmetries, the MSSM gauginos obtain masses via loop effects. Below the messenger scale, we can integrate them out and obtain effective Lagrangian such as

$$\mathcal{L} \supset \frac{1}{4g_a^2(S,\mu)}\mathcal{W}^\alpha\mathcal{W}_\alpha. \tag{A.43}$$

This implies that the gaugino mass is given by

$$M_\lambda = 2\pi \frac{\partial g_a^{-2}}{\partial S}\bigg|_{S=M_m} F_S. \tag{A.44}$$

Using Eq. (A.25), we obtain

$$M_\lambda = \frac{\alpha}{4\pi}\frac{F_S}{M_m}. \tag{A.45}$$

The MSSM scalar fields also obtain masses via two-loop effects [148]. First let us consider the wavefunction renormalization for a chiral superfield in the MSSM Φ':

$$\mathcal{L} \supset \int \mathrm{d}^2\theta \mathrm{d}^2\bar{\theta}^2 Z(S, S^\dagger)\Phi'\Phi'^\dagger, \tag{A.46}$$

which can be rewritten as

$$\mathcal{L} \supset \int \mathrm{d}^2\theta \mathrm{d}^2\bar{\theta}^2 \left[Z + \frac{\partial Z}{\partial S}F_S\theta^2 + \frac{\partial Z}{\partial S^\dagger}F_S^\dagger(\theta^\dagger)^2 + \frac{\partial^2 Z}{\partial S \partial S^\dagger}F_S\theta^2 F_S^\dagger(\theta^\dagger)^2\right]\bigg|_{S=M_m} \Phi'\Phi'^\dagger. \tag{A.47}$$

After canonically normalizing Φ such as

$$\Phi = Z^{1/2}\left[1 + \frac{\partial \log Z}{\partial S}F_S\theta^2\right]\bigg|_{S=M_m}\Phi', \tag{A.48}$$

we obtain

$$\mathcal{L} \supset \int \mathrm{d}^2\theta \mathrm{d}^2\bar{\theta}^2 \left[1 + \frac{\partial^2 \log Z}{\partial \log S \partial \log S^\dagger}\frac{F_S F_S^\dagger}{X X^\dagger}\theta^2(\theta^\dagger)^2\right]\bigg|_{S=M_m}\Phi\Phi^\dagger. \tag{A.49}$$

This implies that the scalar component of Φ obtains a soft mass of

$$m_\Phi^2 = -\frac{\partial^2 \log Z}{\partial \log S \partial \log S^\dagger}\frac{F_S^2}{M_m^2}. \tag{A.50}$$

Using Eq. (A.12), we obtain

$$m_\Phi^2 \simeq 2C_a(\Phi)\frac{\alpha_a^2}{16\pi^2}\frac{F_S^2}{M_m^2}. \tag{A.51}$$

These contributions to the soft masses are much larger than those of gravity-mediated effects explained in the previous subsection. Thus the soft masses are determined by these gauge-mediated effects and the gravitino mass is allowed to be much smaller than the electroweak scale. The rescaling of Eq. (A.48) induces A-terms from superpotential such as

$$Z^{-1/2}\frac{\partial \log Z}{\partial S}\bigg|_{S=M_m} F_S\Phi\frac{\partial W}{\partial Z^{-1/2}\Phi}, \tag{A.52}$$

which leads to

$$A \simeq \frac{2C_a(\Phi)}{b_a}\frac{\alpha_a}{4\pi}\frac{F_S}{M_m}. \tag{A.53}$$

This is suppressed by a factor of $\alpha_a/(4\pi)$ compared with the soft-mass scale and is neglected.

Note that these soft terms are suppressed for energy scales larger than the messenger scale M_m. This is particularly important when a charged field (e.g., an AD field) has a larger VEV than M_m. Here we derive its potential for a VEV larger than M_m. For simplicity, let us consider a $U(1)$ gauge theory under which the messenger fields and another scalar field (an AD field) ϕ are charged. From the superpotential of Eq. (A.42), we have a one-loop Coleman-Weinberg potential such as

$$V_{1-\text{loop}} \simeq |F_S|^2 \frac{y^2}{16\pi^2}\ln\left(\frac{|S|^2}{\mu_0^2}\right). \tag{A.54}$$

We take the renormalization scale μ_0 as the GUT scale. The VEV of S is fixed at the messenger scale M_m. To discuss two-loop effect, we rewrite the one-loop potential such as

$$V_{1,2-\text{loop}} \simeq |F_S|^2 \frac{1}{8\pi^2}\int_{\mu_0}^{|S|} \mathrm{d}\ln\mu\; y^2(\mu). \tag{A.55}$$

Here, since the AD field ϕ is charged under the gauge symmetry and has a large VEV, the gauge symmetry is spontaneously broken by its VEV and the vector supermultiplet acquires an effective mass of order $g\phi$, where g is the gauge coupling constant. Since the messenger fields Q and $\bar{Q}$ are charged under the gauge symmetry, the renormalization running of the coupling constant y in Eq. (A.42) contains contributions from gauge interactions. Therefore, when the AD field ϕ obtains a larger VEV than the messenger scale, the renormalization running of the coupling y is affected and is dependent on $|\phi|$. The renormalization running equation for the Yukawa coupling y is written as [see Eq. (A.12)]

$$\frac{\mathrm{d}y}{\mathrm{dlog}\mu/\mu_0} = -\frac{g_a^2}{4\pi^2}y + \dots, \tag{A.56}$$

where we omit the other terms irrelevant for our discussion. When the vector supermultiplet has an effective mass of $g|\phi|$, the gauge contribution of the running of y is absent below this mass scale. Thus we obtain

$$y(\mu) = y_0 - \frac{g_a^2}{8\pi^2}y\ln\left(\frac{|g\phi|^2}{\mu_0^2}\right) + \dots, \quad \text{for} \quad \mu < g|\phi|, \tag{A.57}$$

where ... represents terms that are independent of $|\phi|$. Therefore, Eq. (A.55) has a $|\phi|$ dependent part for the integral below the energy scale of $g|\phi|$. As a result, we obtain the $|\phi|$ dependent potential such as

$$V(\phi) \simeq |F_S|^2 \frac{y^2 g^2}{128\pi^4} \left[\ln \frac{g^2 |\phi|^2}{M_m^2} \right]^2 . \tag{A.58}$$

This agrees with the result in Ref. [57] for $g|\phi| \gg M_m$, where they have explicitly calculated two-loop diagrams.

Appendix B

Inflation

In this Appendix, we briefly explain inflation. It solves some initial condition problems in the Big Bang theory, including the flatness problem and the horizon problem. It can be realized by a potential of a scalar field called an inflaton when it is spatially homogeneous and slowly rolls towards its potential minimum. After the slow roll ends, the inflaton starts to oscillate around its potential minimum and then decay into radiation. The resulting Universe is then consistent with the Big Bang theory with a negligible curvature in the homogeneous Universe. The inflaton acquires quantum fluctuations during inflation, which are converted to fluctuations of scalar part of metric called curvature perturbations. The perturbations can be observed as the CMB temperature anisotropy.

B.1 Motivations

Here we explain the flatness problem. If the curvature of the Universe is nonzero, the Friedmann equations are written as

$$H^2 = \frac{\rho}{3M_{\rm Pl}^2} - \frac{K}{a^2} \tag{B.1}$$

$$\dot{\rho} = -3H\left(\rho + p\right). \tag{B.2}$$

These can be rewritten as

$$\frac{H^2}{H_0^2} = \Omega_r \left(\frac{a_0}{a}\right)^4 + \Omega_m \left(\frac{a_0}{a}\right)^3 + \Omega_K \left(\frac{a_0}{a}\right)^2, \tag{B.3}$$

$$\Omega_K \equiv -\frac{K}{a_0^2 H_0^2}, \tag{B.4}$$

where Ω_r and Ω_m are abundance of radiation and matter, respectively. Here we omit the dark energy for simplicity. The parameter Ω_K is bounded above as $|\Omega_K| \lesssim 0.01$ by the observation

of CMB temperature anisotropies. However, the curvature term in Eq. (B.3) is proportional to a^{-2}, so that the combination of $|\Omega_K|\,(a_0H_0/aH)^2$ is extremely smaller than unity in the early Universe. Such an extremely small dimensionless parameter is a mystery known as the flatness problem.

The observations of CMB temperature fluctuations show that the background temperature of the Universe is homogeneous up to a factor of of order 10^{-5}. However, if the Universe begins from the radiation or matter dominated era, there is no correlation for the whole observable Universe. There is no reason that the whole Universe is homogeneous without correlations. This is known as the horizon problem.

The above flatness and horizon problems are explained by an era of exponential expansion called inflation. If the early Universe is dominated by the energy density with the equation of state of $p \simeq -\rho$, the Friedmann equation implies that $H = H_{\rm inf} = $ const. and the scale factor exponentially increases such as $a(t) = a(t_{\rm ini})\exp[H_{\rm inf}(t - t_{\rm ini})]$, where $t_{\rm ini}$ is the time at the beginning of inflation. If the constant energy density is converted to radiation at the time denoted by $t_{\rm end}$, then the Universe is filled with the thermal plasma. We define e-folding number as an alternative of time variable during inflation such as $N(t) \equiv \log\left(a(t_{\rm end})/a(t)\right)$.

Suppose that the curvature term in the Friedmann equation is below but comparable to the constant energy density at the beginning of inflation ($t = t_{\rm ini}$). Since the curvature term in the Friedmann equation decreases with time as $\propto a^{-2}$, $|\Omega_K|$ is given by

$$|\Omega_K| = e^{-2N(t_{\rm ini})}\left(\frac{a(t_{\rm end})H(t_{\rm end})}{a_0H_0}\right)^2. \tag{B.5}$$

Since the observation implies that $|\Omega_K| \ll 1$, we require

$$N(t_{\rm ini}) \;\gg\; \log\left(\frac{a(t_{\rm end})H(t_{\rm end})}{a_0H_0}\right). \tag{B.6}$$

The right-hand side can be written as

$$\log\left(\frac{a(t_{\rm end})H(t_{\rm end})}{a_0H_0}\right) \simeq 56 + \frac{1}{3}\log\left(\frac{T_{\rm RH}}{10^9\ {\rm GeV}}\right) + \frac{1}{3}\log\left(\frac{H_{\rm end}}{10^{13}\ {\rm GeV}}\right), \tag{B.7}$$

where $T_{\rm RH}$ is reheating temperature defined in Sec. B.4. Here we assume that the energy density of the Universe decreases as $\propto a^{-3}$ after inflation and before reheating completes. For typical parameters, the required e-folding number is about $50 - 60$.

The correlation length is given by the Hubble horizon $(aH)^{-1}$. When the horizon length at present a_0H_0 is smaller than the one at the beginning of inflation $a(t_{\rm ini})H(t_{\rm ini})$, the observable Universe can have correlation before inflation. Thus we again require the condition of Eq. (B.6) to solve the horizon problem.

B.2 Inflation by a scalar field

Inflation can be realized by a potential energy of a scalar field. If the inflaton is spatially homogeneous, its energy density and pressure are given as

$$\rho = K + V_{\rm inf} \tag{B.8}$$

$$p = K - V_{\rm inf}, \tag{B.9}$$

where K and $V_{\rm inf}$ are kinetic energy and potential energy of inflaton, respectively. When the kinetic energy of inflaton is smaller than the potential energy, we obtain $\rho \simeq -p$ and can realize inflation. We define slow roll parameters ϵ_s and η_s such as

$$\epsilon_s \equiv \frac{1}{2}\left(\frac{V'_{\rm inf}}{V_{\rm inf}}\right)^2, \tag{B.10}$$

$$\eta_s \equiv \frac{V''_{\rm inf}}{V_{\rm inf}}, \tag{B.11}$$

where the prime denotes the derivative with respect to the inflaton field. Then the condition of $K \ll V_{\rm inf}$ can be rewritten as $\epsilon_s \ll 1$. Note that in order to realize inflation for sufficiently long time, we also require $\eta_s \ll 1$. These conditions are called slow-roll conditions. The e-folding number can be calculate as

$$N(t) \simeq \int_t^{t_{\rm end}} H(t){\rm d}t \simeq \int {\rm d}\phi \frac{V_{\rm inf}}{V'_{\rm inf}} = \int \frac{{\rm d}\phi}{\sqrt{2\epsilon_s}}. \tag{B.12}$$

B.3 Curvature perturbation

Quantum fluctuations of the inflaton during inflation is the seed of large scale structure. The fluctuations are converted to those of scalar part of metric called curvature perturbation. The power spectrum of curvature perturbation is parametrized as

$$\mathcal{P}_s(k) = A_s \left(\frac{k}{k_*}\right)^{n_s - 1}, \tag{B.13}$$

where k_* ($= 0.05$ Mpc^{-1}) is the pivot scale, and A_s and n_s are the amplitude and spectral index, respectively. They are calculated as

$$A_s \simeq \frac{V_{\rm inf}}{24\pi^2\epsilon_s} \tag{B.14}$$

$$n_s \simeq 1 - 6\epsilon_s + 2\eta_s. \tag{B.15}$$

The Planck collaboration observes the CMB temperature anisotropies, which give us information of curvature perturbation such as [6]

$$A_s = \left(2.198^{+0.076}_{-0.085}\right) \times 10^{-9} \tag{B.16}$$

$$n_s = 0.9655 \pm 0.0062, \tag{B.17}$$

at the 68% CL. These values put constraints on inflaton potential via Eqs. (B.14), (B.10), and (B.11).

B.4 Reheating

Inflation ends when the slow-roll conditions fail and the inflaton starts to oscillate around the potential minimum. Then the oscillating inflaton gradually decays into radiation. Since the energy density of radiation is given by $\rho_{\rm rad} \simeq (3/5)\rho_{\rm inf}\Gamma_{\rm inf}t$, where $\rho_{\rm inf}$ ($\simeq 3H^2(t)M_{\rm Pl}^2$) is the energy density of inflaton oscillation and $\Gamma_{\rm inf}$ is its decay rate. Thus there is a background plasma with a temperature of

$$T = \left(\frac{36H(t)\Gamma_{\rm inf}M_{\rm Pl}^2}{g_*(T)\pi^2}\right)^{1/4}, \tag{B.18}$$

where g_* is the effective number of relativistic degrees of freedom in the thermal plasma. We define reheating temperature by $H(T_{\rm RH}) = \Gamma_{\rm inf}$, which is then given by

$$T_{\rm RH} \simeq \left(\frac{90}{g_*(T_{\rm RH})\pi^2}\right)^{1/4} \sqrt{\Gamma_{\rm inf}M_{\rm Pl}}. \tag{B.19}$$

The reheating temperature has to be higher than 1 MeV so that the subsequent history of the Universe is consistent with the BBN theory.

B.4.1 Inflaton decay via supergravity effects

Here we briefly explain inflaton decay process via supergravity effects. This puts the lower bound on reheating temperature and gives a non-thermal source of gravitinos.

We specify the SUSY breaking sector to explain the inflaton decay through supergravity effects. We introduce a Polonyi field z, which breaks SUSY in low energy scale, and consider a simple extension of the Polonyi model given as

$$K^{(\rm hidden)} = |z|^2 - \frac{|z|^4}{\Lambda^2}, \tag{B.20}$$

$$W^{(\rm hidden)} = \mu_z^2 z + W_0, \tag{B.21}$$

where Λ is a cutoff scale, μ_z is the SUSY breaking scale, and W_0 is a constant term which makes the cosmological constant (almost) zero in the present Universe. This can be achieved by the O'Raifeartaigh model after integrating out relatively heavy particles [149] or by dynamical SUSY breaking models, including the IYIT model [150, 151]. The important parameters are calculated as

$$\mu_z^2 \simeq \sqrt{3} m_{3/2} M_{\rm Pl}, \tag{B.22}$$

$$m_z^2 \simeq \frac{12 m_{3/2}^2}{\Lambda^2} M_{\rm Pl}^2, \tag{B.23}$$

$$\langle z \rangle \simeq 2\sqrt{3} \left(\frac{m_{3/2}}{m_z} \right)^2 M_{\rm Pl}, \tag{B.24}$$

where m_z is the mass of z and $\langle z \rangle$ is its VEV at the low energy vacuum.

Suppose that inflaton sector is effectively written by the following superpotential at the time around the reheating epoch:

$$W_{\rm inf} = m_{\rm inf} S X. \tag{B.25}$$

This is actually the cases in F-term and D-term hybrid and chaotic inflation models as we explain in Chap. 6. In this case, the supergravity effects induce a soft SUSY breaking B-term of $b m_{3/2} m_{\rm inf} S X$, where b is an $\mathcal{O}(1)$ constant. This implies that they maximally mix with each other and form mass eigenstates of

$$\Phi_\pm \equiv \frac{1}{\sqrt{2}} \left(S \pm X^* \right), \tag{B.26}$$

around the potential minimum [114]. Therefore, when the time scale of inflaton decay $\Gamma_{\rm inf}^{-1}$ is longer than that of the mixing effect $m_{3/2}^{-1}$, we have to consider the decay of $\Phi_\pm$ to investigate the reheating process. Hereafter we consider this case.

Suppose that a first derivative of Kähler potential in terms of inflaton S, K_S, is nonzero at the potential minimum. This results in the decay of the field $\Phi_\pm$ through supergravity effects [114]. First, let us focus on the top Yukawa interaction in the MSSM sector:

$$W^{(\rm top)} = y_t Q_3 H_u u_3^c, \tag{B.27}$$

where y_t is the top Yukawa coupling constant. The relevant interaction terms between X and the MSSM fields are given by

$$\begin{aligned} V &= \frac{1}{M_{\rm Pl}} K_S W^{(\rm top)} W_S^* + \text{c.c.} + \dots, \\ &= \frac{y_t m_{\rm inf} K_S}{M_{\rm Pl}^2} X^* (\tilde{Q}_3 H_u \tilde{u}_3^c) + \text{c.c.} + \dots, \end{aligned} \tag{B.28}$$

where the dots "..." represents the other irrelevant terms. Since the fields $\Phi_\pm$ consist of X as Eq. (B.26), they decay into the MSSM scalar fields through this interaction. They also decay into the MSSM fermion fields, which equally contributes to the $\Phi_\pm$ decay. Thus, the partial decay rate of $\Phi_\pm$ into the MSSM fields is given as

$$\Gamma_{\rm MSSM}\left(\Phi_\pm \to {\rm MSSM}\right) = \frac{3K_S^2}{256\pi^3}\left|y_t\right|^2 \frac{m_{\rm inf}^3}{M_{\rm Pl}^2}. \tag{B.29}$$

When we consider the gaugino mass ($m_{\tilde{g}}$) much smaller than the gravitino mass, the decay rates of S into gauge fields are suppressed by a factor of $(m_{\tilde{g}}/m_{3/2})^2$ and can be neglected.

Next, let us consider the decay of $\Phi_\pm$ into gravitinos [114]. We follow the discussion presented in Ref. [152]. Through nonzero values of K_S and $K_{Sz\bar{z}}$, the field X mixes with the SUSY breaking field z and can decays into goldstino, (i.e., longitudinal component of gravitino). This is because the supergravity effects induce mixing terms such as

$$\begin{aligned} V &= W_S\left(K_S W\right)^* + K_{S\bar{z}}^{-1} W_S W_z^* + {\rm c.c.} + \dots \\ &= m_{\rm inf} d F_z X z^* + {\rm c.c.} + \dots, \end{aligned} \tag{B.30}$$

$$d \equiv \langle K_S \rangle - \langle K_{Sz\bar{z}} \rangle, \tag{B.31}$$

where the dots "..." represent the other irrelevant terms. Thus, the fields X and z mix with each other and the mixing angle is given by

$$\theta_{\rm mix} \simeq d\frac{F_z m_{\rm inf}}{m_z^2}, \tag{B.32}$$

where we use $m_z \gg m_{\rm inf}$. Since the fields $\Phi_\pm$ consist of X, they mix with z and the mixing angle is given by $\theta_{\rm mix}/\sqrt{2}$. Since the SUSY breaking field z has an operator of

$$\mathcal{L} = -2\frac{F_z}{\Lambda^2} z \tilde{z}^\dagger \tilde{z}^\dagger + {\rm h.c.}, \tag{B.33}$$

it decays into goldstino $\tilde{z}$. Together with the mixings between $\Phi_\pm$ and z, the fields $\Phi_\pm$ decays into goldstino through this operator. The partial decay rate of the field $\Phi_\pm$ into goldstino is therefore calculated as [153]

$$\begin{aligned} \Gamma_{\tilde{z}}\left(\Phi_\pm \to \tilde{z}\tilde{z}\right) &\simeq \frac{1}{32\pi}\left(\frac{\theta_{\rm mix}}{\sqrt{2}}\right)^2 \frac{m_z^4}{\left|F_z\right|^2} m_{\rm inf}, \\ &\simeq \frac{d^2}{64\pi}\frac{m_{\rm inf}^3}{M_{\rm Pl}^2}. \end{aligned} \tag{B.34}$$

If the fields S and X do not have other interactions, the branching into gravitinos is given by

$$\mathrm{Br}_{3/2} \;=\; \frac{d^2}{d^2 + 3\left|y_t\right|^2 c^2/(4\pi^2)}. \tag{B.35}$$

Since $d/c = \mathcal{O}(1)$ and $y_t = \mathcal{O}(1)$, the branching ratio is almost unity. The reheating temperature is then given by

$$T_{\mathrm{RH}} \simeq 3 \times 10^8 \text{ GeV} d \left(\frac{m_{\mathrm{inf}}}{10^{13} \text{ GeV}}\right)^{3/2}. \tag{B.36}$$

Bibliography

[1] G. Aad *et al.* [ATLAS Collaboration], Phys. Lett. B **716**, 1 (2012) [arXiv:1207.7214 [hep-ex]].

[2] S. Chatrchyan *et al.* [CMS Collaboration], Phys. Lett. B **716**, 30 (2012) [arXiv:1207.7235 [hep-ex]].

[3] E. Aver, K. A. Olive, R. L. Porter and E. D. Skillman, JCAP **1311**, 017 (2013) [arXiv:1309.0047 [astro-ph.CO]].

[4] Y. I. Izotov, T. X. Thuan and N. G. Guseva, Mon. Not. Roy. Astron. Soc. **445**, no. 1, 778 (2014) [arXiv:1408.6953 [astro-ph.CO]].

[5] R. Cooke, M. Pettini, R. A. Jorgenson, M. T. Murphy and C. C. Steidel, Astrophys. J. **781**, no. 1, 31 (2014) [arXiv:1308.3240 [astro-ph.CO]].

[6] P. A. R. Ade *et al.* [Planck Collaboration], arXiv:1502.01589 [astro-ph.CO].

[7] K. A. Olive *et al.* [Particle Data Group Collaboration], Chin. Phys. C **38**, 090001 (2014).

[8] A. H. Guth, Phys. Rev. D **23**, 347 (1981).

[9] A. A. Starobinsky, Phys. Lett. B **91**, 99 (1980).

[10] A. D. Linde, Phys. Lett. B **108**, 389 (1982).

[11] A. Albrecht and P. J. Steinhardt, Phys. Rev. Lett. **48**, 1220 (1982).

[12] V. F. Mukhanov and G. V. Chibisov, JETP Lett. **33**, 532 (1981) [Pisma Zh. Eksp. Teor. Fiz. **33**, 549 (1981)].

[13] A. H. Guth and S. Y. Pi, Phys. Rev. Lett. **49**, 1110 (1982).

[14] S. W. Hawking, Phys. Lett. B **115**, 295 (1982).

[15] G. Hinshaw *et al.* [WMAP Collaboration], Astrophys. J. Suppl. **208**, 19 (2013) [arXiv:1212.5226 [astro-ph.CO]].

[16] A. D. Sakharov, Pisma Zh. Eksp. Teor. Fiz. **5**, 32 (1967) [JETP Lett. **5**, 24 (1967)] [Sov. Phys. Usp. **34**, 392 (1991)] [Usp. Fiz. Nauk **161**, 61 (1991)].

[17] I. Affleck and M. Dine, Nucl. Phys. B **249**, 361 (1985).

[18] H. Murayama and T. Yanagida, Phys. Lett. B **322**, 349 (1994) [hep-ph/9310297].

[19] M. Dine, L. Randall and S. D. Thomas, Nucl. Phys. B **458**, 291 (1996). [hep-ph/9507453].

[20] V. A. Kuzmin, V. A. Rubakov and M. E. Shaposhnikov, Phys. Lett. B **155**, 36 (1985).

[21] M. Fukugita and T. Yanagida, Phys. Lett. B **174**, 45 (1986).

[22] A. Kusenko, Phys. Lett. **B405** (1997) 108.

[23] A. Kusenko and M. E. Shaposhnikov, Phys. Lett. B **418**, 46 (1998).

[24] K. Enqvist and J. McDonald, Phys. Lett. B **425**, 309 (1998); Nucl. Phys. B **538**, 321 (1999).

[25] S. Kasuya and M. Kawasaki, Phys. Rev. D **61**, 041301(R) (2000); S. Kasuya and M. Kawasaki, Phys. Rev. D **62**, 023512 (2000); S. Kasuya and M. Kawasaki, Phys. Rev. D **64**, 123515 (2001).

[26] S. Coleman, Nucl. Phys. **B262** (1985) 263.

[27] A. G. Cohen, S. R. Coleman, H. Georgi and A. Manohar, Nucl. Phys. B **272**, 301 (1986).

[28] M. Fujii and K. Hamaguchi, Phys. Lett. B **525**, 143 (2002) [hep-ph/0110072]; M. Fujii and K. Hamaguchi, Phys. Rev. D **66**, 083501 (2002) [hep-ph/0205044].

[29] K. Harigaya, A. Kamada, M. Kawasaki, K. Mukaida and M. Yamada, Phys. Rev. D **90**, no. 4, 043510 (2014) [arXiv:1404.3138 [hep-ph]].

[30] A. Kamada, M. Kawasaki and M. Yamada, Phys. Rev. D **91**, no. 8, 081301 (2015) [arXiv:1405.6577 [hep-ph]].

[31] M. Kawasaki and M. Yamada, Phys. Rev. D **91**, no. 8, 083512 (2015) [arXiv:1502.03550 [hep-ph]].

[32] M. Yamada, arXiv:1510.08514 [hep-ph].

[33] M. Yamada, arXiv:1511.05974 [hep-ph].

[34] M. Kawasaki and M. Yamada, Phys. Rev. D **87**, no. 2, 023517 (2013) [arXiv:1209.5781 [hep-ph]].

[35] A. Kamada, M. Kawasaki and M. Yamada, Phys. Lett. B **719**, 9 (2013) [arXiv:1211.6813 [hep-ph]].

[36] V. F. Mukhanov, Int. J. Theor. Phys. **43**, 669 (2004) [astro-ph/0303073].

[37] S. L. Adler, Phys. Rev. **177**, 2426 (1969).

[38] J. S. Bell and R. Jackiw, Nuovo Cim. A **60**, 47 (1969).

[39] G. 't Hooft, Phys. Rev. Lett. **37**, 8 (1976). Phys. Rev. D **14**, 3432 (1976) [Phys. Rev. D **18**, 2199 (1978)].

[40] N. S. Manton, Phys. Rev. D **28**, 2019 (1983). F. R. Klinkhamer and N. S. Manton, Phys. Rev. D **30**, 2212 (1984).

[41] J. A. Harvey and M. S. Turner, Phys. Rev. D **42**, 3344 (1990).

[42] F. Zwicky, Helv. Phys. Acta **6**, 110 (1933).

[43] V. C. Rubin, N. Thonnard, and J. Ford, W. K., *Astrophys. J* **225** (1978) L107.

[44] A. Einstein, Science **84**, 506 (1936).

[45] F. Zwicky, Phys. Rev. **51**, 290 (1937).

[46] D. Harvey, R. Massey, T. Kitching, A. Taylor and E. Tittley, Science **347**, 1462 (2015) [arXiv:1503.07675 [astro-ph.CO]].

[47] S. D. M. White, C. S. Frenk and M. Davis, Astrophys. J. **274**, L1 (1983).

[48] W. Buchmuller, R. D. Peccei and T. Yanagida, Ann. Rev. Nucl. Part. Sci. **55**, 311 (2005) [hep-ph/0502169].

[49] M. Kawasaki, K. Kohri and N. Sugiyama, Phys. Rev. Lett. **82**, 4168 (1999) [astro-ph/9811437]; M. Kawasaki, K. Kohri and N. Sugiyama, Phys. Rev. D **62**, 023506 (2000) [astro-ph/0002127]; M. Kawasaki, K. Kohri and T. Moroi, Phys. Rev. D **71**, 083502 (2005) [astro-ph/0408426]; K. Ichikawa, M. Kawasaki and F. Takahashi, Phys. Rev. D **72**, 043522 (2005) [astro-ph/0505395]; M. Kawasaki, K. Kohri, T. Moroi and A. Yotsuyanagi, Phys. Rev. D **78**, 065011 (2008) [arXiv:0804.3745 [hep-ph]].

[50] M. Ibe and T. T. Yanagida, Phys. Lett. B **709**, 374 (2012) [arXiv:1112.2462 [hep-ph]]; M. Ibe, S. Matsumoto and T. T. Yanagida, Phys. Rev. D **85**, 095011 (2012) [arXiv:1202.2253 [hep-ph]].

[51] T. Gherghetta, C. F. Kolda and S. P. Martin, Nucl. Phys. B **468**, 37 (1996) [hep-ph/9510370].

[52] https://twiki.cern.ch/twiki/bin/view/AtlasPublic/SupersymmetryPublicResults.

[53] https://twiki.cern.ch/twiki/bin/view/CMSPublic/PhysicsResultsSUS.

[54] R. Allahverdi, B. A. Campbell and J. R. Ellis, Nucl. Phys. B **579**, 355 (2000) [hep-ph/0001122].

[55] A. Anisimov and M. Dine, Nucl. Phys. B **619**, 729 (2001) [hep-ph/0008058].

[56] M. Fujii, K. Hamaguchi and T. Yanagida, Phys. Rev. D **63**, 123513 (2001) [hep-ph/0102187].

[57] A. de Gouvea, T. Moroi and H. Murayama, Phys. Rev. D **56**, 1281 (1997) [hep-ph/9701244].

[58] S. Kasuya, M. Kawasaki and F. Takahashi, JCAP **0810**, 017 (2008) [arXiv:0805.4245 [hep-ph]].

[59] E. J. Copeland, A. R. Liddle, D. H. Lyth, E. D. Stewart and D. Wands, Phys. Rev. D **49**, 6410 (1994) [astro-ph/9401011].

[60] G. R. Dvali, Q. Shafi and R. K. Schaefer, Phys. Rev. Lett. **73**, 1886 (1994) [hep-ph/9406319].

[61] M. Kawasaki, M. Yamaguchi and T. Yanagida, Phys. Rev. Lett. **85**, 3572 (2000) [hep-ph/0004243].

[62] R. Kallosh and A. Linde, JCAP **1011**, 011 (2010) [arXiv:1008.3375 [hep-th]].

[63] P. Binetruy and G. R. Dvali, Phys. Lett. B **388**, 241 (1996) [hep-ph/9606342].

[64] E. Halyo, Phys. Lett. B **387**, 43 (1996) [hep-ph/9606423].

[65] K. Enqvist and J. McDonald, Phys. Rev. Lett. **83**, 2510 (1999) [hep-ph/9811412]; Phys. Rev. D **62**, 043502 (2000) [hep-ph/9912478].

[66] M. Kawasaki and F. Takahashi, Phys. Lett. B **516**, 388 (2001) [hep-ph/0105134].

[67] C. F. Kolda and J. March-Russell, Phys. Rev. D **60**, 023504 (1999) [hep-ph/9802358].

[68] K. Mukaida and K. Nakayama, JCAP **1301**, 017 (2013) [JCAP **1301**, 017 (2013)] [arXiv:1208.3399 [hep-ph]].

[69] S. Kasuya and M. Kawasaki, Phys. Rev. Lett. **85**, 2677 (2000) [hep-ph/0006128].

[70] M. Fujii, K. Hamaguchi and T. Yanagida, Phys. Lett. B **538**, 107 (2002) [hep-ph/0203189].

[71] F. Capozzi, G. L. Fogli, E. Lisi, A. Marrone, D. Montanino and A. Palazzo, Phys. Rev. D **89**, 093018 (2014) [arXiv:1312.2878 [hep-ph]].

[72] P. A. R. Ade *et al.* [Planck Collaboration], arXiv:1502.02114 [astro-ph.CO].

[73] T. Hiramatsu, M. Kawasaki and F. Takahashi, JCAP **1006**, 008 (2010) [arXiv:1003.1779 [hep-ph]].

[74] G. R. Dvali, A. Kusenko and M. E. Shaposhnikov, Phys. Lett. B **417**, 99 (1998) [hep-ph/9707423].

[75] F. Doddato and J. McDonald, JCAP **1106**, 008 (2011) [arXiv:1101.5328 [hep-ph]].

[76] F. Doddato and J. McDonald, JCAP **1206**, 031 (2012) [arXiv:1111.2305 [hep-ph]].

[77] J. Hisano, M. M. Nojiri and N. Okada, Phys. Rev. D **64**, 023511 (2001) [hep-ph/0102045].

[78] M. Laine and M. E. Shaposhnikov, Nucl. Phys. B **532**, 376 (1998) [hep-ph/9804237].

[79] R. Banerjee and K. Jedamzik, Phys. Lett. B **484**, 278 (2000) [hep-ph/0005031].

[80] M. Fujii and T. Yanagida, Phys. Lett. B **542**, 80 (2002) [hep-ph/0206066].

[81] L. Roszkowski and O. Seto, Phys. Rev. Lett. **98**, 161304 (2007) [hep-ph/0608013]; O. Seto and M. Yamaguchi, Phys. Rev. D **75**, 123506 (2007) [arXiv:0704.0510 [hep-ph]].

[82] I. M. Shoemaker and A. Kusenko, Phys. Rev. D **80**, 075021 (2009); S. Kasuya and M. Kawasaki, Phys. Rev. D **84**, 123528 (2011) [arXiv:1107.0403 [hep-ph]]; F. Doddato and J. McDonald, JCAP **1307**, 004 (2013) [arXiv:1211.1892 [hep-ph]]; S. Kasuya, M. Kawasaki and M. Yamada, Phys. Lett. B **726**, 1 (2013) [arXiv:1211.4743 [hep-ph]].

[83] ATLAS-CONF-2013-047 [ATLAS Collaboration].

[84] J. L. Feng, P. Kant, S. Profumo and D. Sanford, Phys. Rev. Lett. **111**, 131802 (2013) [arXiv:1306.2318 [hep-ph]].

[85] O. Buchmueller *et al.*, Eur. Phys. J. C **74**, no. 3, 2809 (2014) [arXiv:1312.5233 [hep-ph]].

[86] K. Harigaya, M. Kawasaki, K. Mukaida and M. Yamada, Phys. Rev. D **89**, no. 8, 083532 (2014) [arXiv:1402.2846 [hep-ph]].

[87] B. C. Allanach, Comput. Phys. Commun. **143**, 305 (2002) [hep-ph/0104145].

[88] T. Falk, R. Madden, K. A. Olive and M. Srednicki, Phys. Lett. B **318**, 354 (1993) [hep-ph/9308324].

[89] S. Heinemeyer, W. Hollik and G. Weiglein, Comput. Phys. Commun. **124**, 76 (2000) [hep-ph/9812320].

[90] S. Heinemeyer, W. Hollik and G. Weiglein, Eur. Phys. J. C **9**, 343 (1999) [hep-ph/9812472].

[91] G. Degrassi, S. Heinemeyer, W. Hollik, P. Slavich and G. Weiglein, Eur. Phys. J. C **28**, 133 (2003) [hep-ph/0212020].

[92] M. Frank, T. Hahn, S. Heinemeyer, W. Hollik, H. Rzehak and G. Weiglein, JHEP **0702**, 047 (2007) [hep-ph/0611326].

[93] T. Hahn, S. Heinemeyer, W. Hollik, H. Rzehak and G. Weiglein, Phys. Rev. Lett. **112**, 141801 (2014) [arXiv:1312.4937 [hep-ph]].

[94] O. Buchmueller, R. Cavanaugh, M. Citron, A. De Roeck, M. J. Dolan, J. R. Ellis, H. Flacher and S. Heinemeyer *et al.*, Eur. Phys. J. C **72**, 2243 (2012) [arXiv:1207.7315].

[95] H. Baer, V. Barger, A. Lessa and X. Tata, JHEP **0909**, 063 (2009) [arXiv:0907.1922 [hep-ph]].

[96] H. Baer, V. Barger, A. Lessa and X. Tata, Phys. Rev. D **86**, 117701 (2012) [arXiv:1207.4846 [hep-ph]].

[97] G. Belanger, F. Boudjema, A. Pukhov and A. Semenov, Comput. Phys. Commun. **185**, 960 (2014) [arXiv:1305.0237 [hep-ph]].

[98] L. Baudis, Phys. Dark Univ. **4**, 50 (2014) [arXiv:1408.4371 [astro-ph.IM]].

[99] E. Aprile [XENON1T Collaboration], arXiv:1206.6288 [astro-ph.IM].

[100] L. Baudis [DARWIN Consortium Collaboration], J. Phys. Conf. Ser. **375**, 012028 (2012) [arXiv:1201.2402 [astro-ph.IM]].

[101] J. Billard, E. Figueroa-Feliciano and L. Strigari, Phys. Rev. D **89**, 023524 (2014) [arXiv:1307.5458 [hep-ph]].

[102] J. McDonald and O. Seto, JCAP **0807**, 015 (2008) [arXiv:0801.2102 [hep-ph]].

[103] S. Kasuya and F. Takahashi, Phys. Lett. B **736**, 526 (2014) [arXiv:1405.4125 [hep-ph]].

[104] C. M. Lin and J. McDonald, Phys. Rev. D **74**, 063510 (2006) [hep-ph/0604245].

[105] W. Buchmuller, V. Domcke, K. Kamada and K. Schmitz, JCAP **1407**, 054 (2014) [arXiv:1404.1832 [hep-ph]].

[106] W. Buchmuller, C. Wieck and M. W. Winkler, Phys. Lett. B **736**, 237 (2014) [arXiv:1404.2275 [hep-th]]; W. Buchmuller, E. Dudas, L. Heurtier and C. Wieck, JHEP **1409**, 053 (2014) [arXiv:1407.0253 [hep-th]]; W. Buchmuller and K. Ishiwata, Phys. Rev. D **91**, no. 8, 081302 (2015) [arXiv:1412.3764 [hep-ph]]; W. Buchmuller, E. Dudas, L. Heurtier, A. Westphal, C. Wieck and M. W. Winkler, JHEP **1504**, 058 (2015) [arXiv:1501.05812 [hep-th]].

[107] K. Harigaya, M. Ibe, M. Kawasaki and T. T. Yanagida, arXiv:1506.05250 [hep-ph].

[108] M. Hindmarsh, Prog. Theor. Phys. Suppl. **190**, 197 (2011) [arXiv:1106.0391 [astro-ph.CO]].

[109] P. A. R. Ade *et al.* [Planck Collaboration], Astron. Astrophys. **571**, A25 (2014) [arXiv:1303.5085 [astro-ph.CO]].

[110] Z. Arzoumanian *et al.* [NANOGrav Collaboration], arXiv:1508.03024 [astro-ph.GA].

[111] G. Janssen *et al.*, PoS AASKA **14**, 037 (2015) [arXiv:1501.00127 [astro-ph.IM]].

[112] M. Bastero-Gil, S. F. King and Q. Shafi, Phys. Lett. B **651**, 345 (2007) [hep-ph/0604198].

[113] K. Nakayama, F. Takahashi and T. T. Yanagida, JCAP **1012**, 010 (2010) [arXiv:1007.5152 [hep-ph]].

[114] S. Nakamura and M. Yamaguchi, Phys. Lett. B **638**, 389 (2006) [hep-ph/0602081]; M. Kawasaki, F. Takahashi and T. T. Yanagida, Phys. Lett. B **638**, 8 (2006) [hep-ph/0603265]; T. Asaka, S. Nakamura and M. Yamaguchi, Phys. Rev. D **74**, 023520 (2006) [hep-ph/0604132]; M. Dine, R. Kitano, A. Morisse and Y. Shirman, Phys. Rev. D **73**, 123518 (2006) [hep-ph/0604140]; M. Endo, K. Hamaguchi and F. Takahashi, Phys. Rev. D **74**, 023531 (2006) [hep-ph/0605091]; M. Kawasaki, F. Takahashi and T. T. Yanagida, Phys. Rev. D **74**, 043519 (2006) [hep-ph/0605297]; M. Endo, M. Kawasaki, F. Takahashi and T. T. Yanagida, Phys. Lett. B **642**, 518 (2006) [hep-ph/0607170].

[115] T. Moroi, H. Murayama and M. Yamaguchi, Phys. Lett. B **303**, 289 (1993).

[116] M. Bolz, A. Brandenburg and W. Buchmuller, Nucl. Phys. B **606**, 518 (2001) [Erratum-ibid. B **790**, 336 (2008)] [hep-ph/0012052].

[117] J. Pradler and F. D. Steffen, Phys. Rev. D **75**, 023509 (2007) [hep-ph/0608344].

[118] W. Buchmuller, K. Schmitz and G. Vertongen, Nucl. Phys. B **851**, 481 (2011) [arXiv:1104.2750 [hep-ph]].

[119] W. Buchmuller, L. Covi and D. Delepine, Phys. Lett. B **491**, 183 (2000) [hep-ph/0006168].

[120] F. Takahashi and M. Yamada, arXiv:1510.07822 [hep-ph].

[121] W. Buchmuller, V. Domcke and K. Schmitz, JCAP **1304**, 019 (2013) [arXiv:1210.4105 [hep-ph]].

[122] W. Buchmuller, V. Domcke and K. Kamada, Phys. Lett. B **726**, 467 (2013) [arXiv:1306.3471 [hep-th]].

[123] W. Buchmuller, V. Domcke and K. Schmitz, JCAP11(2014)006 [arXiv:1406.6300 [hep-ph]].

[124] R. Battye, B. Garbrecht and A. Moss, Phys. Rev. D **81**, 123512 (2010) [arXiv:1001.0769 [astro-ph.CO]].

[125] M. Kawasaki, M. Yamaguchi and T. Yanagida, Phys. Rev. D **63**, 103514 (2001) [hep-ph/0011104].

[126] K. Nakayama, F. Takahashi and T. T. Yanagida, JCAP **1308**, 038 (2013) [arXiv:1305.5099 [hep-ph]].

[127] A. Kamada and M. Yamada, Phys. Rev. D **91**, 063529 (2015) [arXiv:1407.2882 [hep-ph]].

[128] A. Kamada and M. Yamada, JCAP **1510**, no. 10, 021 (2015) [arXiv:1505.01167 [hep-ph]].

[129] K. Kamada, Y. Miyamoto and J. Yokoyama, JCAP **1210**, 023 (2012) [arXiv:1204.3237 [astro-ph.CO]].

[130] K. Kamada, Y. Miyamoto, D. Yamauchi and J. Yokoyama, Phys. Rev. D **90**, no. 8, 083502 (2014) [arXiv:1407.2951 [astro-ph.CO]].

[131] K. Mukaida and M. Yamada, arXiv:1506.07661 [hep-ph].

[132] Y. Okada, M. Yamaguchi and T. Yanagida, Prog. Theor. Phys. **85**, 1 (1991). Phys. Lett. B **262**, 54 (1991).

[133] J. R. Ellis, G. Ridolfi and F. Zwirner, Phys. Lett. B **257**, 83 (1991). Phys. Lett. B **262**, 477 (1991).

[134] J. McDonald, Phys. Lett. B **456**, 118 (1999) [hep-ph/9902416].

[135] R. Kitano, H. Murayama and M. Ratz, Phys. Lett. B **669**, 145 (2008) [arXiv:0807.4313 [hep-ph]].

[136] J. Hisano, K. Kohri and M. M. Nojiri, Phys. Lett. B **505**, 169 (2001) [hep-ph/0011216].

[137] G. Arcadi and P. Ullio, Phys. Rev. D **84**, 043520 (2011) [arXiv:1104.3591 [hep-ph]].

[138] M. Ibe, A. Kamada and S. Matsumoto, Phys. Rev. D **87**, no. 6, 063511 (2013) [arXiv:1210.0191 [hep-ph]].

[139] N. Arkani-Hamed and S. Dimopoulos, JHEP **0506**, 073 (2005) [hep-th/0405159]; G. F. Giudice and A. Romanino, Nucl. Phys. B **699**, 65 (2004) [Erratum-ibid. B **706**, 65 (2005)] [hep-ph/0406088]; N. Arkani-Hamed, S. Dimopoulos, G. F. Giudice and A. Romanino, Nucl. Phys. B **709**, 3 (2005) [hep-ph/0409232].

[140] J. D. Wells, Phys. Rev. D **71**, 015013 (2005) [hep-ph/0411041].

[141] L. J. Hall and Y. Nomura, JHEP **1201**, 082 (2012) [arXiv:1111.4519 [hep-ph]].

[142] L. Randall and R. Sundrum, Nucl. Phys. B **557**, 79 (1999) [hep-th/9810155].

[143] G. F. Giudice, M. A. Luty, H. Murayama and R. Rattazzi, JHEP **9812**, 027 (1998) [hep-ph/9810442].

[144] B. Bhattacherjee, M. Ibe, K. Ichikawa, S. Matsumoto and K. Nishiyama, JHEP **1407**, 080 (2014) [arXiv:1405.4914 [hep-ph]].

[145] J. Fan and M. Reece, JHEP **1310**, 124 (2013) [arXiv:1307.4400 [hep-ph]].

[146] H. P. Nilles, Phys. Rept. **110**, 1 (1984).

[147] J. Wess and J. Bagger, Princeton, USA: Univ. Pr. (1992) 259 p

[148] G. F. Giudice and R. Rattazzi, Nucl. Phys. B **511**, 25 (1998) [hep-ph/9706540].

[149] R. Kallosh and A. D. Linde, JHEP **0702**, 002 (2007) [hep-th/0611183].

[150] K. I. Izawa and T. Yanagida, Prog. Theor. Phys. **95**, 829 (1996) [hep-th/9602180].

[151] K. A. Intriligator and S. D. Thomas, Nucl. Phys. B **473**, 121 (1996) [hep-th/9603158].

[152] K. Nakayama, F. Takahashi and T. T. Yanagida, Phys. Lett. B **718**, 526 (2012) [arXiv:1209.2583 [hep-ph]].

[153] K. Nakayama, F. Takahashi and T. T. Yanagida, Phys. Lett. B **734**, 358 (2014) [arXiv:1404.2472 [hep-ph]].